

ACIT5900
MASTER THESIS
in
Applied Computer and Information
Technology (ACIT)
May 2023
Robotics and Control
Development and Control
of a Low Cost Solar Powered
Autonomous Surface Vessel for Water Quality
Investigation and Monitoring

Jan-Philip Radicke

Department of Computer Science
Faculty of Technology, Art and Design

OSLOMET

Preface

This thesis explores the design and development of a low-cost, solar-powered unmanned surface vessel (USV) for water quality inspection and monitoring in coastal areas and fjords. The project was inspired by the need for a more accessible and efficient method of water quality monitoring, as traditional methods can be time-consuming and expensive.

Given my interest in robotics and diverse fields, I saw this project as an opportunity to gain valuable experience, combining 3D-modeling and printing, electronics, mechanics, programming, and practical construction. Overall, I am happy for getting the chance to contribute to water quality monitoring with my thesis, and I have thoroughly enjoyed the time I spent designing and constructing the USV. Nevertheless, this project has been challenging and stressful at times and I could not have accomplished it without the excellent guidance and support of my supervisors, Alex Alcocer and Tønnes Nygaard.

I would also like to thank Aksel Johan Frafjord, Alexander Halseth, and Pierre Boniface for not only creating an amazing working environment, but also for the invaluable input and the motivation they have provided me.

Lastly, I would like to thank my family and friends for their unwavering support and encouragement during this challenging journey.

This thesis aims to contribute to the development of a low-cost and accessible method of water quality monitoring, and I sincerely hope that it can serve as a foundation for future research in this field.

Oslo, May 14, 2023

A handwritten signature in black ink that reads "Jan-Philip Radicke". The script is cursive and fluid, with the first letters of each name being capitalized and prominent.

Jan-Philip Radicke

Abstract

This thesis presents an unmanned surface vessel (USV) which was designed with the goal of providing a low-cost, highly accessible, and autonomous platform for water quality inspection and monitoring in coastal areas and fjords. Traditional water quality monitoring methods often require expensive equipment and highly trained personnel, limiting their accessibility and scalability. Solutions for this present unmanned surface vessels which can be used for water quality inspection, but are often too expensive and time consuming to deploy. By contrast, the solar-powered USV based on a stand-up-paddle (SUP) board offers a fast, easy-to-deploy, and highly maneuverable platform for water quality investigation and monitoring.

The USV is equipped with solar panels to reduce its reliance on external power sources and various sensors for water quality investigation and monitoring. The use of Ardupilot facilitates the operation of the vessel, which can be controlled remotely from a shore-based station. All hardware is housed in cases mounted to an aluminum frame, which provides durability.

The USV was tested at 30% and 50% throttle, and it was found to be more efficient at 30% throttle, providing power for three hours of operation, provided enough sunlight. However, future work aims to improve the solidity of the frame, fine-tune the PID controller of the vessel, and map the sensor data taken during missions.

The use of off-the-shelf components with high market availability makes the USV a viable option for mass production, costing around 50.000NOK. The development of the USV offers a promising solution for affordable and accessible water quality monitoring and inspection, which is crucial for maintaining the health of coastal ecosystems and preserving the livelihoods of coastal communities.

Contents

| | | |
|----------|--|-----------|
| 1 | Introduction | 1 |
| 1.1 | Research Objectives and Scope | 2 |
| 1.2 | Ethical Contributions and Considerations | 3 |
| 1.2.1 | United Nations' Sustainable Development Goals | 3 |
| 1.2.2 | Considerations and Potential Harms | 4 |
| 1.3 | Thesis Layout | 5 |
| 2 | Background | 6 |
| 2.1 | Overview of USVs and Applications | 7 |
| 2.1.1 | Definition of an USV | 7 |
| 2.1.2 | History and Usage of USVs | 7 |
| 2.2 | Previous Work on Low Cost Unmanned Surface Vessels | 7 |
| 3 | Theory | 11 |
| 3.1 | Aquatic Data Collection and Sensors | 11 |
| 3.1.1 | Definition and Importance of Aquatic Ecosystems | 11 |
| 3.1.2 | Measurements of Water Quality | 12 |
| 3.1.3 | Ideal Values for Salt Water and Fresh Water | 14 |
| 3.2 | Probes | 14 |
| 3.2.1 | Dissolved Oxygen Probes | 14 |
| 3.2.2 | pH Probes | 15 |
| 3.2.3 | Temperature Probes | 15 |
| 3.2.4 | Conductivity Probes | 15 |
| 3.3 | Hull Types | 16 |
| 3.4 | Global Positioning System (GPS) | 18 |
| 3.5 | Power Consumption | 19 |
| 3.6 | Properties and Considerations of Metals in Marine Environments | 20 |
| 3.7 | Finite Element Method | 21 |
| 3.7.1 | Von Mises | 21 |
| 4 | Materials | 22 |
| 4.1 | Mechanics | 22 |
| 4.2 | Software | 23 |
| 4.3 | Hardware | 24 |
| 5 | Prototypes and Discarded Ideas | 27 |
| 5.1 | Early Frames | 27 |
| 5.2 | ROS and Websocket | 28 |
| 6 | Methodology | 30 |

| | | |
|-----------|--|-----------|
| 6.1 | Design | 30 |
| 6.1.1 | Frame | 30 |
| 6.1.2 | Handles | 35 |
| 6.2 | Mechanics | 37 |
| 6.2.1 | Kinematics | 37 |
| 6.2.2 | Finite Element Method | 40 |
| 6.3 | Constructing the Physical Frame | 41 |
| 6.4 | Hardware | 43 |
| 6.4.1 | Thruster Model | 46 |
| 6.5 | Software and Control | 48 |
| 6.5.1 | Autopilot Setup | 48 |
| 6.5.2 | Navigation and Control Algorithm | 50 |
| 6.6 | Probe Setup | 51 |
| 6.6.1 | Taking Continuous Measurements | 52 |
| 7 | Results | 55 |
| 7.1 | Price | 55 |
| 7.2 | Building the Vessel | 56 |
| 7.3 | Transportation and Assembly | 56 |
| 7.4 | Initial Test | 59 |
| 7.5 | Second Test | 67 |
| 7.6 | Operation Time | 71 |
| 7.7 | Sensor Data | 72 |
| 7.8 | Frame Stability during Operation | 73 |
| 8 | Discussion and Future Work | 74 |
| 8.1 | Price | 74 |
| 8.2 | Design | 75 |
| 8.3 | Hardware | 76 |
| 8.4 | Software and Navigation | 78 |
| 8.5 | Sensor Data | 79 |
| 8.6 | Ethical Concerns | 80 |
| 9 | Conclusion | 82 |
| 10 | Appendix | 89 |

List of Figures

| | | |
|------|---|----|
| 1.1 | 3D model of the USV | 2 |
| 1.2 | United Nations' global goals [32] | 3 |
| 2.1 | 3D model of the wave- and solar powered USV[12] | 8 |
| 2.2 | Kayak drone [58] | 9 |
| 2.3 | Isometric overview of the paddleboard USV[23] | 9 |
| 2.4 | Water environmental mobile observer (WeMo) [29] | 10 |
| 2.5 | USV prototype [62] | 10 |
| 3.1 | pH scale | 12 |
| 3.2 | Different exchanges of ions [47] | 15 |
| 3.3 | Common types of hulls | 17 |
| 3.4 | GPS position of a receiver at the intersection of four satellites | 18 |
| 4.1 | Aqua Marina Hyper [6] | 23 |
| 4.2 | Pixhawk 4 [57] | 24 |
| 4.3 | Herelink Video Transmission System [3] | 24 |
| 4.4 | Blue Robotics T200 Thrusters [41] | 25 |
| 4.5 | Sunpower SPR-E-Flex-110 [4] | 25 |
| 4.6 | Solar charge controller [4] | 25 |
| 4.7 | Atlas Scientific probes from left to right: pH probe [50], DO probe [48], temperature probe [51], conductivity probe [43] | 26 |
| 5.1 | Frame with mounting for solar panels | 27 |
| 5.2 | Initial design of V-shaped thruster arm | 28 |
| 5.3 | Initial Hardware Structure | 29 |
| 6.1 | Securing the arm during operation | 31 |
| 6.2 | Securing the bolt at the end of the thruster arm | 31 |
| 6.3 | Folding process of the frame | 32 |
| 6.4 | Complete USV model | 33 |
| 6.5 | Technical drawing of the main frame | 34 |
| 6.6 | Technical drawing of the thruster arm and side frame | 34 |
| 6.7 | Bracket for the handle | 35 |
| 6.8 | Handles that lock the frame in place | 36 |
| 6.9 | Body-fixed vehicle coordinate system of the USV | 38 |
| 6.10 | Simplified model of the thruster arm | 40 |
| 6.11 | Force exerted on the thruster and Von Mises | 41 |
| 6.12 | Force exerted on the thruster and Von Mises | 41 |
| 6.13 | Assembling the main- and side frames | 41 |
| 6.14 | Assembled frames with hinges | 41 |

| | | |
|------|---|----|
| 6.15 | Completed, unfolded frame | 42 |
| 6.16 | Completed, folded frame | 42 |
| 6.17 | Fastening mechanism of the handles | 42 |
| 6.18 | Setup for the solar charge controller | 43 |
| 6.19 | Power module connections | 44 |
| 6.20 | Thruster profiles 3D-modelled (left) and 3D-printed (right) | 45 |
| 6.21 | Fastening of thruster and cables | 45 |
| 6.22 | 2D drawings of the T200 thrusters | 46 |
| 6.23 | Thrust at 16V [41] | 46 |
| 6.24 | Current Draw at 16V [41] | 47 |
| 6.25 | Efficiency at 16V [41] | 47 |
| 6.26 | Servo output | 48 |
| 6.27 | Thruster responses during movement options | 49 |
| 6.28 | Diagram for Guidance Logic [38] | 50 |
| 6.29 | Sensor readings in terminal (without probes) | 53 |
| 6.30 | Directory structure for the probe setup | 54 |
| | | |
| 7.1 | All parts on a trolley | 57 |
| 7.2 | Inflating the SUP board | 58 |
| 7.3 | Putting the frame in place | 58 |
| 7.4 | Opening and strapping the frame to the SUP board | 58 |
| 7.5 | Strapping the solar panels to the hull | 58 |
| 7.6 | Connecting solar panels, battery, and the load to the solar charge controller | 58 |
| 7.7 | Lowering the thruster arms and deploying the USV | 58 |
| 7.8 | Completed USV during operation | 59 |
| 7.9 | Map data from the initial test | 59 |
| 7.10 | Throttle performance during Manual, where throttle right is displayed in red, and throttle left is displayed in green | 60 |
| 7.11 | Winding the spool during Loiter test | 61 |
| 7.12 | Throttle performance during Loiter, where throttle right is displayed in red, and throttle left is displayed in green | 61 |
| 7.13 | Path of the USV during guided- and RTL-mode | 62 |
| 7.14 | Throttle performance during Guided and RTL, where throttle right is displayed in red, and throttle left is displayed in green | 63 |
| 7.15 | The measured current of the battery during the entire initial test | 64 |
| 7.16 | The measured current of the battery during the Guided- and RTL mission | 64 |
| 7.17 | The measured speed of the USV during the entire test | 65 |
| 7.18 | The measured speed of the USV during the Guided- and RTL mission | 65 |
| 7.19 | The cross-track error for the RTL/ Guided mission | 66 |
| 7.20 | Completed USV during the second test | 67 |
| 7.21 | Predefined waypoints for the Auto mission | 68 |
| 7.22 | Map data from the Auto mission | 68 |
| 7.23 | Thruster performance during Auto mission | 69 |
| 7.24 | Measured current during Auto mission | 69 |
| 7.25 | Measured speed during Auto mission | 70 |
| 7.26 | Cross-track error during the Auto mission | 70 |

| | | |
|-------|---|----|
| 7.27 | Estimated operation time at 30% throttle | 71 |
| 7.28 | Estimated operation time at 50% throttle | 71 |
| 7.29 | Estimated operation time at 30% throttle without solar panels . . | 72 |
| 7.30 | Estimated operation time at 50% throttle without solar panels . . | 72 |
| 8.1 | Current formatting of data | 80 |
| 10.1 | SUP board | 90 |
| 10.2 | Solar panel | 90 |
| 10.3 | pelican case | 91 |
| 10.4 | T200 thruster | 91 |
| 10.5 | Bolt | 91 |
| 10.6 | Nut | 91 |
| 10.7 | Angle bracket 75x75mm | 91 |
| 10.8 | Hinge (consisting of three parts) | 91 |
| 10.9 | Ratrig angle bracket | 92 |
| 10.10 | Ratrig aluminium profile | 92 |
| 10.11 | Ratrig screw | 92 |
| 10.12 | Thruster profile | 92 |
| 10.13 | Handle | 92 |
| 10.14 | Handle bracket | 92 |

List of Tables

| | | |
|-----|--|----|
| 3.1 | Overview of ideal fresh- and saltwater parameters [63] | 14 |
| 6.1 | USV coordinate system [21] | 38 |
| 7.1 | Bill of Materials | 55 |
| 7.2 | ArduRover flight modes | 60 |
| 7.3 | Efficiency comparison between 30% and 50% throttle | 72 |
| 8.1 | Efficiency comparison between 30% and 50% throttle | 77 |
| 8.2 | Comparison of findings against ideal parameters | 80 |

Chapter 1

Introduction

Aquatic ecosystems play a crucial role in maintaining the health and balance of the environment. However, smaller coastal areas and fjords are currently threatened by pollution, climate change, habitat destruction and overfishing. When these issues become unmanageable, they should be taken seriously because water may not be able to completely neutralize contaminants[25]. It is therefore crucial to monitor the current state of water bodies, such as lakes, streams, rivers or fjords, in order to identify any threatening longterm changes [23].

Conventional methods for water quality evaluation are often not sufficient to cover concerns of this degree. They are often costly as well as and time- and labour intensive. In addition, large parts of water bodies are often hard to reach or directly inaccessible [11]. These methods are also susceptible to human errors during sample collection, such as sample cross contamination or misidentification, incorrect transportation, and the use of wrong laboratory equipment [2].

In modern days, monitoring can be performed by readily available unmanned surface vessels equipped with sensors to identify changes in water quality. These vessels can cover large areas faster due to some degree of autonomy, but they are often too expensive as well as impractical and time consuming to deploy [23].

The above mentioned limitations display the need for vessels with focus on being low cost, fast to deploy, having higher degree of autonomy, and a generally higher accessibility. This may be achieved by using more off-the-shelf components with higher marked availability, allowing for the mass production of vessels for the use of more effective water quality monitoring [29].

1.1 Research Objectives and Scope

In light of the previously mentioned issues, this project focuses on the design and production of a low cost, solar powered unmanned surface vessel (USV). The following objectives are included in the design process of this USV:

The USV will be based on a Stand-up-Paddle (SUP) board, which is fast to deploy, easy to transport, and highly maneuverable. The frame carrying the hardware will be simple, fast to construct, and made of lightweight materials that can withstand marine environments. The USV will be equipped with solar panels to prolong the battery life and reduce reliance on external power sources. It will also house various sensors for water quality investigation and monitoring. The USV will have some degree of autonomy alongside GPS (global positioning system) tracking.

This project does not aim to develop a finished product but instead to create an operational vessel that can prove the suitability of the concepts and ideas mentioned in this Section. Figure 1.1 visualizes the idea of the design.

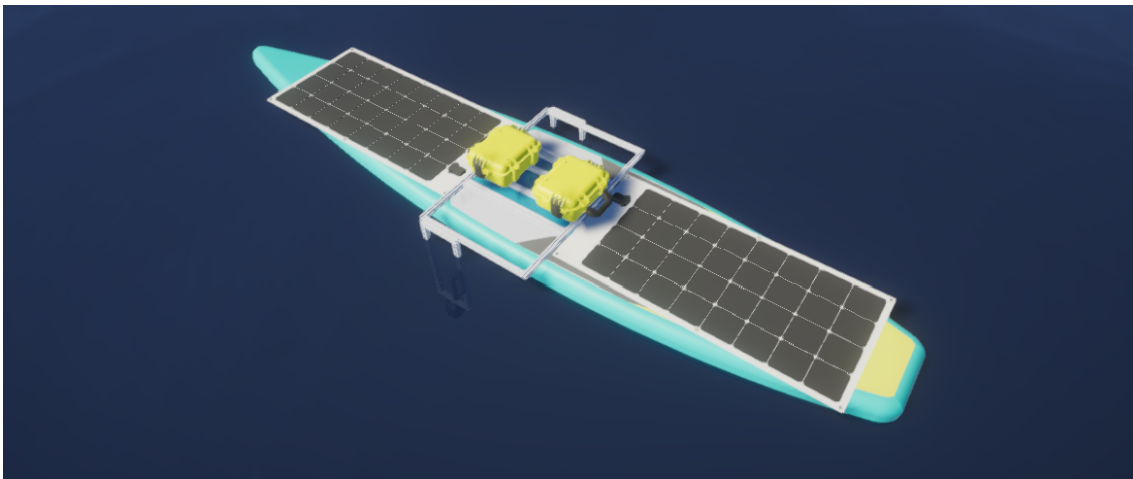


Figure 1.1: 3D model of the USV

1.2 Ethical Contributions and Considerations

With every project, there are different ethics that need to be taken into consideration. The following Sections present what considerations were taken during the design process and construction of the USV, in addition to the contributions this project makes to the environment.

1.2.1 United Nations' Sustainable Development Goals

United Nations has adopted 17 different sustainable development goals, presented in Figure 1.2, which aim to protect the planet. As some of these goals specifically refer to water quality, the quality of life under water, and the global climate[36], this project makes natural contributions to achieving these goals. The following Sections elaborate on these goals, and how the production of a low-cost, solar powered, USV plays a part in achieving them. The complete list of all goals is shown in Figure 1.2



Figure 1.2: United Nations' global goals [32]

Clean Water and Sanitation This project contributes to UN's SDG 6, which aims to "protect and restore water-related ecosystems, including mountains, forests, wetlands, rivers, aquifers and lakes" [35]. This project contributes to this goal by providing a cheap and fast method of monitoring the quality of these water bodies.

Life Below Water Similar to SDG 6, this project contributes to the quality of SDG 14: Life below Water. This goal aims to "sustainably manage and protect marine and coastal ecosystems from pollution, as well as address the impacts of ocean acidification" [34]. While measuring water quality specifically contributes to SDG 6, it assists SDG 14 indirectly. As elaborated on later, in Section 3.1.2, water quality indicates the state of the environments at which life below water exists, and thus provides information on the well-being of aquatic life.

Global Climate While SDGs 6 and 14 are more pivotal in this project, water quality also plays a role in adjusting SDG 13: climate action. The global climate does not only impact water quality, but water quality does also impact the global climate [33]. Water bodies host algae, which mitigate rising atmospheric CO₂ levels [37]. Similar to SDG 14, water quality monitoring can assist in assuring growth of algae and other aquatic life.

1.2.2 Considerations and Potential Harms

While a USV can have positive impacts on the environment, there are potential harms that need to be addressed and taken in to consideration when the vehicle is being designed and operated. The following Sections address some of these potential risks.

Hazardous Materials The USV might sink, capsize, or lose parts during operations, which can lead to environmental damage. Plastics, electronic devices, batteries, and metals pose threats to aquatic ecosystems which are not easily reversible. A sinking USV can also damage fragile ecosystems such as coral reefs and seagrass beds.

Navigation and Collision The USV might be susceptible to collisions with other vessels, structures, objects, or people in the water. This can result in damage to the USV, other vessels, or even injury. These concerns apply to both the autopilot and manual operation.

Environmental Sensitivity The USV can cause disturbances to marine environments, habitats, or water quality. During navigation, the USV can also cause disturbing noise to not only marine environments, but other nearby people and life.

1.3 Thesis Layout

The rest of the thesis is structured as follows.

Background explains what a USV is and presents various previous research that is conducted in regards to low cost.

Theory covers relevant principles that should be known for this thesis. It covers common parameters that can be measured for monitoring water quality, hull types, GPS, power consumption, etc.

The Materials Section of this report presents all major components and materials used for this project.

The Methodology explains how the USV is designed and constructed. It presents some previous prototyping ideas, the current design, and how the frame, hardware, and software is set up. Lastly, it explains the probe- and Raspberry Pi setup.

The Results Section demonstrates the viability of the components and design chosen for this project. In addition, the Section presents results from the various tests that were performed.

The Discussion reflects on the results of the USV and aims to suggest possible improvements for future attempts.

The Conclusion of this report summarizes the complete thesis.

Lastly, the Appendix contains a link to the Github repository of this project and shows figures of the 3D models that were created for this thesis.

Chapter 2

Background

The following Chapter provides a literature review, history and use cases for USVs, and previous and related work in the context of this thesis.

For this thesis, most of the sources were obtained from Google Scholar. In regards to publishing dates, all sources regarding USVs and their technical specifications were retrieved from 2019 and onwards due to the rapid technological advancements in recent years. Common searches for this topic included "Unmanned Surface Vessel," "Autonomous Surface Vessel," "Water Quality Monitoring," and "Low Cost USV."

Sources related to fundamental aspects of water quality, such as water quality measurements and parameters were not limited to a specific publishing year. Information on these topics was found on blogs, academic papers, and books.

Figures were sourced from their original location, such as the websites on which they were purchased or official websites. Information on the parts used in the Materials Section was retrieved from official documentation or the websites where they were purchased.

The workings of the probes are explained according to the information provided by their vendor, Atlas Scientific, and are cited in their respective sections.

2.1 Overview of USVs and Applications

The following Section defines what a USV is and presents an overview of their historical development and common applications.

2.1.1 Definition of an USV

USVs are ships or boats that do not require operators on board. Instead they get controlled from afar and thus produce several benefits, such as lower development and operation costs, improved personnel safety and security, and extended operational range [27].

USVs usually have some, although varying, degree of autonomy. Therefore, they are often called autonomous surface vessels, but the two terms are often used interchangeably, depending on the context and industry. Generally, USVs have some level of autonomy or self-navigation capabilities, which can range from basic waypoint following to more advanced capabilities such as obstacle detection, obstacle avoidance, decision making, and adaptive mission planning [39].

2.1.2 History and Usage of USVs

The idea of USVs can be traced back to World War II, when the first remotely-controlled boats were developed for military purposes. Since then, the technology has evolved and expanded to other areas such as scientific research, oceanography, environmental monitoring, offshore oil and gas, and shipping [59]. USVs are also used in general robotic research and development to improve their autonomy, navigation, and decision-making capabilities. Lastly, USVs are used for public purposes such as search and rescue and disaster response [31].

2.2 Previous Work on Low Cost Unmanned Surface Vessels

Previous research on cheap and reproducible unmanned surface vehicles (USVs) has focused on developing low-cost, easy-to-build platforms for a variety of applications. These applications include oceanography, environmental monitoring, and search and rescue operations.

For instance, researchers at OsloMet have build a low-cost USV operated by wave and solar energy. The vessel, depicted in Figure 2.1, is composed of a surface unit and a submerged unit, linked together with a tether, both electrically and mechanically. The hull is a multihull, and is created using fiberglass, and polyvinyl chloride (PVC) was chosen for the frame due to its mechanical properties and low weight. The frame was then manufactured using a 3D CNC router and assembled using stainless steel bolts and locknuts. A server is created that allows users to set new waypoints and see the collected data. The vessel takes

measurements of conductivity, pH (power of hydrogen), dissolved oxygen (DO), and temperature [12].

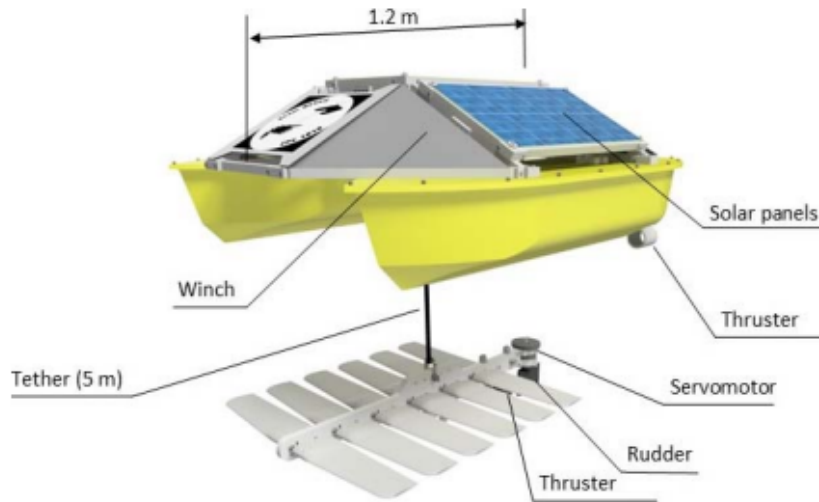


Figure 2.1: 3D model of the wave- and solar powered USV[12]

Another solution has focuses on an autonomous raft vehicle (ARV), which has as its purpose to improve ARV navigation with the A-star (A*) pathfinding algorithm over multi-way-point. The ARV is build as a raft-like vessel, containing two PVC pipes and an aluminium frame to connect the two hulls [13].

Researchers at the Institute of Marine Research present a prototype USV, named the Kayak Drone, which was built to fulfill experimental and operational needs such as:

- inshore and shallow water acoustic monitoring
- offshore comparison of echo sounder recordings
- monitoring natural fish schooling behavior
- monitoring seabird-fish behavioral interactions

The Kayak Drone shown below was built using off-the-shelf hardware and existing open-source software, resulting in a modular and low-cost USV based on an expedition double kayak hull. In situ experiments demonstrate that the Kayak Drone produces very little noise and can record echo sounder data of fish near the surface without disturbing their natural distribution and behavior. This was achieved by silent propulsion and a slim hull as to minimize the pressure field. The Kayak Drone was also able to navigate within a couple of meters from swimming seabirds without triggering escape, making it a useful tool for observing predation by seabirds on fish schools without interfering with their natural behavior. Overall, the authors foresee that the Kayak Drone can be utilized in many different experiments where a silent platform is needed [58].

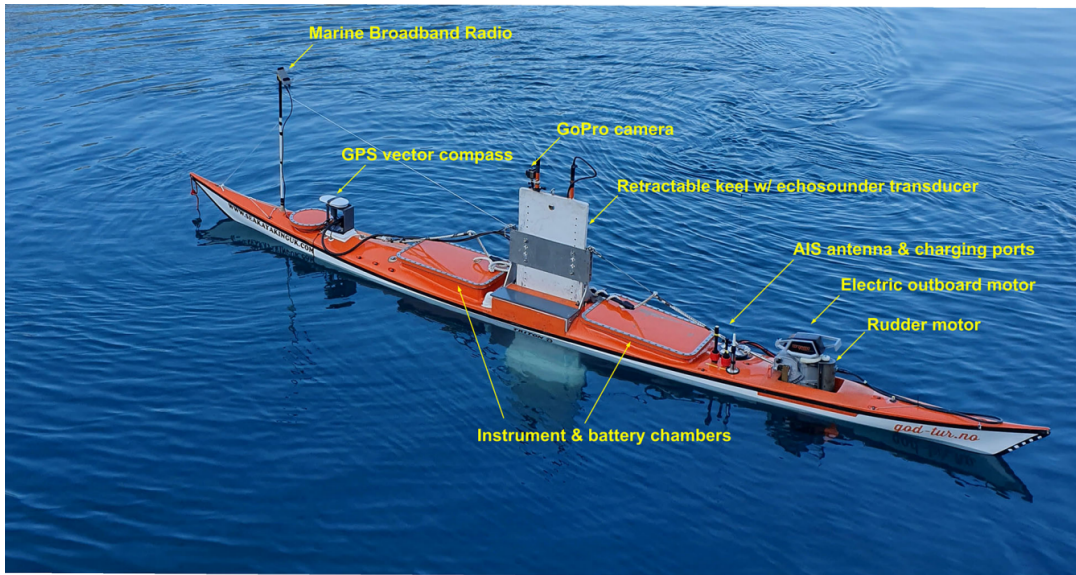


Figure 2.2: Kayak drone [58]

[23] provided work done on a SUP board-based USV that proved itself to be portable and capable of performing surveys at several sites in Rhode Island. A frame made of carbon fiber tubes was mounted to the SUP board. The frame can be folded such that transport is made easier, and may be attached to the board by fastening strips. For the hardware, the vessel makes use of off-the-shelf components like the Orange Cube autopilot and T200 thrusters. The total weight of the USV is 21kg. An isometric overview of this design is depicted in Figure 2.4.

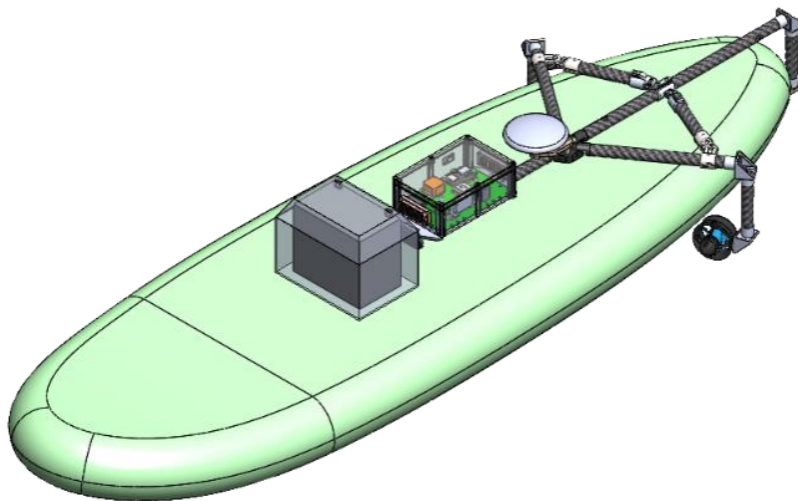


Figure 2.3: Isometric overview of the paddleboard USV[23]

Another solution that has focus on cost-effectiveness and reproducibility is the water environmental mobile observer (WeMo). The vehicle has been realized exploiting off-the-shelf components and is provided with an array of sensors to measure chemical and physical parameters. With the vessel being more reproducible, it aims to create an eco-system of USVs for local communities and administrations, with the purpose of monitoring ecological statuses.

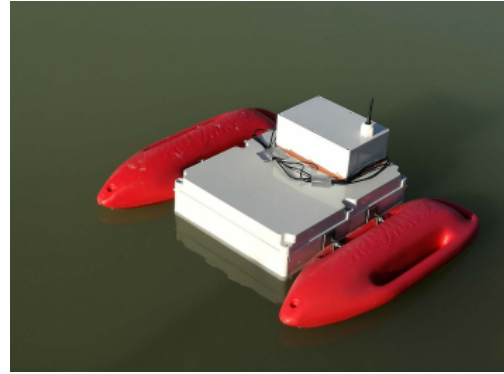


Figure 2.4: Water environmental mobile observer (WeMo) [29]

The vessel is built by the use of an ABS plastic box and two lateral rescue cans. Using various sensors, it measures pH, ORP (Oxidation-Reduction Potential), salinity, DO, flow rate, and water depth [29].

[62] discusses the challenges of water sampling and proposes the use of USVs to collect water samples and analyze them. This USV focuses on shallow water bathymetry mapping, which is the process of measuring and mapping the depth and topography of underwater environments. The USV was equipped with two BlueRobotics T200 thrusters, a 1D sonar sensor, a 14.8V 7200mAh 4S LiPo battery, a microcontroller, ESCs, and other sensors. All electronics were placed in waterproof containers, with wires entering through water-tight cable penetrators and waterproof epoxy. The compass was placed in a separate container and shielded with aluminum foil to prevent false readings. A plastic cover and a rope frame were added to prevent water from entering the upper cavity and provide a quick connection point for the retrieval rope. The prototype USV weighs 6.44kg.



Figure 2.5: USV prototype [62]

Chapter 3

Theory

This Chapter presents information on relevant principles and theory such as hull design, GPS, probes, power consumption, and the use of metals in marine environments.

3.1 Aquatic Data Collection and Sensors

The following Sections provide information on aquatic ecosystems and present different parameters that can be measured when monitoring water quality. Section 3.1.3 provides an overview of ideal parameters for fresh- and saltwater.

3.1.1 Definition and Importance of Aquatic Ecosystems

Aquatic ecosystems are water-based environments, such as lakes, rivers, and oceans, where living organisms interact with both physical and chemical features of the environment. Aquatic ecosystems and life perform several valuable functions for the environment. Among others, the ecosystem recycles nutrients, maintains streamflow, recharges ground water, produces food, and purifies water. On a larger scale, aquatic ecosystems contribute by regulating the global climate, through the exchange of carbon dioxide between the atmosphere and the ocean. The ocean absorbs about 30% of the carbon dioxide released into the atmosphere by human activities, which helps to mitigate the effects of climate change.[25].

However, aquatic ecosystems are facing numerous threats, including pollution, climate change, overfishing, and habitat destruction. Monitoring the health of aquatic ecosystems is important for understanding their current state. Water has the ability to neutralize contamination, but if the contamination becomes uncontrolled, the self-generating capacity can be lost. Therefore, it is important to identify any changes that could threaten their long-term sustainability [5]. USVs have proven as a valuable tool in regards to monitoring aquatic ecosystems by the help of sensors, which provides information about the health of aquatic ecosystems and the impacts of human activities on these systems [12].

3.1.2 Measurements of Water Quality

There are several parameters that can be measured to monitor the water quality of aquatic ecosystems. Some of the most common measurements that are taken are as follows.

pH level The pH level of water (Power of Hydrogen) can affect the survival and growth of aquatic organisms. It measures the the acidity or alkalinity of water, with a pH of 1 being strongly acidic, a pH of 7 being neutral, and a pH of 14 being strongly basic (also called alkaline). The pH scale is logarithmic. This means that each number below 7 is 10 times more acidic than the previous number when counting down, and vice versa, as demonstrated in Figure 3.1. Different species of aquatic life have different pH tolerances [18].

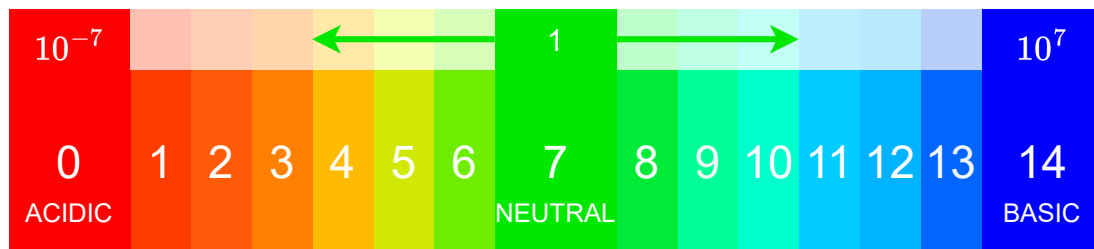


Figure 3.1: pH scale

Dissolved Oxygen (DO) DO is a measure of the level of free, non-compound oxygen present in water and explains how much oxygen is dissolved in the water. It is measured in units of milligrams of oxygen gas (O_2) dissolved in each litre of water (mg/L). Similar to organisms on land, DO is necessary for aquatic life including fish, invertebrates, bacteria and plants. The concentration of DO is heavily dependant on a number of factors, such as diffusion and aeration, photosynthesis, respiration and decomposition. In freshwater systems it also varies by season, location and water depth. Different aquatic life requires different concentration. For example, shallow water fish need higher levels of DO (4-15 mg/L), while bottom feeders such as crabs and worms need minimal amounts of oxygen (1-6 mg/L) [44][17].

Turbidity, Water Clarity, and Total Suspended Solids Turbidity is a measure of how cloudy the water is. It can affect the amount of light that reaches underwater plants and can impact the feeding and behavior of aquatic animals. Turbidity is measured in nephelometric turbidity units (NTU) [19].

Water clarity is defined by how clear or transparent water is. It is measured by how deep the sun light reaches, which is also known as the photic zone. The deeper the photic zone reaches, the higher the chances are for photosynthetic production. The photic zone can reach depths up to 200m and is limited as a result of the light absorption properties of water. Water clarity is measured in

meters by lowering a measuring device into the water until it is no longer visible. Turbidity and water clarity are inversely correlated, meaning that as turbidity increases, water clarity decreases [19].

Total suspended solids (TSS) are particles that are larger than $2\mu m$ found in the water column, and includes anything drifting or floating in the water. Examples of TSS may be sediment, silt, and sand and even plankton and algae [19]. When the concentration of total solids is too low, there might not be enough nutrients in the environment to support aquatic life. On the other hand, too high TSS can indicate high turbidity or pollution [56].

Conductivity and Salinity Conductivity is a measurement of how effectively water can conduct an electrical current and is usually measured in micro- or millisiemens per centimeter ($\mu S/cm$ or mS/cm). It is related to the amount of dissolved ions and minerals in the water and can help researchers understand the salinity of the water [16].

Salinity refers to the total concentration of all dissolved salts in water and is measured in parts per thousand (ppt). In practice, high salt levels can disrupt the natural balance of the ecosystem and harm fish, plants, and other aquatic organisms. Aquatic organisms have varying levels of tolerance for salinity, and salinity levels can differ among different aquatic environments [16].

Water Temperature Water temperature is a physical property and expresses how hot or cold the water is, which is defined as the average kinetic energy of the atoms and molecules. The temperature changes due to heat transfer, which can come from sun light, other water sources, thermal pollution, and air. Alone, water temperature affects the metabolic rates and biological activity of aquatic organisms and the habitats that come with them. On a larger scale, water temperature affects almost all other parameters used for measuring water quality as it alters the physical and chemical properties of water [20]. Some of the parameters affected by temperature are:

- Water Density
- pH Level
- Conductivity and salinity
- Dissolved oxygen
- Metabolic rates and photosynthesis production[20]

Chlorophyll concentration Chlorophyll is the pigment that gives plants their green color and is used in photosynthesis, and indicates the amount of phytoplankton in water [14]. Phytoplankton are organisms that live in water bodies, and are responsible for converting solar energy into organic matter - a process

known as primary production. Primary production is what provides fish, sea birds, marine mammals, and humans with food. Measuring chlorophyll concentration in water can thereby give an indication of the amount of plant life present in the water. Chlorophyll concentration is usually measured in milligram per litre of water (mg/L). Large phytoplankton populations also cause water to appear greener as a result of high chlorophyll concentrations [15].

3.1.3 Ideal Values for Salt Water and Fresh Water

For means of comparisson, the following Table lists and summarizes some important water quality parameters with their freshwater- and saltwater ideal ranges.

Table 3.1: Overview of ideal fresh- and saltwater parameters [63]

| Water Quality Parameter (SI Unit) | Freshwater Ideal Range | Saltwater Ideal Range |
|-----------------------------------|------------------------|-----------------------|
| pH | 6.5 - 8.5 | 7.5 - 8.4 |
| DO (mg/L) | 5 - 14 | 5 - 11 |
| Turbidity (NTU) | < 5 | < 5 |
| Water Clarity (m) | > 1 | > 1 |
| TSS (mg/L) | < 50 | < 50 |
| Conductivity (μ S/cm) | 50 - 1500 | 50,000 - 70,000 |
| Salinity (ppt) | < 0.5 | 30 - 40 |
| Water Temperature ($^{\circ}$ C) | 5 - 25 | 5 - 25 |
| Chlorophyll (μ g/L) | < 10 | < 10 |

3.2 Probes

This project utilizes probes to measure DO, pH, conductivity, and temperature. The following Sections provide an overview of the functions of the specific probes used in this project. Thus, it is important to note that the information presented here may not be applicable to probes manufactured by other companies.

3.2.1 Dissolved Oxygen Probes

Dissolved oxygen (DO) probes are a common way to measure dissolved oxygen in water. They work by defusing oxygen molecules through the membrane at a constant rate. The molecules are thereafter reduced at the cathode, an electrode from which a conventional current leaves a polarized electrical device, and a small voltage is produced. At 0mV, the probe indicates the absence of oxygen. As the level of oxygen increases, the mV output of the probe will also increase. This signal is then read by the DO probe and is displayed on a meter [45].

The probe requires an electrolyte solution which must create an electrochemical reaction at the sensing element that generates a voltage. The electrolyte solution acts as a conductor, allowing ions to move between the cathode and anode and complete the electrochemical reaction. Without the solution, there is no current. The electrolyte solution depletes when the probe reacts with oxygen in water and must therefore be replaced when the solution is low [45] [49].

3.2.2 pH Probes

A pH meter determines pH by measuring the voltage that a solution produces. The meter uses three components for this; the pH meter itself as well as two probes - a reference pH electrode, and a pH probe that is inserted into the solution being tested. There are usually two electrodes in the body of the probe. The first electrode is used as reference and contains a neutral electrolyte, meaning it has a pH value of 7, while the second is used for measuring. As depicted in Figure 3.2, the probe measures pH by swapping hydrogen ions with the tested solution. The more ions that enter the solution, the more acidic the solution is, and vice versa.

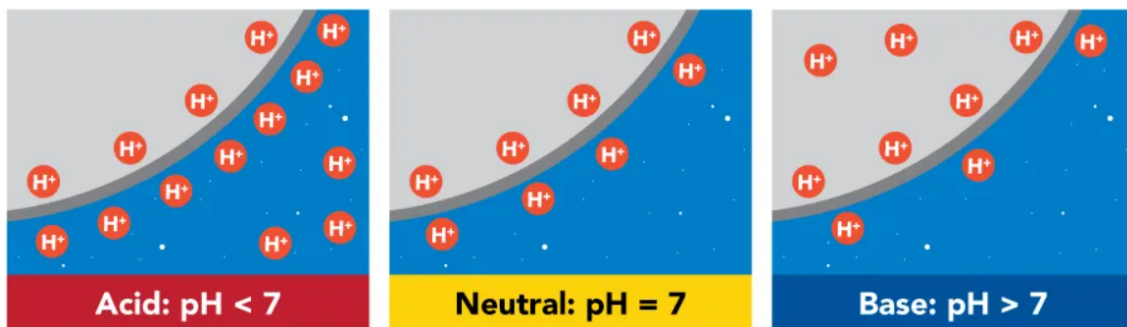


Figure 3.2: Different exchanges of ions [47]

3.2.3 Temperature Probes

Temperature probes contain two metals that generate an electrical voltage or resistance during changing temperatures. They then measure the voltage and convert it to temperature. As platinum has a linear correlation between resistance and temperature, it is often used as the industry standard for temperature probes. The tips of the probes are made of steel, and therefore conduct the heat from the environment to the platinum sensor in the probe [46] [52].

3.2.4 Conductivity Probes

As previously mentioned, conductivity is the measurement of the electrical current of a solution, often measured in micro-Siemens per centimeter ($\mu S/cm$). In practice, conductivity probes contain two electrodes set apart a specific distance. An electrical current will flow between the electrodes, determined by the ion concentration in the solution. The higher the ion concentration is, the higher the conductivity of the tested solution is, which results in a faster electric current, and vice versa [53].

As stated in Section 3.1.2, conductivity is heavily affected by the water temperature, because high and low water temperatures increase and decrease the ion movement respectively. This dependency requires calibration before use, and also suggests importance of simultaneously measuring the temperature of the solution [53].

3.3 Hull Types

All vessels, regardless of size, type, purpose, and complexity, can be categorized into three broad categories based on the kind of hulls used; displacement hulls, planing hulls, and semi-displacement hulls. Displacement hulls displace the water around them and thus move at a slower but steadier pace. Planing hulls are designed to plane on top of the water which reduces drag and allows the boat to travel at higher speeds. Lastly, semi-displacement hulls are a combination of displacement hulls and planing hulls. These three categories can further be split into sub-categories that all have different use cases [22]. The following hulls are also illustrated in Figure 3.3.

Flat-Bottom Hulls A flat-bottom hull is a type of planing hull that has a flat or nearly flat bottom surface that allows the boat to plane at high speeds. The flat bottom creates lift, reduces drag, and allows the boat to skim across the water's surface. They tend to be very stable, but do not perform well at open sea, as they can more easily capsize due to waves [7] [42].

Round-Bottomed Hulls Round-bottomed hulls are displacement hulls that are designed for stability and maneuverability, especially in rough water, but they typically do not achieve high speeds [7] [42].

Multi-Hulls Depending on the specific design of the multi-hull, they can belong to either planing hulls or displacement hulls. Typical examples of multi-hulls are catamarans or trimarans, which may provide increased stability, speed, and carrying capacity. Their downside is a decreased turning radius [7] [42].

V-Shaped Hulls V-shaped hulls have a sharp entry at the bow, which provides higher stability at the cost of higher power usage. These hulls may also be classified as either planing- or displacement-hulls, depending on the v-shape [7] [42].

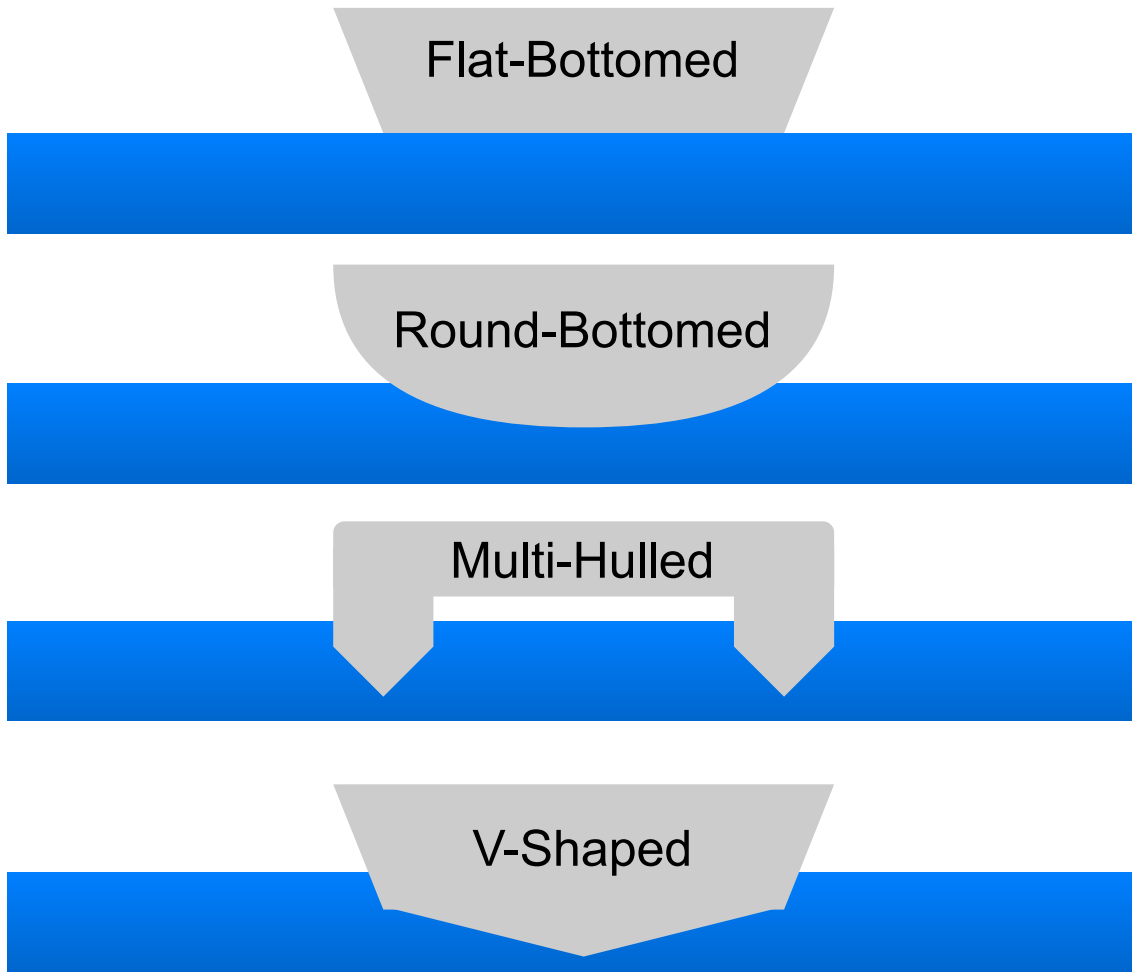


Figure 3.3: Common types of hulls

3.4 Global Positioning System (GPS)

GPS is a network of satellites and receiving devices used to determine the location of a given object [61]. Commonly, there are 24 satellites circulating Earth, with each satellite making a full orbit of Earth every 12 hours. Satellites consistently send signals for objects to receive [30].

Satellites emit signals enabling receivers to determine their location and time. Each GPS satellite carries an atomic clock that provides precise time information, which is transmitted with the signals. The receiver calculates the distance to each satellite by measuring the time difference between the time the signal was broadcast and the time of signal reception. The receiver also makes adjustments for propagation delays caused by the ionosphere and troposphere. By using information from four satellites, the receiver can compute its three-dimensional position and the time. The calculations require an atomic clock synchronized to GPS, but a fourth satellite measurement can replace the need for an atomic clock. The four satellites used by the receiver compute latitude, longitude, altitude, and time [1]. An illustration of these workings is presented in Figure 3.4.

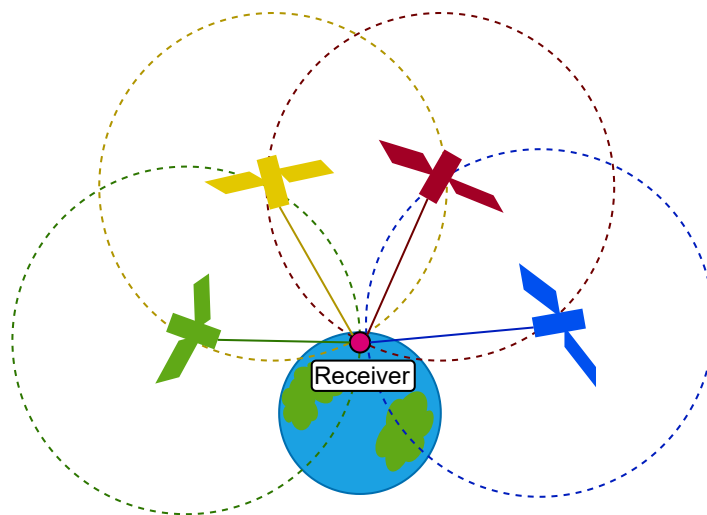


Figure 3.4: GPS position of a receiver at the intersection of four satellites

Once the receiver's position is determined, it has received a fix. The accuracy of the fix depends on a variety of factors, including the quality of the GPS signal, the number of satellites in view, and the geometry of the satellite constellation relative to the user's position. Almanac was introduced as a memory the receiver would keep in order to predict the satellites that would be visible for a given time and position on Earth. The almanac is transmitted along with the signals to GPS receivers, and helps the receivers from a "cold" or "warm" start. These terms refer to the initial state of a GPS receiver, and while their definitions may vary among manufacturers, the following paragraphs provide a general description of these states [28].

Cold start means that the GPS receiver has no position or time, and usually occurs at the beginning of each day. In addition, the GPS does not always have an almanac [54] [26].

A warm start, on the other hand, usually occurs when the receiver has been turned off for a short period of time or has been moved to a new location since its last use. In a warm start, the GPS receiver usually has information about the satellite constellation and current time, so it can acquire a fix more quickly than in a cold start. The time it takes for a GPS receiver to obtain a fix is also known as "Time to first Fix", or TTFF, and is measured in seconds [54] [26].

3.5 Power Consumption

Power consumption refers to the amount of energy consumed by an electrical device or system over a given period of time, and is typically measured in watts (W) or kilowatts (kW). The principles and fundamental equations related to power consumption are based on basic electrical concepts, such as voltage, current, and resistance [24].

These three parameters are related as such:

$$V = IR \tag{3.1}$$

where:

- V = Voltage (volts)
- I = Current (amperes)
- R = Resistance (ohms)

Furthermore, power can be calculated using the following equation:

$$P = VI \tag{3.2}$$

where:

- P = Power (watts)
- V = Voltage (volts)
- I = Current (amperes)

The unit of electric charge, measured in milliampere-hours (mAh), is commonly used to measure the capacity of a battery or the amount of charge a battery can store. It represents the total amount of charge that a battery can deliver over a specific period of time, and is calculated as the power (W) during an amount of hours (h), divided by the voltage (V) [24].

$$C = mAh = \frac{Wh}{V} \tag{3.3}$$

where:

- C = Battery capacity (mAh)
- mAh = Milliampere-hours
- W = Power (watts)
- h = Time duration (hours)
- V = Voltage (volts)

The power consumption, which describes how long a system can run, is calculated as the total time duration of the system in hours (h) being equal to the battery capacity (C), subtracted by the change in power in the system (ΔP).

$$h = C - \Delta P \quad (3.4)$$

where ΔP is equal to the power that leaves the system, subtracted from the power that enters the system ($P_{in} - P_{out}$).

3.6 Properties and Considerations of Metals in Marine Environments

When working in marine environments, it is important to consider the correct materials, as seawater may cause chemical, physical, and biological deterioration.

For metals, deterioration is known as corrosion, and is a result of oxidation. This generally happens when metals lose electrons to oxygen and other substances. Rust is a subcategory of corrosion that specifically refers to the oxidation of iron or steel in the presence of oxygen and moisture [60].

Metals can be split into two categories: ferrous and non-ferrous metals. The following paragraphs explain the two, and name metals that are most common for use in marine environments.

Non-Ferrous Metals Non-ferrous metals do not contain iron, and thus have lower tensile strength than ferrous metals and are often more expensive. Due to the lack of iron however, they naturally provide stronger resistance to corrosion, and generally have a lower weight than ferrous metals. Common metals in this category include aluminium, copper, lead, and zinc [10].

Ferrous Metals Ferrous metals are metals that contain iron and steel. One of the key properties of ferrous metals is their strength and durability. This makes them suitable for use in applications where strength and load-bearing capacity are important, such as in the construction, or in the manufacturing of heavy machinery and equipment. However, ferrous metals are susceptible to corrosion, particularly in marine environments. Common solutions to this problem

is stainless steel or galvanization.

Stainless steel is a ferrous metal, which is an alloy that contains chromium, nickel, and molybdenum to provide corrosion resistance. The chromium in stainless steel reacts with oxygen in the air to form a layer of oxide on the surface of the metal. The oxide then acts as a protective, self-renewing, barrier against corrosion.

Galvanized steel usually involves coating the metal with a layer of zinc and is usually done by hot-dip galvanization or electroplating. In hot-dip galvanization, the metal is immersed in a bath of molten zinc, while in electroplating, the metal is placed in a solution containing zinc ions. In contrast to stainless steel, galvanization does not provide a self-renewing coat, thus making the metal subject to corrosion once scratched or damaged. In all, stainless steel is more expensive, but more resistant than galvanized steel [10].

3.7 Finite Element Method

Finite element method (FEM) is a numerical technique that predicts how an object might behave under various physical conditions. In short, the method splits the structure of an object into simpler parts (finite elements), with each part represented by a set of element equations, and then reconnects the elements at points (nodes), creating a global system of equations for the final calculation [40].

3.7.1 Von Mises

Von Mises stress, σ_v , is a value used to determine if a given material will yield or fracture, and is often used in FEM. A material will yield when the stress applied to it exceeds its yield strength. Yield strength is the amount of stress required to permanently deform a material. When a material is under stress, there are three limits to take into consideration [55]:

- **Elastic Limit:** The elastic limit, or yield stress, is the region where the deformations of a material are reversible. If the stress on the material remains below the elastic limit, it will return to its original shape once the stress is removed.
- **Upper Yield Strength:** Once the stress on a material exceeds the upper yield strength, the deformations the material experiences are irreversible. This type of deformation is also known as plastic deformation.
- **Rupture Strength:** Rupture strength, or the ultimate strength, is when a material is deformed to the point where it fractures or breaks apart [8][9].

Chapter 4

Materials

This Section provides an overview of the hardware and software utilized in this project, including their respective versions as of the report's writing. Citations for other materials are indicated at their corresponding usage locations, while appendices are provided for supplementary materials. This Section is divided into Mechanics, Software, and Hardware.

4.1 Mechanics

The following paragraphs present the components that constitute the construction of the USV. These components include the hull, the hardware housing, and the frame components. Each paragraph also provides explanation of the choice of materials for the respective component.

Hull As mentioned in Section 3.3, the correct type of hull needs to be considered for the right use. Considering a USV that should monitor in fjords and coastal areas, it was decided that maneuverability should be the highest priority. A Stand-Up-Paddle (SUP) board is chosen as the hull. SUP boards have a high marked availability, are easy to transport, and are deployed quickly and efficiently in various locations. In addition, they are considered as flat-bottom hulls which can provide a number of benefits. SUP boards are designed for maneuverability and are easy to turn and control. This is an advantage in narrow fjords and other coastal areas where tight turns and precise navigation may be required. The drawback of a SUP board can be that it can more easily capsize during moments with higher waves, meaning they are not suited for use in harsh environments

The SUP board of choice is the Aqua Marina Hyper, shown in Figure 4.1, which is an inflatable board that has dimensions of 3500x750x150mm and supports a payload of 150kg. The fairly large dimensions provide enough space for two solar panels in addition to the frame and hardware.



Figure 4.1: Aqua Marina Hyper [6]

Aluminium Profiles To mount the hardware to the hull, a frame is created which consists of 20x20mm extruded aluminium profiles, known as ratrig. In total, two ratrig starter packages are purchased which provides a total of 24 x 500mm aluminium profiles, 16 angle brackets, 64 x M5 8mm bolts and 64 x M5-T washers. As mentioned in Section 3.6, aluminium has advantages in marine environments, such as low weight and higher resistance to corrosion. They are also practical in terms of construction and marked availability.

Peli Case The housing of the hardware was decided to be a Peli Case IM2050. Peli Cases are durable and fully waterproof. In addition, they are relatively large and can accommodate several parts of hardware. For this project, two cases are used; one for the autopilot and one for the solar charge controller and battery.

4.2 Software

The software, SolidWorks 2021 was run on a MSI GV62 7RE.

The 3D printing was performed on the FlashForge Adventurer 3 for prototyping, and Ultimaker 2+ Connect for finalized attempts. The respective software used for these printers is Flashprint 5 and UltiMaker Cura 5.2.2. Both printers make use of polylactic acid (PLA).

The Raspberry Pi makes use of Raspberry Pi OS, a port of Debian Buster.

Ardupilot was chosen as the software for the USV. It is an open source autopilot software with an active forum and sufficient documentation. Ardupilot makes use of Mission Planner; a program that provides an interface for planning, monitoring, and controlling ArduPilot-powered vehicles. The already existing interface, an autopilot, and number of configurations is what makes Ardupilot the software of choice for this project. For this project, Mission Planner 1.3.80 Build 1.3.8479.20539 was used.

4.3 Hardware

This Section covers all hardware that is used for this project. It is important to not that while the use of these parts is recommended, they must not specifically be used for any replication of this project.

Pixhawk 4 The Pixhawk 4 is an autopilot designed for academic and commercial use. It features a 32-bit ARM Cortex M7 processor, a built-in barometer, magnetometer, and other sensors that allow it to accurately measure altitude, orientation, and other parameters. While it is most often used for drones, it works for maritime purposes as well.



Figure 4.2: Pixhawk 4 [57]

Pixhawk 4 GPS Module The GPS module for the Pixhawk 4 is a component that provides the autopilot with position, velocity, and timing information. It simply connects to the GPS port of the Pixhawk and does not require any further configuration or software.

Herelink HD Video Transmission System The controller for the USV is the Herelink 2.4GHz HD Video Transmission System. It is a long-range video transmission system designed for use with remote-controlled (RC) models. The Herelink system includes a ground station and a remote controller, which communicate with each other using a long-range radio link, supports various flight modes and can transmit live video and telemetry data in real-time.



Figure 4.3: Herelink Video Transmission System [3]

Herelink Air Unit The Herelink Air Unit is a Wifi module connects to the Pixhawk 4 and creates a connection between the Herelink Transmission System and the Pixhawk 4. It features two antennas which connect to the ANT-ports.

Holybro Pixhawk 4 Power Module (PM07) The Power Management Board (PM Board) serves the purpose of a Power Module as well as a Power Distribution Board. In addition to providing power to Pixhawk 4, through designated ports, and the ESCs, it sends information to the autopilot about battery's voltage and current supplied to the flight controller and the motors.

Thrusters For the thrusters, Blue Robotics' T200 thrusters were chosen for this project, inspired by the related research that was conducted. Blue Robotics T200 thrusters are underwater brushless electric thrusters designed for use in marine robotics applications. The T200 thrusters are rated for a maximum depth of 200 meters and can produce up to 5.25 of thrust at full power at 16V. They have a maximum power consumption of 200 watts, and are therefore sufficient for this project in regards to power output, power consumption, price, and maximum depth.



Figure 4.4: Blue Robotics T200 Thrusters [41]

Solar Panels This project makes use of two Sunpower SPR-E-Flex-110 solar panels that are strapped to the hull. The solar panels each have a peak power output of 110 watts each, so two of these panels will provide a total peak power output of 220 watts. While it is not estimated that these panels can power the USV alone, using solar panels to recharge the battery is an effective way to extend the operational time of the ArduPilot setup and reduce reliance on external power sources. In addition, the solar panels are flexible and weather-resistant.

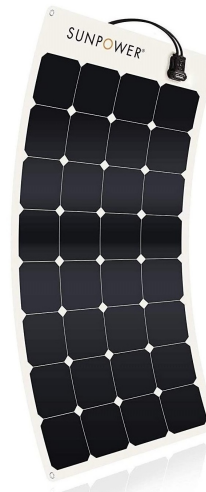


Figure 4.5: Sunpower SPR-E-Flex-110 [4]

Solar Charge Controller The solar charge controller used in this USV is a 40A MPPT (Maximum Power Point Tracking) solar charge controller designed for 12V and 24V systems. MPPT maximizes the charging efficiency and ensuring optimal performance. In addition, the controller features an LCD screen for monitoring and control.

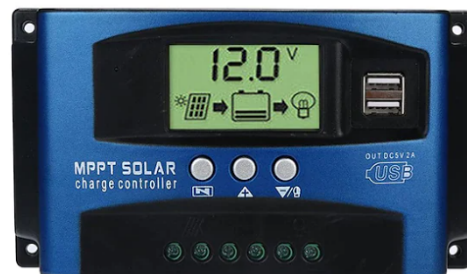


Figure 4.6: Solar charge controller [4]

With multiple load control modes, it provides flexibility in managing power distribution to different loads, making it suitable for this project. This controller is seen in Figure 4.6

Probes This project makes use of Atlas Scientifics' DO-, pH-, conductivity, and temperature probes. These probes are specifically chosen as they cover a variety of measurements that properly describe water quality, as the information in Section 3.1.2 presented. Related and previous research have also used these probes to measure the same parameters. In addition, they have a high marked availability and a relatively low cost. All probes are able to take their respective measurements in both fresh- and salt water and are fully submersible up to the Sub-Miniature version A (SMA) connector. In addition, this project makes use of the Atlas Scientific EZO-DO Circuits which take the readings for each of the probes. The following Figure displays these probes.



Figure 4.7: Atlas Scientific probes from left to right: pH probe [50], DO probe [48], temperature probe [51], conductivity probe [43]

Whitebox T3 To simplify the hardware structure of the payload, this project makes use of the Whitebox T3, a stackable add-on board for the Raspberry Pi allowing for simplified connections between the probes and the Raspberry Pi. The board features two isolated- and one non-isolated port for the EZO circuits. This means that two of the ports are isolated such that other readings and noise does not interfere with readings. Each port also features an SMA connector for the connection of Atlas Scientific probes.

Battery The battery used for this project is a 16000mAh, 4 cell lithium battery. It has a nominal voltage of 14.8V and 16.8V when fully charged.

Chapter 5

Prototypes and Discarded Ideas

This Chapter details the initial ideas and designs of this thesis. These discarded ideas had a significant impact on the thesis, but were ultimately replaced with superior alternatives. The reasons for their dismissal will also be explained.

5.1 Early Frames

The entire design of the USV relies upon a trial and error approach, where the initial ideas were drawn on paper. Ideas that were considered as sufficient were those that indicated a modular, simple, and cheap design. Such ideas were later visualised in Solidworks to give a better representation on their design in practice.

The earliest 3D model of the frame included mounting for the solar panels, as seen in figure 5.1. The plan was to mount the solar panels to the frame with 5mm bolts and nuts, while fastening the Pelican cases with reclosable fastening strips. While not shown in the model, it was planned to have one thruster arm connected to each side of the frame. Overall, the design was discarded because it would require large amounts of aluminium profiles, which would also drastically increase the weight of the USV. This results in frame being more difficult to transport, both in terms of weight and size.

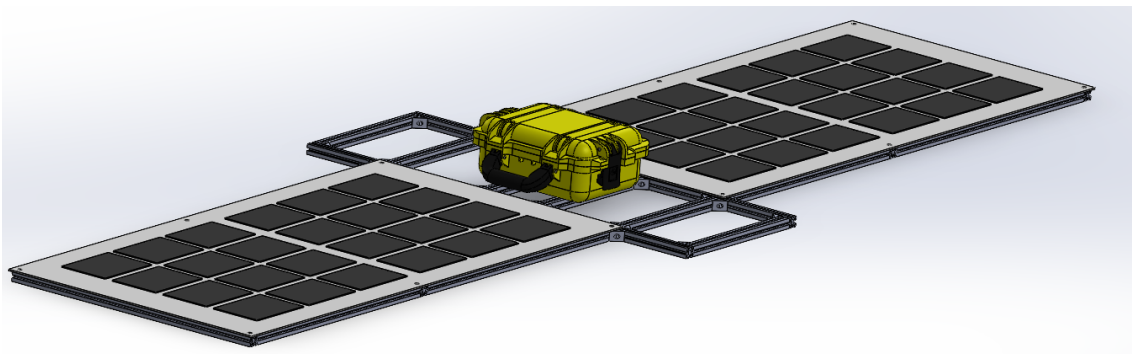


Figure 5.1: Frame with mounting for solar panels

Strapping the solar panels directly to the SUP board saves approximately 8m of aluminium profiles and decreases the weight by roughly 7kg. Newer designs would therefore be lighter and more practical to transport. The frame has undergone multiple adjustments in its design process afterwards.

Initially, the arms were designed to be in a V-shape, as it was initially assumed that the arm might not tolerate the thrust elseways. However, a finite element analysis, shown in a later section, proves that this assumption was wrong. In addition, the arms were rigid, which would likely create problems later on as the frame cannot lay flat on any surface. It was therefore decided that the frame should have foldable arms that can be raised on land and lowered during operation as mentioned in later sections.

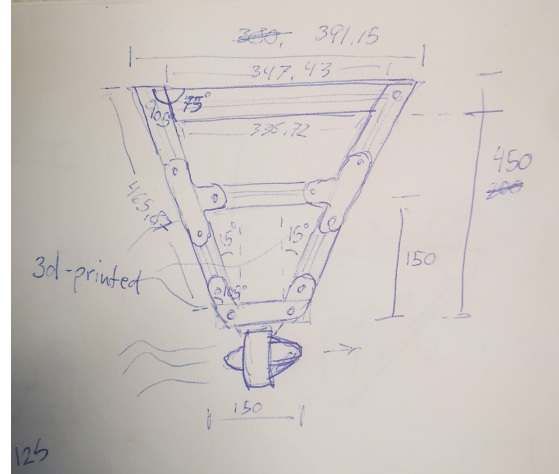


Figure 5.2: Initial design of V-shaped thruster arm

5.2 ROS and Websocket

The initial idea for the hardware- and software structure was to create a websocket on a Raspberry Pi Model 4b that would host a server that users could connect to. The server was planned to have a graphical user interface (GUI) that would allow control from the server, in addition to the ability to create waypoints, and watch the camera feedback and sensor data. To control the hardware and software, the use of the Robot Operating System (ROS) was considered. ROS is a meta-operating system that builds on top of Linux Ubuntu, with the goal of simplifying large processes with multiple sensors and actuators. The use of ROS eliminates the use of threading, as it allows for running multiples processes simultaneously. The benefit of running a server on a Raspberry Pi4, is that it would be a cheaper method than for the finalized product. In addition, it was planned that any host machine could connect to the server given correct authentication. The drawback is that creating this is not only time consuming, weakening the reproducibility, but also prone to more errors during creation. An illustration was created highlighting the hardware setup of this idea in Figure 5.3. The setup is detailed below.

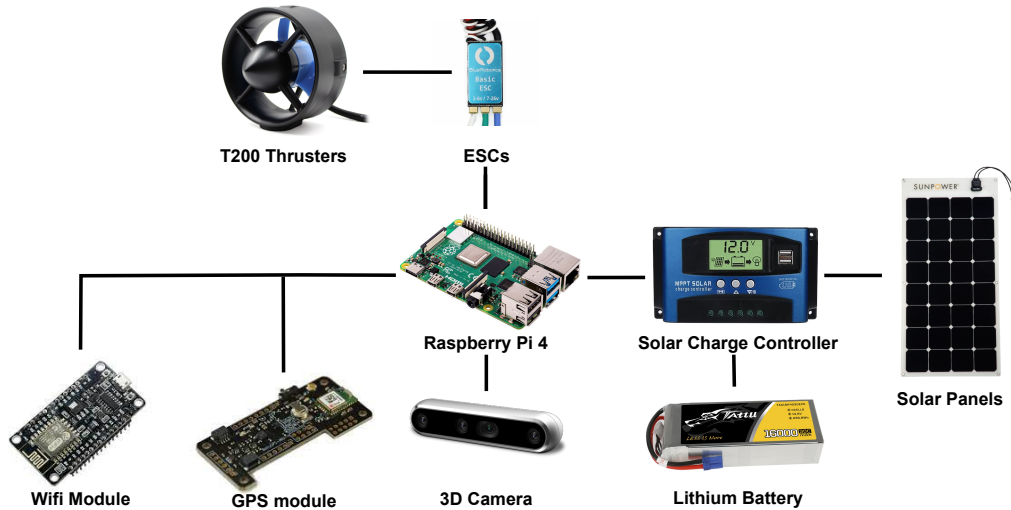


Figure 5.3: Initial Hardware Structure

In the above Figure, the entire system is connected to a solar charge controller, which in turn is connected to a 16 000mAh, 4 cell, lithium battery. The battery is charged by two 110W solar panels.

The hardware is controlled by a Raspberry Pi that is connected to an Intel Real Sense D435 3D camera. The camera is used for object detection, which allows the USV to detect and avoid obstacles in its path. To enable remote control of the USV, an ESP8266 WiFi module is included in the system. The module creates a server that users can connect to and control the USV, inspired by the idea presented in [12]. Positioning is determined using a BerryGPS module, which features GPS, accelerometer, gyroscope, compass, and barometer sensors. This allows the module to determine the USV's position, velocity, heading, and altitude. Finally, the Raspberry Pi is connected to BlueRobotics Electronic Speed Controllers (ESCs), which control two T200 thrusters.

Chapter 6

Methodology

This Chapter presents the methodology of the thesis in its current design. It details the design of the USV and explains the process from designing to building it. Kinematics and mechanics of the vessel are also presented. Then, the hardware and software structure is explained, before the setup of the probes is shown.

6.1 Design

This Section explains the mechanical decisions taken for the USV, including both the frame and hull. As previously mentioned, the USV was first designed in Solid-Works to give a better representation of potential advantages and downsides, before constructing the physical model. The construction of the physical model is described later, in Section 6.3.

6.1.1 Frame

Unlike the heavy and impractical prototype design, the new frame is designed to improve upon these weaknesses, thus being more cost-effective¹. Therefore, the solar panels should now only be strapped to the board with wires, instead of being mounted to the frame. The frame is also designed to be more modular, inspired by [23]. Originating from the initial design, it was found that the frame could be designed in such a way that it could be folded in to a case for transportation. This idea is made possible by dividing the frame in to three separate parts:

- Main frame
- Side frame
- Thruster arm

The main frame is the middle piece that both Peli cases are connected to. There are two side frames, one on each side of the main frame, connected to it with hinges. Lastly, one thruster arm is connected to each of the side frames. To

¹Figures of all individual components are to be found in the Appendix 10

achieve a modular design, the thruster arms are able to rotate around one point such that they can be lifted, as shown in Figure 6.1. In the figure, (1) represents the point where the arm is connected to the side frame with a 5mm bolt that is fastened to the threads of the side frame's aluminium profile. This is the point which the arm rotates around. (2) visualizes the point where the arm is secured to the side frame with a 5mm nut and bolt when the arm is lowered for operation. When the arm is to be lifted, the nut and bolt is removed, thus allowing the arm to be rotated up, as seen in Figure 6.2, before it is fastened at the bottom end of the thruster arm.

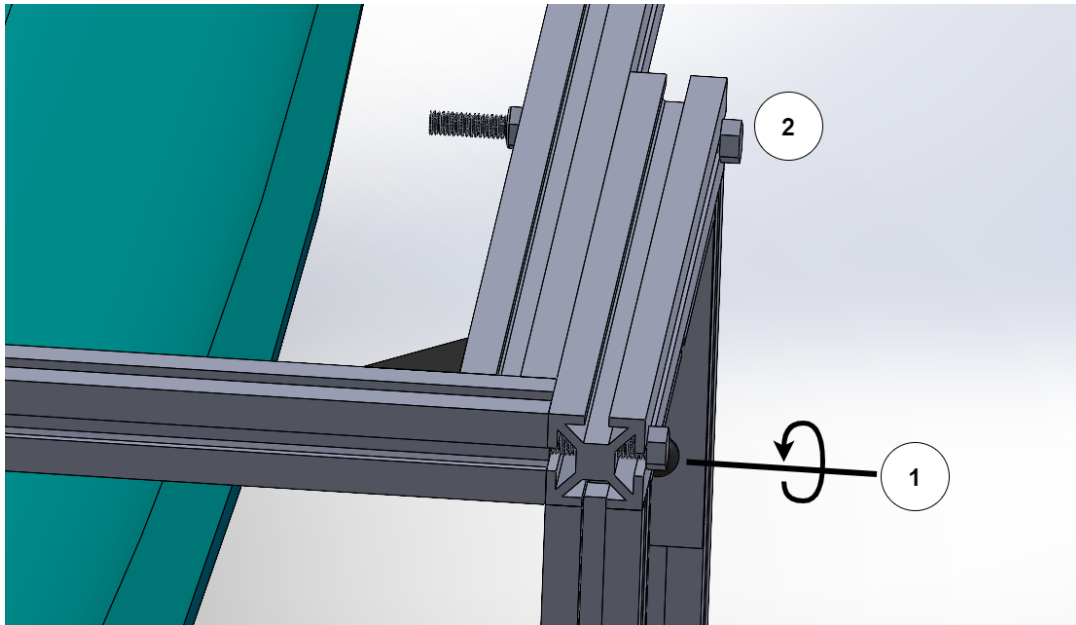


Figure 6.1: Securing the arm during operation

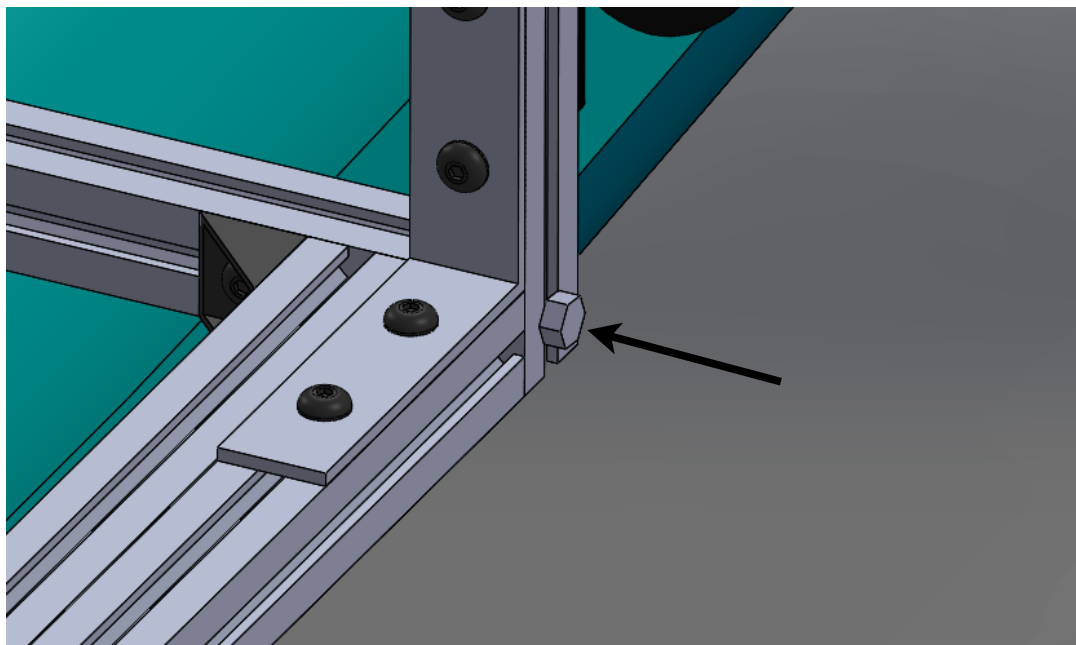


Figure 6.2: Securing the bolt at the end of the thruster arm

With the arms being able to rotate, the frame can be shaped into a case by also rotating the side frames. This entire idea is demonstrated in Figure 6.3. In the figure, the steps are as follows:

- (1) Either bolt is removed such that the thruster arms can be rotated up.
- (2) When the thruster arms are raised, the bolts are then fastened at the end of the thruster arm.
- (3) The side frames are raised such that the thruster arms connect at the top and form a case.

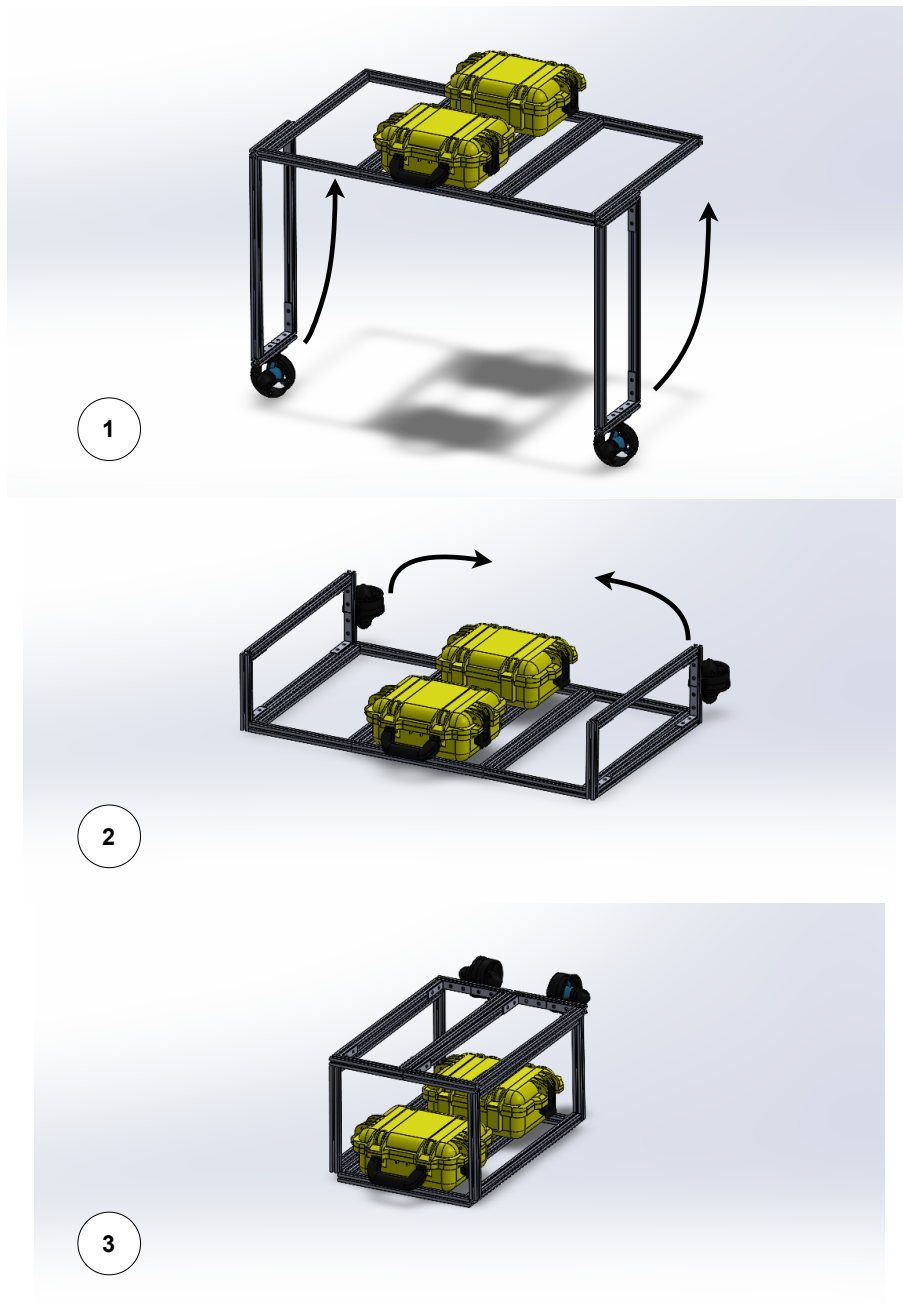


Figure 6.3: Folding process of the frame

The complete 3D model is presented in Figure 6.4. In SolidWorks, the SUP board was created with the same width, height, and length as the physical model. However, due to the lack of precise information about the board's actual shape, the model is not entirely accurate and is used primarily for visualization purposes.

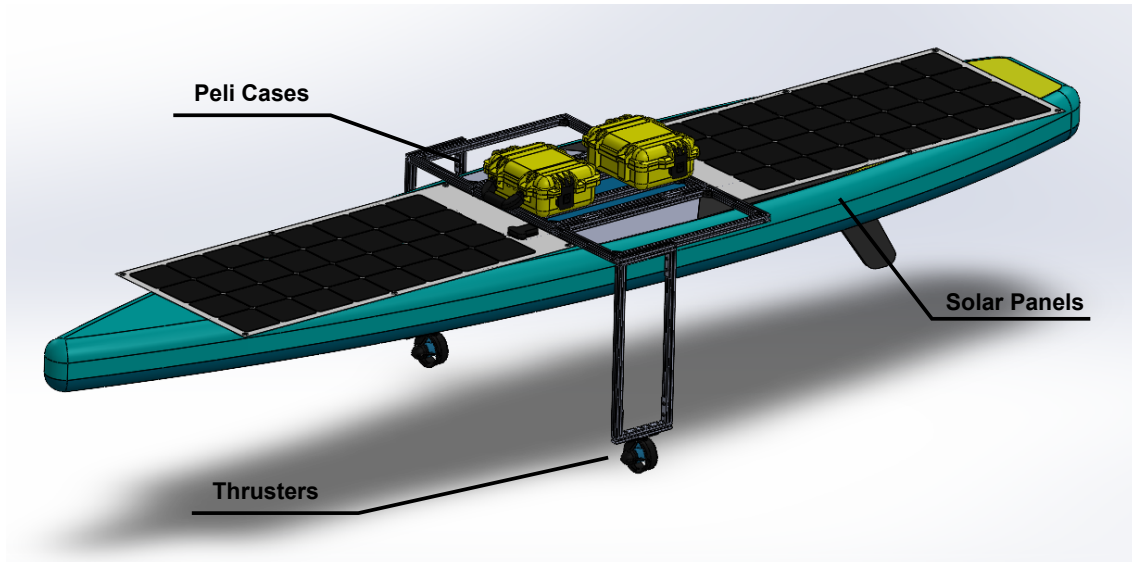
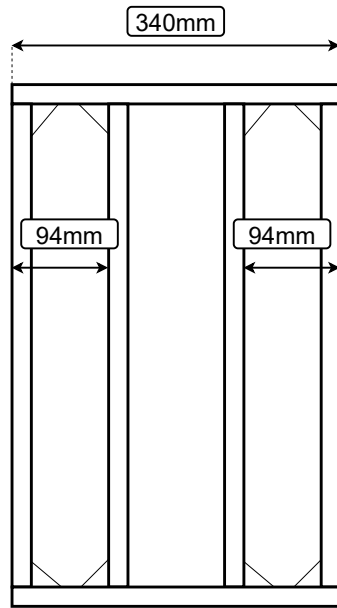


Figure 6.4: Complete USV model

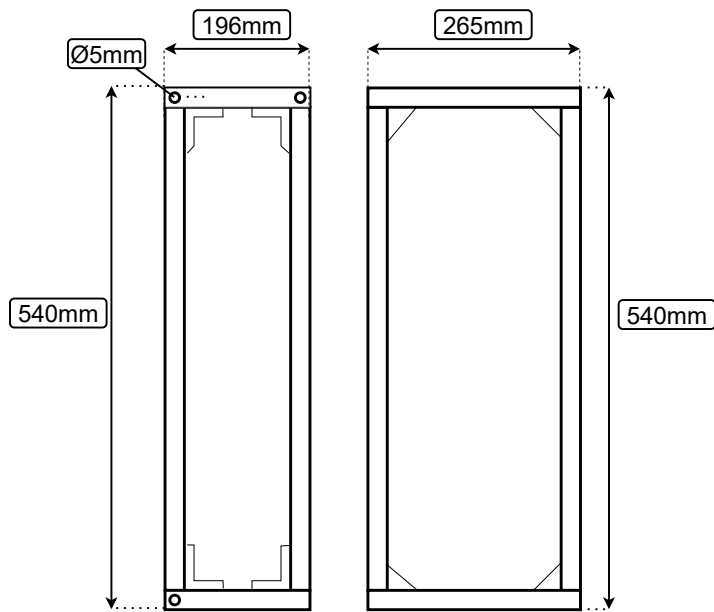
As opposed to the prototype, the aluminium profiles are now kept uncut in length, and remain at 500mm, which is the length at which they are produced, meaning that less time is used on cutting parts of the frame.

Lastly, technical drawings of the parts were created with the measurements used in Solidworks. These drawings are the ones that the physical model is to be based on, and are illustrated in the Figures below.



Main Frame

Figure 6.5: Technical drawing of the main frame



Thruster Arm

Side Frame

Figure 6.6: Technical drawing of the thruster arm and side frame

6.1.2 Handles

As the side frames are connected to the main frame with hinges, the folded frame might not be rigid enough for transportation. To solve for this, handles are created that are mounted on top of each thruster arm as to lock them in place and simplify transportation.

The handles are created with the goal of mounting them without bolts. Therefore, a bracket is first designed, as depicted in Figure 6.7, which is then mounted to the thruster arm. The bracket is to be mounted to the arm with the same 5mm bolts that come included in the ratrig package. A handle is designed which is slid onto the bracket and locks in place at the end. In addition, the handle has a cut out and an extruded part, which means that two handles may be connected together.

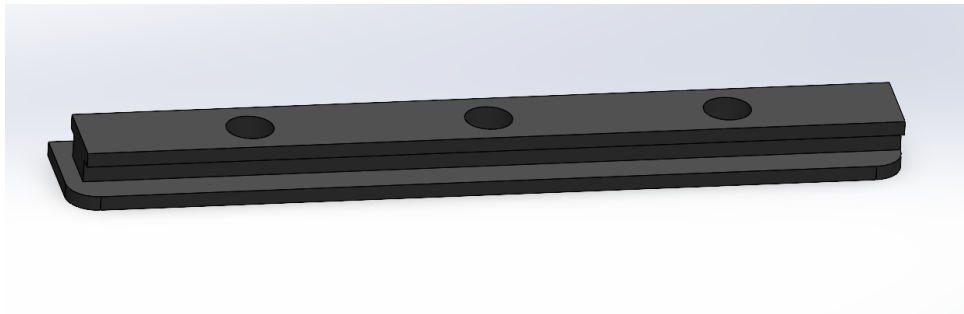


Figure 6.7: Bracket for the handle

The complete idea of the handles locking in place is shown in Figure 6.8. The process is as follows:

- (1) One bracket is mounted on each of the thruster arms with 5mm bolts and ratrig washers.
- (2) The first handle is slid all the way on top of one of the brackets, as seen in (3).
- (4) The second handle is slid on top of the other bracket.
- (5) The brackets now lock the thruster arms such that they are connected, and the side frames cannot be lowered. (i.e. the brackets lock movement in the x-axis)

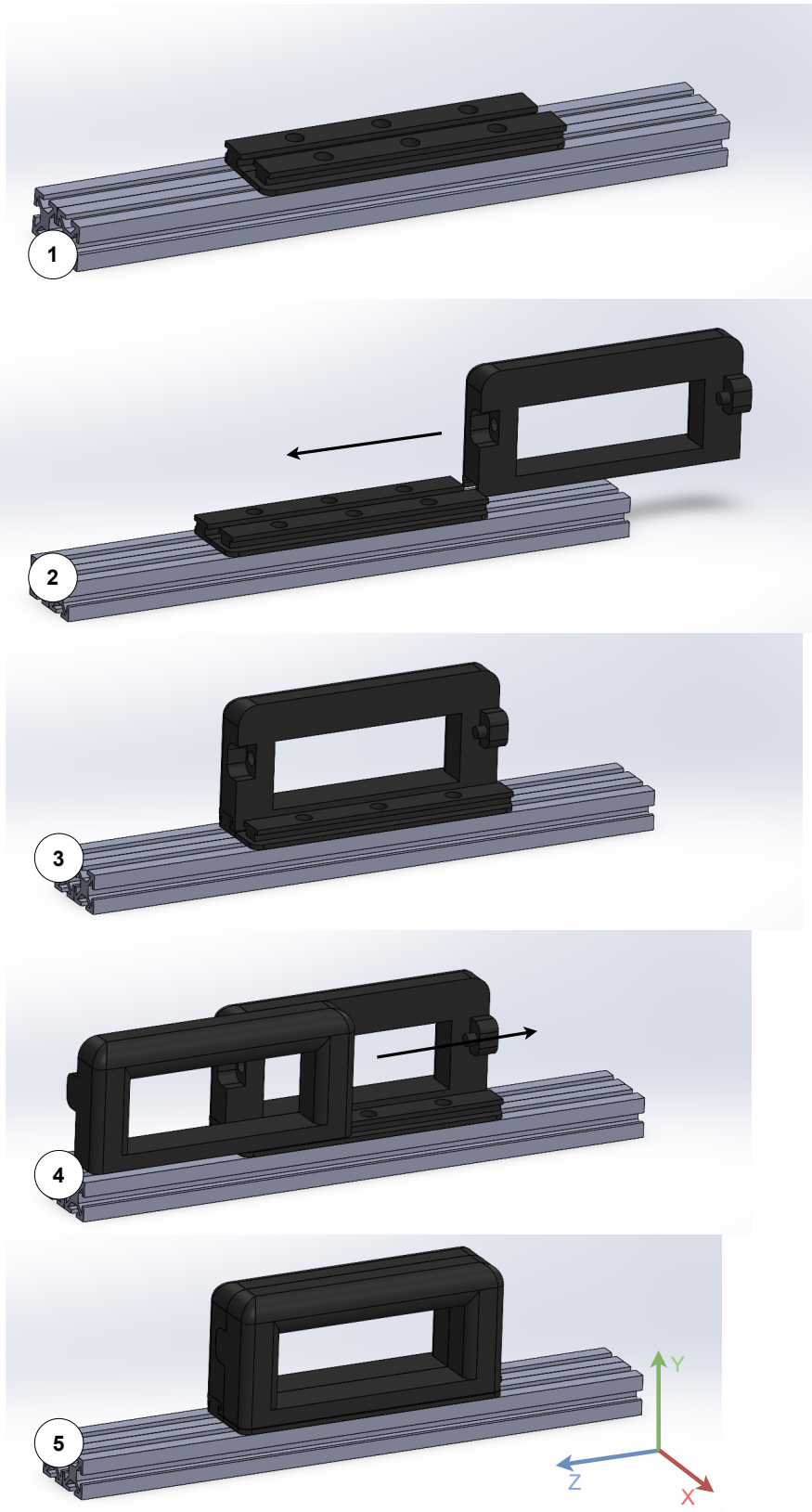


Figure 6.8: Handles that lock the frame in place

6.2 Mechanics

The mechanical performance and motions of the USV are covered in the following Sections. The kinematics of the USV are first defined, including the derivation of its forward and rotational motion equations. Next, a FEM analysis of the thruster arms is presented to evaluate their structural integrity.

6.2.1 Kinematics

The kinematics of the USV describe its forward and rotational motion. The forward motion of the USV is defined as the speed of the USV, also known as linear velocity, while the rotational motion is defined as the rate of rotation of the USV about its axes.

In order to derive the relevant equations of motion, two coordinate systems are defined: the North-East-Down (NED) coordinate system and the Body-Fixed reference frame. The NED coordinate system defines the vessel's position relative to the Earth's surface, and is denoted as:

$$n = (x_n, y_n, z_n) \quad (6.1)$$

where the

- x_n -axis points towards true North
- y_n -axis points towards East
- z_n -axis points downwards, normal to the Earth's surface

The Body-Fixed reference frame, on the other hand, describes the vessel's motion relative to its own orientation. With the origin o_b , the Body-Fixed frame is denoted:

$$b = (x_b, y_b, z_b) \quad (6.2)$$

where the axes are defined as

- x_b - longitudinal axis
- y_b - transversal axis
- z_b - normal axis

This coordinate system is illustrated in Figure 6.9, using a right-hand reference [21].

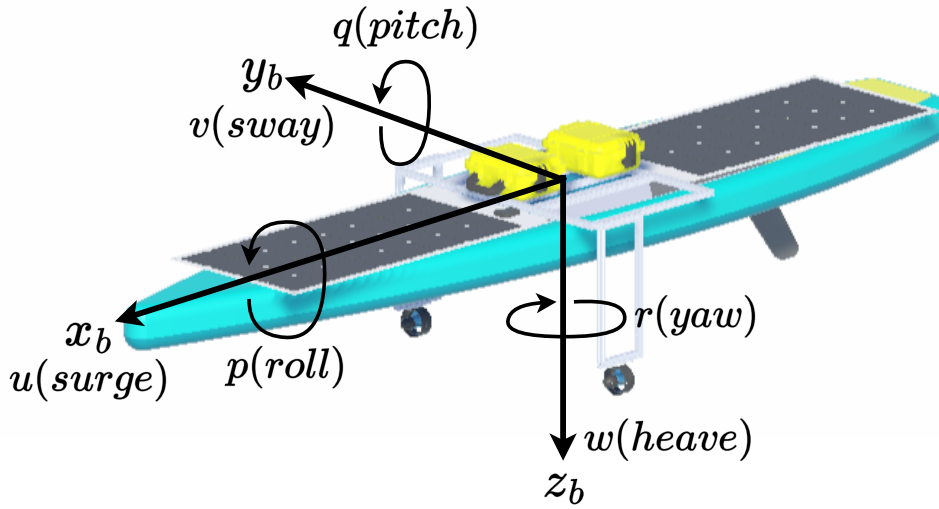


Figure 6.9: Body-fixed vehicle coordinate system of the USV

In the figure, the linear velocities along the x-, y-, and z-axis are respectively noted as u , v , and w . The rotational velocities around the same axes are p , q , and r . The forces along the respective directions are X , Y , Z , K , M , and N . All mentioned directions are known as degrees of freedom (DoF) meaning that there are six DoF, which applies to all marine vessels [21]. These DoF motions are summarized in the following Table.

Table 6.1: USV coordinate system [21]

| Degrees of freedom (DoF) | Forces and moments | Linear and angular velocities |
|--|--------------------|-------------------------------|
| 1. Motions in the x_b -direction (surge) | X | u |
| 2. Motions in the y_b -direction (sway) | Y | v |
| 3. Motions in the z_b -direction (heave) | Z | w |
| 4. Motions in the x_b -axis (roll) | K | p |
| 5. Motions in the y_b -axis (pitch) | M | q |
| 6. Motions in the z_b -axis (yaw) | N | r |

To create a linearized model of vessel motion, the six forces and moments can be broken down into components along the six directions, and create the following six equations.

$$X_1 = X_u u + X_v v + X_w w + X_p p + X_q q + X_r r + X_{\dot{u}} \dot{u} + X_{\dot{v}} \dot{v} + X_{\dot{w}} \dot{w} + X_{\dot{p}} \dot{p} + X_{\dot{q}} \dot{q} + X_{\dot{r}} \dot{r} \quad (6.3)$$

⋮

$$N_1 = N_u u + N_v v + N_w w + N_p p + N_q q + N_r r + N_{\dot{u}} \dot{u} + N_{\dot{v}} \dot{v} + N_{\dot{w}} \dot{w} + N_{\dot{p}} \dot{p} + N_{\dot{q}} \dot{q} + N_{\dot{r}} \dot{r} \quad (6.4)$$

where X_u, \dots, N_r are the linear damping coefficients and $X_{\dot{u}}, \dots, N_{\dot{r}}$ represent hydrodynamic added mass.

This model can be simplified by reducing the DoF from six to three, thus creating a horizontal-plane model. Such a model only considers surge, sway and

yaw (u , v , and r), meaning that the entire vessel may be defined in a two-dimensional coordinate system. Reducing the model to three DoF leaves the following three equations.

$$X_1 = X_u u + X_v v + X_r r + X_{\dot{u}} \dot{u} + X_{\dot{v}} \dot{v} + X_{\dot{r}} \dot{r} \quad (6.5)$$

$$Y_1 = Y_u u + Y_v v + Y_r r + Y_{\dot{u}} \dot{u} + Y_{\dot{v}} \dot{v} + Y_{\dot{r}} \dot{r} \quad (6.6)$$

$$N_1 = N_u u + N_v v + N_r r + N_{\dot{u}} \dot{u} + N_{\dot{v}} \dot{v} + N_{\dot{r}} \dot{r} \quad (6.7)$$

The equations of motion for the model can further be expressed in matrix form [21]:

$$\dot{\boldsymbol{\eta}} = \mathbf{R}(\psi) \mathbf{v} \quad (6.8)$$

The position and heading vector, $\boldsymbol{\eta}$, is equal to:

$$\boldsymbol{\eta} = [x, y, \psi]^T \quad (6.9)$$

The velocity vector, \mathbf{v} , is equal to:

$$\mathbf{v} = [u, v, r]^T \quad (6.10)$$

Lastly, the rotation matrix, $\mathbf{R}(\psi)$, transforms the velocity vector from the Body-Fixed frame to the NED frame and is expressed as [21]:

$$\mathbf{R}(\psi) = \begin{bmatrix} \cos(\psi) & -\sin(\psi) & 0 \\ \sin(\psi) & \cos(\psi) & 0 \\ 0 & 0 & 1 \end{bmatrix} \quad (6.11)$$

6.2.2 Finite Element Method

To verify the solidity of the thruster arm, finite element method (FEM) was performed in Solidworks Simulation. For a lower computation time and higher simplicity, a new thruster model, with the same measurements, is created. The simpler model replaces the actual T200 thruster model for simulation purposes, and is presented in Figure 6.10. In addition, screws are not included in this model. Next, materials are chosen for each part.

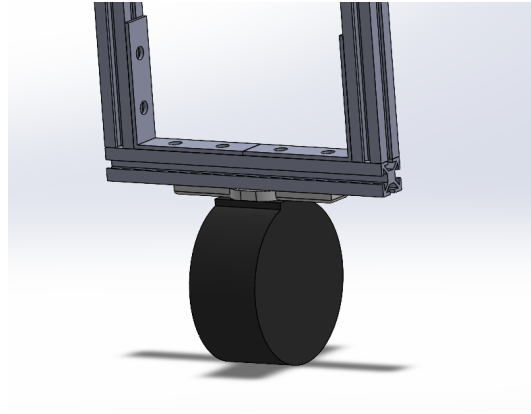


Figure 6.10: Simplified model of the thruster arm

The thruster arm is made of the following parts that each need to have a material assigned:

- T200 thruster (Simplified)
- thruster bracket
- ratrig aluminium profiles
- angle brackets

While the vendors of the ratrig and angle brackets have not specified their specific material, common materials for these parts are 6063-T5 aluminium and AISI 304 steel, respectively. The T200 thrusters are mounted to a 3D printed PLA bracket. However, since PLA is not available, a material of similar quality, PET, is considered. Lastly, the T200 thruster is largely made of polycarbonate plastic [41].

Finally, the model needs a force exerted on the thruster and a fixture on the thruster arm. The fixture is placed inside the holes where the bolts are, as that is where the arm is fixed to the side frame. As verification, the force added in the simulation is the full thrust of the T200 thrusters at the nominal voltage of 16V. According to Blue Robotics' technical information on the T200 thrusters, the full throttle thrust at 16V is estimated as 5.25kgf [41], which is equivalent to 51.48N.

The result of the FEM, presented in Figures 6.11 and 6.12, shows that the arm hardly experiences any stress and remains below the upper yield strength, which suggests that the design is suited for use on the physical USV.

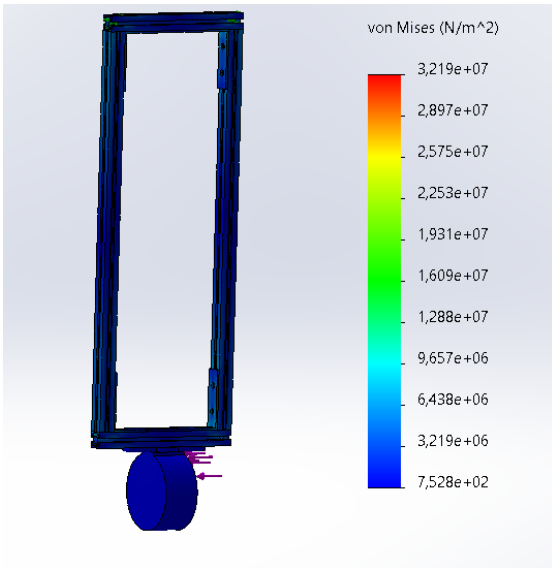


Figure 6.11: Force exerted on the thruster and Von Mises

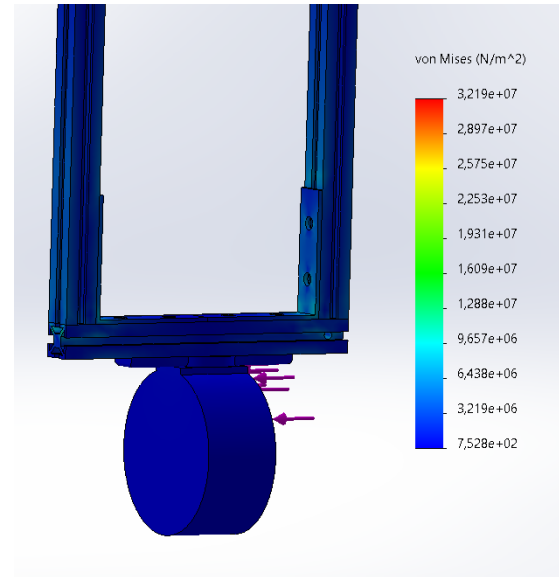


Figure 6.12: Force exerted on the thruster and Von Mises

6.3 Constructing the Physical Frame

The frame is assembled in accordance with the technical drawings shown previously, in Figures 6.5 and 6.6. First, the main frame and side frames are assembled, and later cut to the correct dimensions, as seen below. Two hinges are then fastened to each of the side frames, connecting them to the main frame.



Figure 6.13: Assembling the main- and side frames



Figure 6.14: Assembled frames with hinges

The thruster arms are assembled similar to the rest. Holes are cut into the arms, as shown in the technical drawings, which are then used to mount them to the frame with 5mm nuts and bolts. To strengthen the arms, they are constructed with 75mmx20mm angle brackets, instead of the brackets that come with the ratrig package.

As, the aluminium profiles have screw threads on each end, the screws are

fastened at the bottom end of the thruster arms, connecting them to the side frames.

Both the angle brackets and hinges are constructed from galvanized steel, which can rust quickly when exposed to salt water. However, during the prototyping phase, it was decided to use these parts as they are more affordable and widely available, which was deemed as a reasonable trade-off.

The completed frame, in both folded and unfolded position, is shown below. The Peli cases are then kept in place by the use of reclosable fastening strips which are taped to the two middle beams of the main frame. The complete frame is then strapped to the hull.

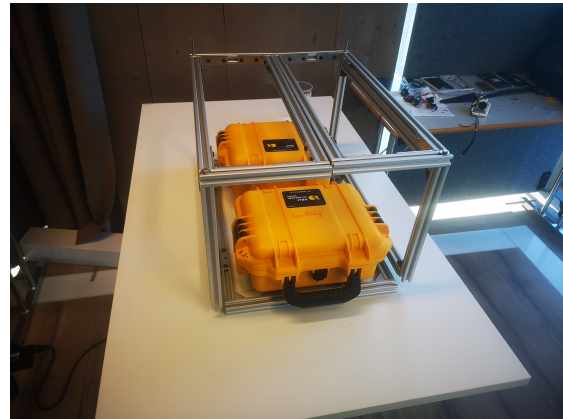


Figure 6.15: Completed, unfolded frame

Figure 6.16: Completed, folded frame

Lastly, the handles and handle brackets are 3D-printed with two top- and bottom-layers, supports enabled, and an infill of 20%. In practice, the brackets are then mounted centered on the thruster arms, and the handles are slid in place as initially depicted in Figure 6.8. The mounting of the physical handles is shown in Figure 6.17



Figure 6.17: Fastening mechanism of the handles

6.4 Hardware

This Section explains how the hardware for the USV is connected. This is done in several steps. As visualized in (1) in Figure 6.18, the 16V 4-cell lithium battery is first connected to the center of the solar charge controller. The setting of the controller must be set to B01 (Lithium battery), and can be found by shuffling through the menu with the left button. This ensures that the battery is properly regulated and charged by the solar panels. Next, the two solar panels are connected to the solar charge controller using MC4 plugs, which come with the panels.

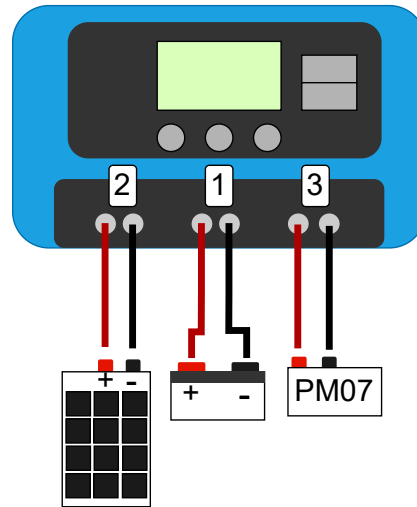


Figure 6.18: Setup for the solar charge controller

To extend the cables of these panels, additional MC4 plugs and solar cables were purchased so that the cables could stay connected to the solar charge controller and be disconnected at the solar panels instead. After connecting the solar panels, the PM07 power distribution board is connected to the solar charge controller, as shown in (3). Since the solar charge controller can handle an input voltage of 46V, the solar panels are connected in series.

Next, the Pixhawk 4 is connected to the power distribution board using the PWR1/PWR2, I/O-PWM-in, and FMU-PWM-in ports. The PWR-ports ensure that the Pixhawk receives power from the board, while the I/O- and FMU-ports receive PWM signals for the ESCs and servos respectively. The GPS module is then connected to the GPS-port on the Pixhawk.

The signal wires of the ESCs (white) are connected to the M1- and M3-ports of the power distribution board, and the GND wires (black) to the 8-pin rail of the board. The usage of these ports requires the soldering of pins on the specific ports being used. Finally, the ESC power- and ground-cables are connected to their respective ports on the board. This ensures that the ESCs receive proper power and can be controlled by the Pixhawk.

Lastly, the Herelink Air Unit is connected to the B+ ground- and power-ports. This ensures that the Herelink Air Unit receives proper power and can communicate with the other hardware on the USV.

An overall objective of the hardware is to incorporate connectors wherever feasible, avoiding the need for gluing or permanent fixings of components. All components soldered to the board are using XT60 and XT30 connectors with the goal to make upgrading and replacing future components less time consuming.

A simplified illustration of the power distribution board setup is depicted in Figure 6.19.

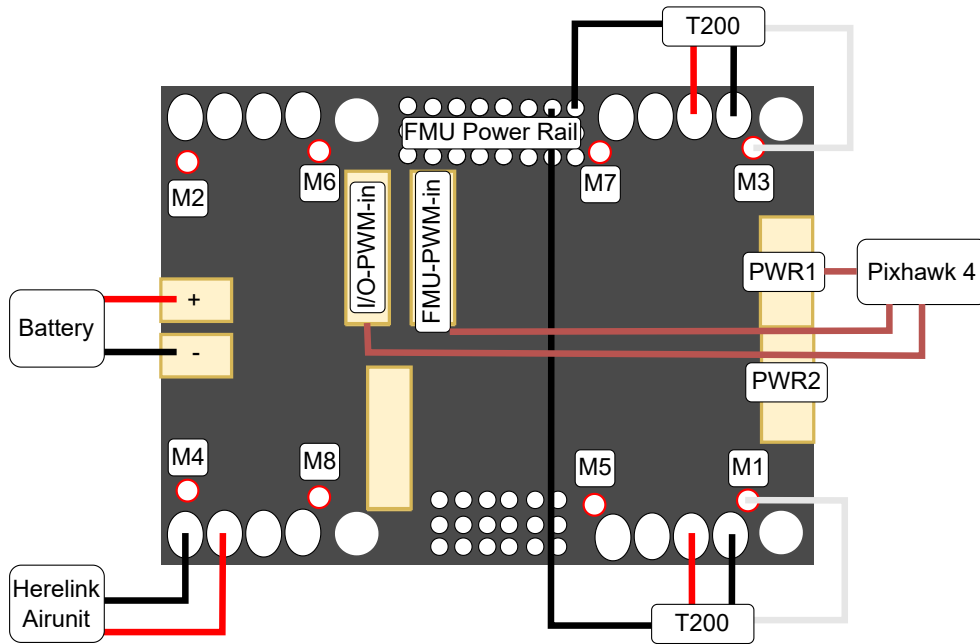


Figure 6.19: Power module connections

The hardware is then distributed in the two Peli cases. The battery and solar charge controller is kept in place in the back case by the use of reclosable fastening strips. The power distribution board, Pixhawk 4, GPS module, and Herelink Airunit is placed in the front case. To keep a good structure inside the case, a small mounting is designed to keep all components in place, before 3D-printing it. First, the components are organized inside the cases. They are then measured and 3D modeled. All components are then fastened with fastening strips. The Herelink antennas are mounted on top of the front case with double sided tape.

All cables exiting either case are tightened and made waterproof by using water- and dust-proof cable glands. There are in total nine cables that exit either case. All these cables have a diameter between 3mm and 8mm. Therefore, ten cable glands that cover this range are purchased. These are first glued to the Peli cases with two-component epoxy adhesive to lock them in place, and are later secured with a glue gun to further waterproof the connections.

Lastly, mountings for the T200 thrusters are 3D-printed as shown in the Figure below. The thrusters are first fastened to the mountings with the 5mm bolts included in the ratrig package. The thrusters and mountings are the mounted centered on either thruster arm. The thruster cables are led along the aluminium frame and can be squeezed inside the profiles, as shown in Figure 6.21. One problem that was found during this project is that the cables are too short for this particular frame, and had to be extended by soldering additional 400mm of high temperature silicone wires (16AWG) between the thrusters and ESCs.

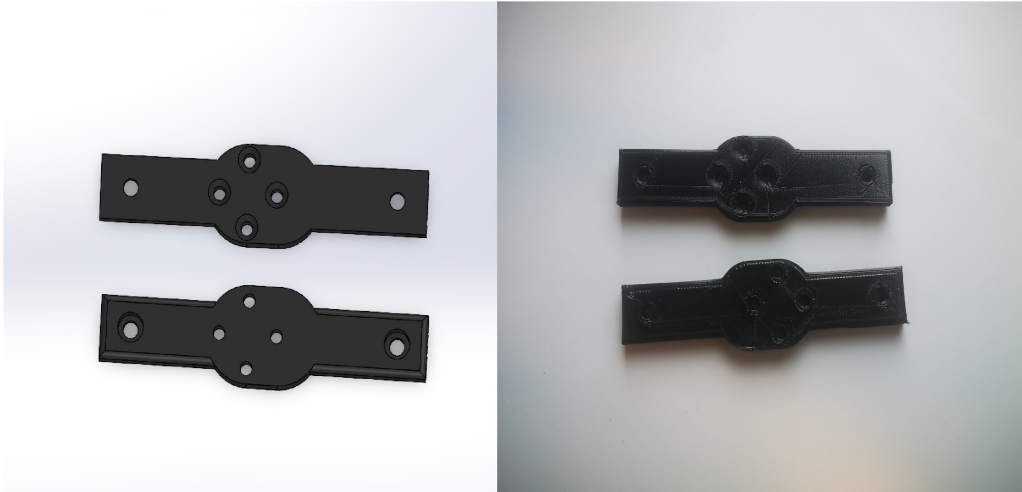


Figure 6.20: Thruster profiles 3D-modelled (left) and 3D-printed (right)



Figure 6.21: Fastening of thruster and cables

6.4.1 Thruster Model

The Blue Robotics T200 thruster is a three-phase brushless outrunner motor with a fully-flooded design for underwater use. The thruster is optimized to run at 16 V and has a full throttle current of 24A (390W) at this voltage.

The thruster's physical dimensions are depicted below, and are 113mm in length and 100mm in diameter, with a propeller diameter of 76mm. It weighs 344g in air and 156g in water, and its wetted materials include polycarbonate, epoxy, stainless steel, plastic, and polyurethane.

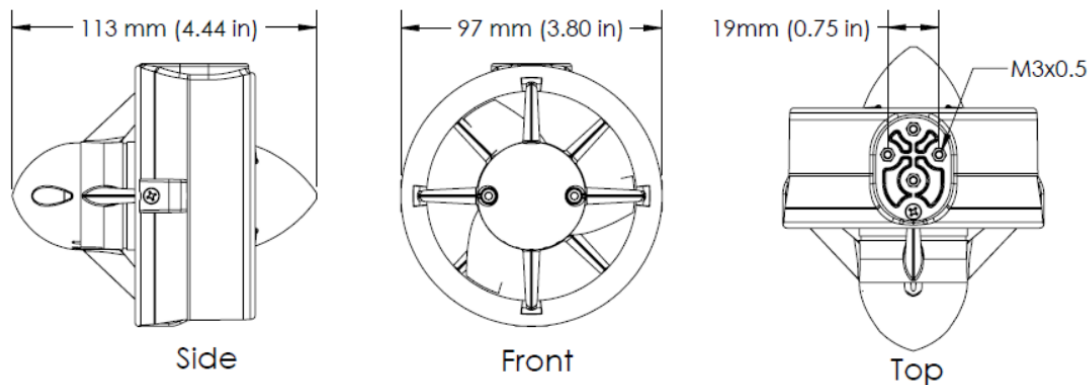


Figure 6.22: 2D drawings of the T200 thrusters

The thruster requires a sensorless brushless electronic speed controller (ESC) to run. It is recommended to operate the thruster at 12-16 V for the best balance of thrust and efficiency, although operation at up to 20 V is allowable.

In this specific project, the thrusters are operated at 16V with the Blue Robotics Basic ESC. At the nominal voltage of 16V, the thrust, current draw, and efficiency are respectively presented in Figures 6.23 - 6.25 [41].

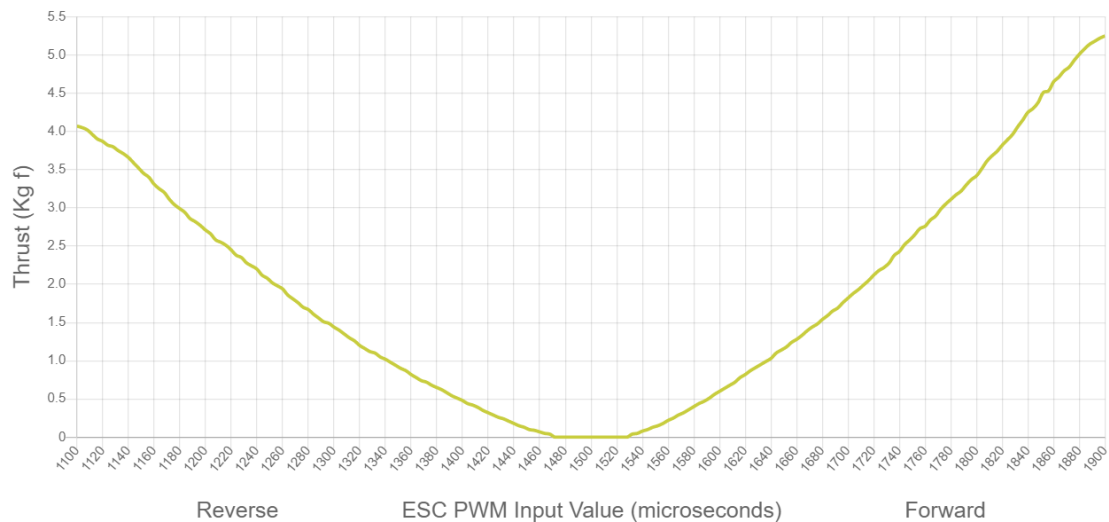


Figure 6.23: Thrust at 16V [41]

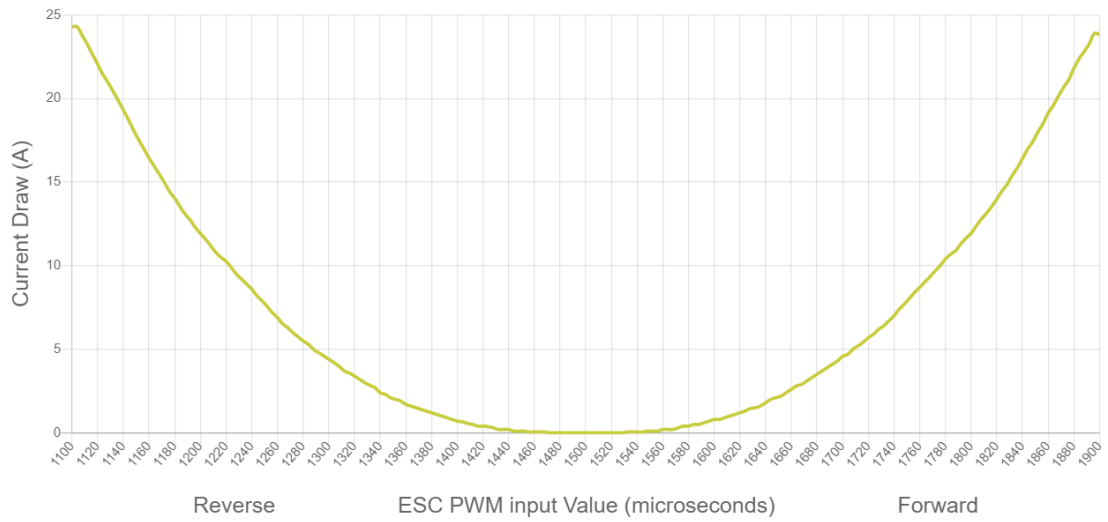


Figure 6.24: Current Draw at 16V [41]

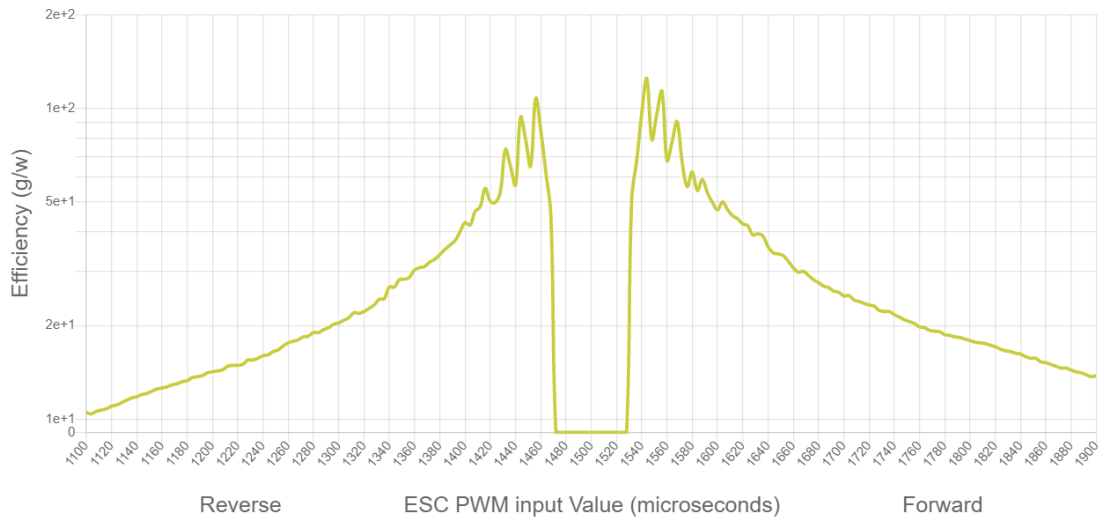


Figure 6.25: Efficiency at 16V [41]

6.5 Software and Control

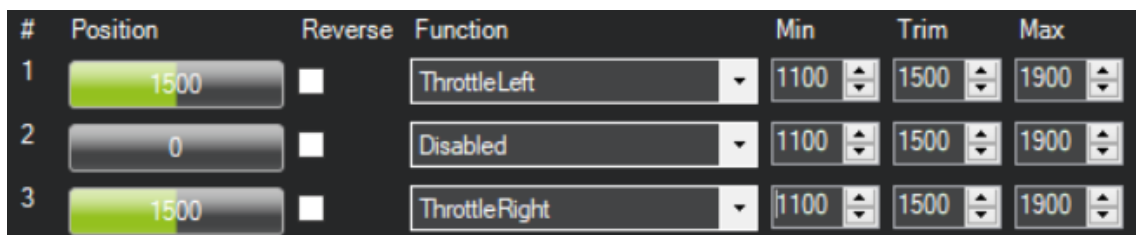
The following software Section describes the development and implementation of the software component for the USV. This includes the use of ArduPilot for autonomous navigation, as well as the principles of path following and the control strategy of ArduPilot.

6.5.1 Autopilot Setup

The ArduPilot is set up by first connecting the Pixhawk 4 to the computer via USB and opening Mission Planner. The connection and data rate is then configured using the drop-down boxes in the upper-right portion of the screen. Specifically, the COM port is set to **COM4**, and the data rate is automatically assigned. Once the connection is established by clicking on **Connect**, the Pixhawk 4 is calibrated using the setup tab.

The following pages are required to run ArduPilot: **Frame Type, Acceleration Calibration, Compass, Radio Calibration, Servo Output, Flight Modes, Fail-Safe, HW ID, and ADSB**. For this project, **ESC calibration** is not needed. In the case of boats, the **Frame Type** is set to **2**, which equals ArduRover, a particular version of ArduPilot for ground vehicles and boats.

The thruster control is defined in **Servo Output**. **Throttle Left** is set as **1**, and **Throttle Right** is set as **3**. The minimum value for both thrusters is set to 1100, and the maximum to 1900, in accordance with the Blue Robotics T200 documentation. The Trim was set to 1500. These particular settings are demonstrated in Figure 6.26



| # | Position | Reverse | Function | Min | Trim | Max |
|---|----------|--------------------------|---------------|------|------|------|
| 1 | 1500 | <input type="checkbox"/> | ThrottleLeft | 1100 | 1500 | 1900 |
| 2 | 0 | <input type="checkbox"/> | Disabled | 1100 | 1500 | 1900 |
| 3 | 1500 | <input type="checkbox"/> | ThrottleRight | 1100 | 1500 | 1900 |

Figure 6.26: Servo output

With the GPS connected to the Pixhawk, it automatically receives a fix with the TTFF depending on the start. After a cold start, the TTFF can take up to 10 minutes. A warm start requires less time, and the GPS often receives a fix after a minute. Thereafter, the Herelink Transmission System is connected to the Pixhawk.

Before being able to arm the USV, several safety parameters must be turned off. As the vessel does not contain a physical safety switch, the parameter **BRD_SAFETYENABLE** must be set to **0**. Then, the remaining safety options that are kept on are **Barometer, Compass, GPS lock, RC Channels, Battery Level,**

and **GPS Configuration**. This means that if one or multiple of these parameters are not cleared, the vehicle may not be armed².

To test the thrusters, they were armed by holding the right stick to the right, after which the left stick controlled straight movement, while the right stick controlled turns. The thruster responses during movement options are illustrated in Figure 6.27.

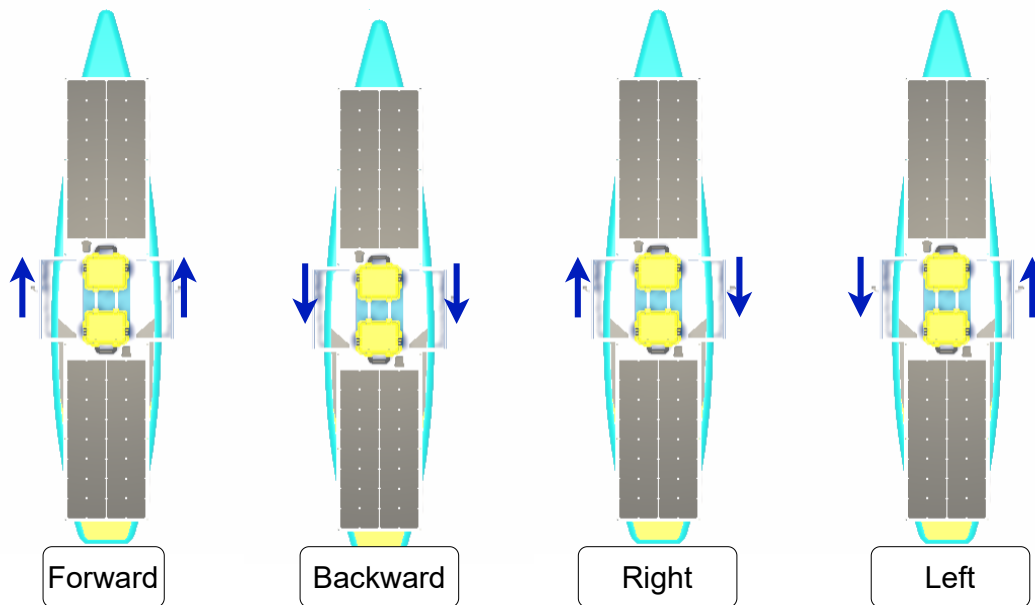


Figure 6.27: Thruster responses during movement options

From the graphs depicted in Section 6.4.1, it is apparent that the thrust and current draw drastically increase as the PWM value is increased. In addition, the efficiency of the thrusters is highest at low PWM values. Under **Basic Tuning** in Mission Planner, the throttle of the thrusters is therefore initially set to 30%, or 1380/1620rpm while moving backwards/forwards, and with **Cruise Speed** equalling 1m/s, with the goal of keeping a high efficiency and low current draw, while operating at a sufficient speed.

The PID (Proportional-Integral-Derivative) values for the steering rate and throttle of the vessel were kept unchanged and are thus:

- P = 0.200
- I = 0.200
- D = 0.000

²The complete parameter list is to be found on the Github repository.

6.5.2 Navigation and Control Algorithm

The navigation algorithm used by the USV is the L1 controller which is based on this paper [38].

The paper describes a guidance logic that uses a reference point on the desired path, a distance L_1 forward of the vehicle, to generate a lateral acceleration command. The lateral acceleration command is determined by:

$$a_{s_{cmd}} = 2 \frac{v^2}{L_1} \sin(\eta) \quad (6.12)$$

where:

- v = vehicle velocity
- η = Angle created from V to the line L_1
- R = radius of the circle the vehicle must follow to reach the reference point

The guidance logic is visualized in Figure 6.28. The direction of the acceleration depends on the sign of the angle between the L_1 line segment and the vehicle velocity vector. In the context of this figure, the selected reference point is to the right of the vehicle velocity vector, prompting the vessel to accelerate to the right.

A circular path can be defined at any given moment by the position of the reference point, the vehicle's current position, and the tangential direction of the vehicle's velocity vector, as represented by the dotted line in Figure 6.28.

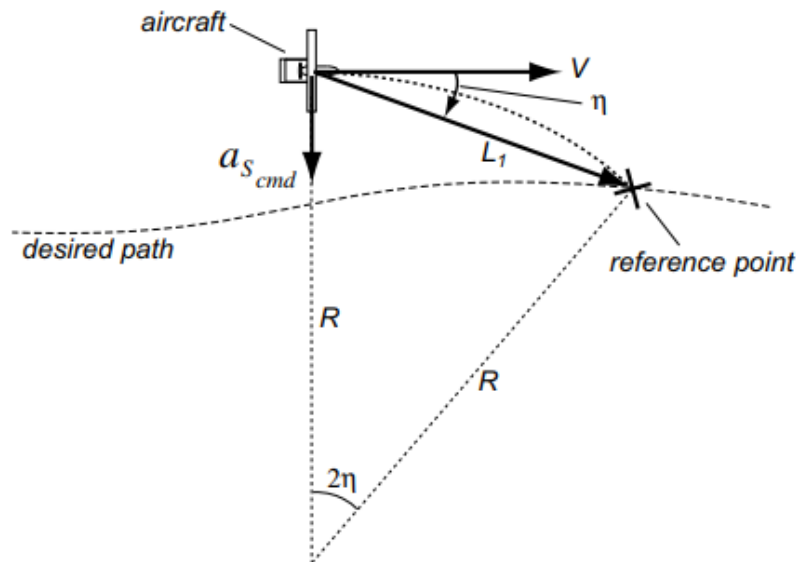


Figure 6.28: Diagram for Guidance Logic [38]

In addition, the guidance logic tends to rotate the vehicle so that its velocity direction approaches the desired path at a large angle when it is far away from the desired path, and at a small angle when it is close to the desired path, thus

resulting in a smooth convergence to the reference point [38].

As previously mentioned, the L1 controller that ArduRover uses is based on the mathematics explained above. The distance L1 is defined along a line between the original position and the destination, which is measured starting from the point closest to the vehicle along the target path and a distance defined as:

$$L_1 = 0.3\zeta T v \quad (6.13)$$

where

- ζ = damping
- T = period
- v = velocity

Damping and period are user-set parameters, while the velocity is measured on site.

The desired lateral acceleration, a_d , is then calculated as:

$$a_d = \frac{4\zeta^2 v^2 \sin(Nu_1 + Nu_2)}{L_1} \quad (6.14)$$

where Nu_1 is the angle between the intended vehicle track and the line drawn from the vehicle to the point a distance L1 ahead of the vehicle's along-track point, while Nu_2 is the angle between the vehicle's velocity and its intended path. A PID controller is then used to calculate the desired steering output, resulting in the desired lateral acceleration which brings the vehicle back to the line between the origin and destination.

6.6 Probe Setup

The probes are kept in the same case as the solar charge controller and battery, but form a separate system from the USV. This means that the probes are instead controlled by a Raspberry Pi while being powered by the solar charge controller. The probes used in this project are, as previously mentioned, Atlas Scientific's pH probe, temperature probe, DO probe, and conductivity probe. To simplify the hardware setup needed, two Whitebox T3 MkII for the Raspberry Pi are used, along with a Raspberry Pi 4 Model B. The Whitebox is a stackable add-on board allowing for the use of three sensors for one board. The EZO circuits and probes are connected to the two Whitebox boards, which are then stacked on top of the Raspberry Pi.

The setup and calculation of the probes is done in accordance with the official documentation of these parts, provided by Atlas Scientific.

6.6.1 Taking Continuous Measurements

For a simple prototype, the idea is for the probes to start measuring and writing the measured values to a CSV (comma-separated values) file in addition to the time and date when the system is powered on. Once the USV is done operating, the Raspberry Pi can then be connected to a PC allowing the data to be extracted.

The available console provides several functions one can make use of, but for such a prototype, these functions are not necessary. Therefore, the available script for the console, **ic2.py**, is copied and adjusted. In the new script, **ic2_continuous.py**, much of the original code stays the same, but some simplifications and adjustments are made. Firstly, to keep a good structure, every time the script is run, it will create a new file named after the current timestamp, which, for simplification, is referred to as "**filename**".

```
filename = "logged_data_" + datetime.datetime.now().strftime("%d-%m-%Y  
↪ %H:%M:%S") + ".csv"
```

Then, the while loop is primarily adjusted to automatically take measurements every 30 seconds. Inside the loop, the script iterates over each device in the **device_list** obtained from the **get_devices()** function. For each device, it sends the command R using the **write()** method from the **AtlasI2C** library, instructing each of the devices to take a single reading.

```
while True:  
  
    for dev in device_list:  
        dev.write("R")
```

Thereafter, the script pauses for 1.5 seconds, which is the timeout needed to query readings and calibrations, allowing the EZO devices in the **device_list** to complete the process of taking readings. The script then iterates through all the devices while opening "**filename**" in append mode.

```
time.sleep(1.5)  
for dev in device_list:  
    with open("path/to/file" + filename, "a") as file:  
        try:
```

Finally, the script gets the current timestamp, **timestamp** and appends it to "**filename**" alongside the sensor reading, **sensor_data**. For bug testing, this information is also printed to the console. The script then delays for 30 seconds before taking new measurements.

```
try:  
  
    #get and print current timestamp  
    timestamp = datetime.datetime.now().strftime("%d -%m-%Y %H:%M:%S")
```

```

print(str(timestamp))

#print sensor data
print(dev.read())

#get sensor data
sensor_data = dev.query("R")
# write data and timestamp to the file
file.write(timestamp + " " + str(sensor_data) + "\n")

except IOError:
    print("Query failed ...")

```

An example of the output from the terminal is shown in Figure 6.29.

```

pi@raspberrypi: ~
File Edit Tabs Help
pi@raspberrypi:~ $ sudo python atlas/whitebox-raspberry-ezo/i2c_continuous.py
--> D0 97
- pH 99
- EC 100
- RTD 102
-----
26-04-2023 17:21:56
Success D0 97: 33.45
-----
26-04-2023 17:21:58
Success pH 99: 14.000
-----
26-04-2023 17:21:59
Success EC 100: 0.00,0,0.00,1.000
-----
26-04-2023 17:22:01
Success RTD 102: -1023.000

```

Figure 6.29: Sensor readings in terminal (without probes)

To fully automate this process, the script must automatically run on startup. A new launcher file, **launcher.sh**, is therefore created which accesses the terminal, navigates to the correct directory, and runs the new code, **ic2_continuous.py**.

```

#!/bin/sh
# launcher.sh

cd /
cd /home/pi/atlas/whitebox-raspberry-ezo
sudo python i2c_continuous.py

```

Then, in the **pi/home** directory, a new **logs** directory is added where error logs are to be saved. Crontab, a background (daemon) process, is then used to launch

launcher.sh on startup. To open Crontab, the following command is used.

```
sudo crontab -e
```

By then adding the following entry, Crontab runs the script upon startup and saves error logs to the newly created **logs** directory.

```
@reboot sh /home/pi/bbt/launcher.sh >/home/pi/logs/cronlog 2>&1
```

For clarification, the complete directory structure of this setup is illustrated in Figure 6.30

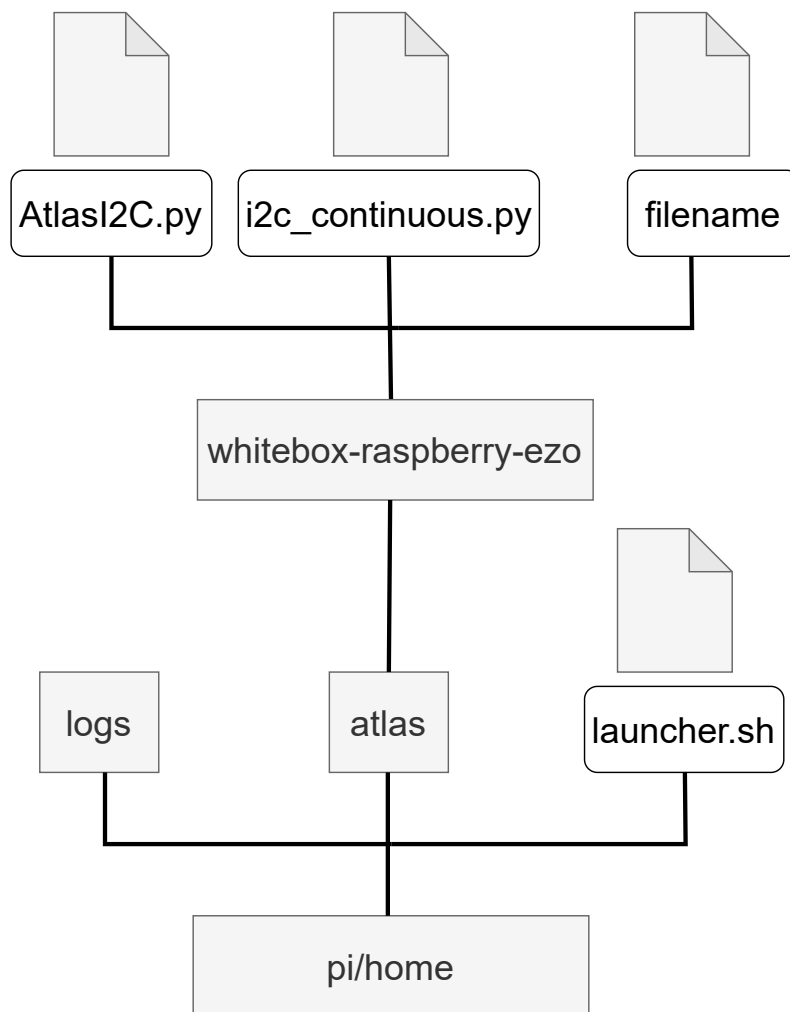


Figure 6.30: Directory structure for the probe setup

Chapter 7

Results

This Section highlights the results of this thesis and is split up to cover the various aspects of the USV, demonstrating their advantages and short comings. As a significant part of this project has been the design of the USV and the viability for mass production, the following Sections will address it's price, weight, and ease of assembly and transport. In addition, the various flight modes of the USV, as well as the results for the probes are covered.

7.1 Price

The components used for this project are all off-the-shelf and are specifically chosen for their low price and availability. The Table below shows a list of all main components and their prices, as of the writing of this report. The table is divided in three parts; the component, vendor, and price. The price is calculated in Norwegian kroner (NOK) and shipping prices are not included. Note that the vendor refers to the entity or company from which the component was purchased, and is not necessarily the manufacturer of that product.

Table 7.1: Bill of Materials

| Component | Vendor | Price(NOK) |
|---|------------------|------------|
| SUP board | Bauhaus | 4 999 |
| Ratrig Starter Package (x2) | Kjell & Company | 1 998 |
| Peli Case IM2050 (x2) | Nordicase | 2 042 |
| Pixhawk 4/ PM07/ GPS | Elfa Distrelec | 3 754 |
| Herelink Ground Station / Air Unit | 3DXR | 11 622 |
| T200 Thrusters (x2) | Blue Robotics | 4 876 |
| Sunpower SPR-E-Flex-110 Solar Panels (x2) | Watski | 2 998 |
| Solar Charge Controller | Light in the Box | 289 |
| Lithium Battery | Elefun | 1 795 |
| dH Probe | Atlas Scientific | 888 |
| DO Probe | Atlas Scientific | 2 519 |
| Temperature Probe | Atlas Scientific | 248 |
| EZO carrier board (dH) | Atlas Scientific | 413 |
| EZO carrier board (DO) | Atlas Scientific | 516 |
| EZO carrier board (Temperature) | Atlas Scientific | 310 |
| Whitebox T3 (x2) | Whiteboxes | 2180 |
| Raspberry Pi 4 Model B Starter Pack | Dustin Home | 945 |

The price of the complete table is thus estimated to be 43.000 NOK. However,

due to other parts, such as PLA, wires, fastening strips, hinges, shipping prices, connectors, etc, not being listed here, the correct price is higher.

7.2 Building the Vessel

As the design of the USV should be simple but effective, this Section explains the viability of the design and its ability to effectively be build, assembled, transported, and deployed.

With all equipment and components present, the assembly of the frame was achieved in about five hours . The cutting of the frame was performed with an angle grinder, while the fastening of angle brackets and hinges was done with a drill. The drilling of holes was achieved with the help of a pillar drilling machine.

The Peli cases were mounted to the frame and the components were put in place. Connecting all parts, soldering included, did also take five hours. Assembling and preparing the sensor payload is done within an hour with the code found on Github.

7.3 Transportation and Assembly

The USV was first tested at Aker Brygge, Oslo, where it was deployed for approximately one hour. During this initial test, transportation, assembly, and several flight modes were performed and analyzed. The following paragraphs present the USV's ability to be transported and deployed during this initial test.

Transportation In regards to transportation, the disassembled USV comes in five major parts. These parts and their respective weights are as follows:

- the deflated SUP board = 10.5kg
- the pump = 1.6kg
- the folded frame = 10.5kg
- two solar panels = 4.4kg

In addition, there are the straps and ground station that can be kept in a box or bag when transporting the vessel. In all, the complete deflated USV weighs in at 27kg. All parts mentioned above are depicted in Figure 7.1, where they were carried on a trolley for the initial test.



Figure 7.1: All parts on a trolley

Assembling the Vessel During the initial testing of the USV, it was found that the USV can be assembled and made ready for operation in roughly 30 minutes, when performed with a team of three people. The process for this is as follows:

- Inflate the SUP board.
- Unfold the frame and strap it to the center of the SUP board.
- Strap the sensor payload below the USV.
- Strap one solar panel on each end of the board.
- Connect the solar panels to the MC4 plugs of the solar charge controller.
- Power the USV and Raspberry Pi by initiating the load on the solar charge controller, and turn on the camera.
- Power the Herelink ground station, and wait for a GPS fix.
- *When disassembling the USV, the order of operation is reversed.*

Visual representations taken from the initial test of this project can be found in the following six Figures.



Figure 7.2: Inflating the SUP board



Figure 7.3: Putting the frame in place



Figure 7.4: Opening and strapping the frame to the SUP board



Figure 7.5: Strapping the solar panels to the hull

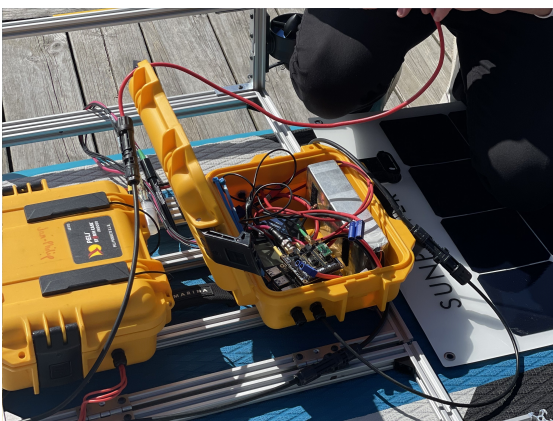


Figure 7.6: Connecting solar panels, battery, and the load to the solar charge controller



Figure 7.7: Lowering the thruster arms and deploying the USV

7.4 Initial Test

As mentioned above, the initial test was performed at Aker Brygge, Oslo on the 28th of April 2023. The USV was tested at 12:00, with still water conditions and little-to-no wind. During the initial test, the USV was secured with a wire from a wire spool. It should be noted that the area is highly trafficked by other boats, which resulted in occasional waves during the testing. The complete USV can be seen operating in Figure 7.8, while Figure 7.9 shows the map data during the initial test.

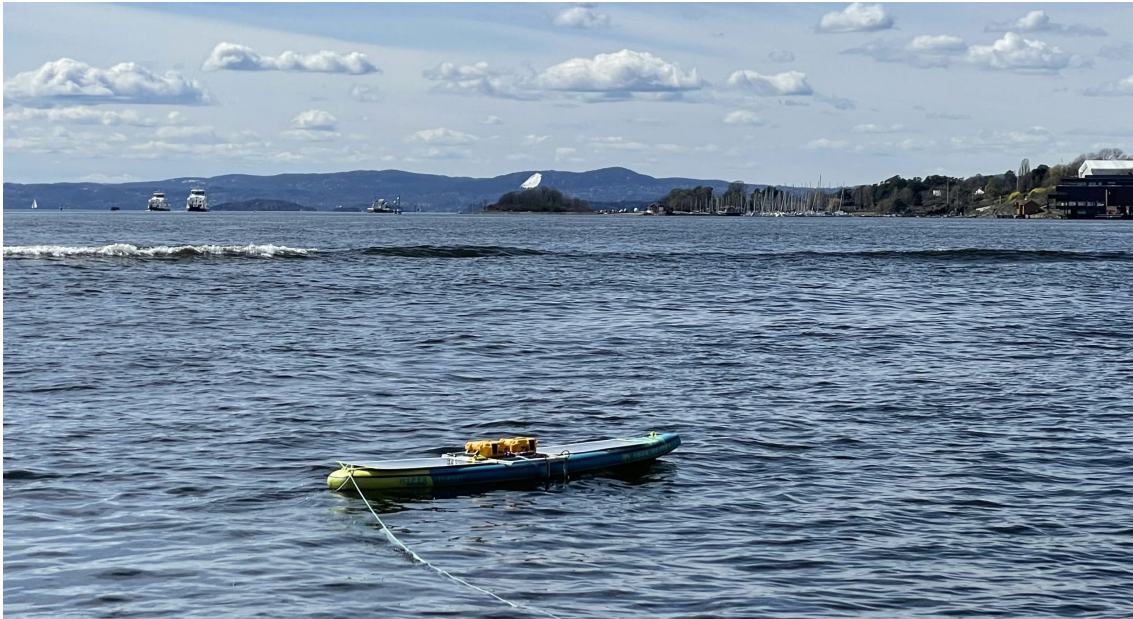


Figure 7.8: Completed USV during operation

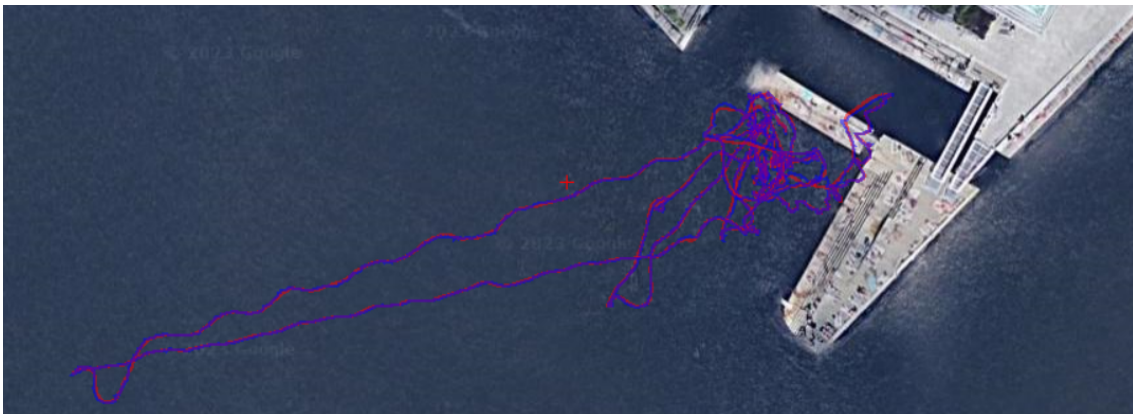


Figure 7.9: Map data from the initial test

The operation of the vessel is facilitated by the implementation of Ardupilot. Once the vessel is deployed and armed, ArduRover provides a range of supported flight modes that are accessible to the operator. These flight modes are summarized in the following table.

Table 7.2: ArduRover flight modes

| Flightmode | Function |
|---------------|--|
| Manual | Enables manual control of the vessel |
| Auto | Enables the operator to upload premade waypoints for predefined missions |
| Loiter | The vessel will attempt to hold its position |
| Acro | Used for tuning the vehicle |
| Guided | The vessel will attempt to navigate to a set point |
| RTL | (Return to Launch) The vessel will attempt to navigate back to its launch position |

During this test, Manual, Loiter, Guided, and RTL were attempted, with their respective results listed below.

Manual control allows the operator to steer the vessel. While maneuvering, the thrusters perform differently depending on the direction of movement, providing maximum thrust of 30% during forward and backward motion, and 100% during turning. This setup enables the vessel to be responsive and quick during turns but relatively slow when moving straight. The throttle performance, measured in rpm, during Manual mode is shown in Figure 7.10.



Figure 7.10: Throttle performance during Manual, where throttle right is displayed in red, and throttle left is displayed in green

Loiter means that the USV holds the current position. This flight mode was attempted while the USV was stationary in the water. In loiter mode, it was attempted to wind the wire such that the USV is pulled back towards the pier. This resulted in the USV trying to counter this force by moving back to the initial position. The test is visualized in Figure 7.11. The throttle performance during this test is presented in Figure 7.12.



Figure 7.11: Winding the spool during Loiter test

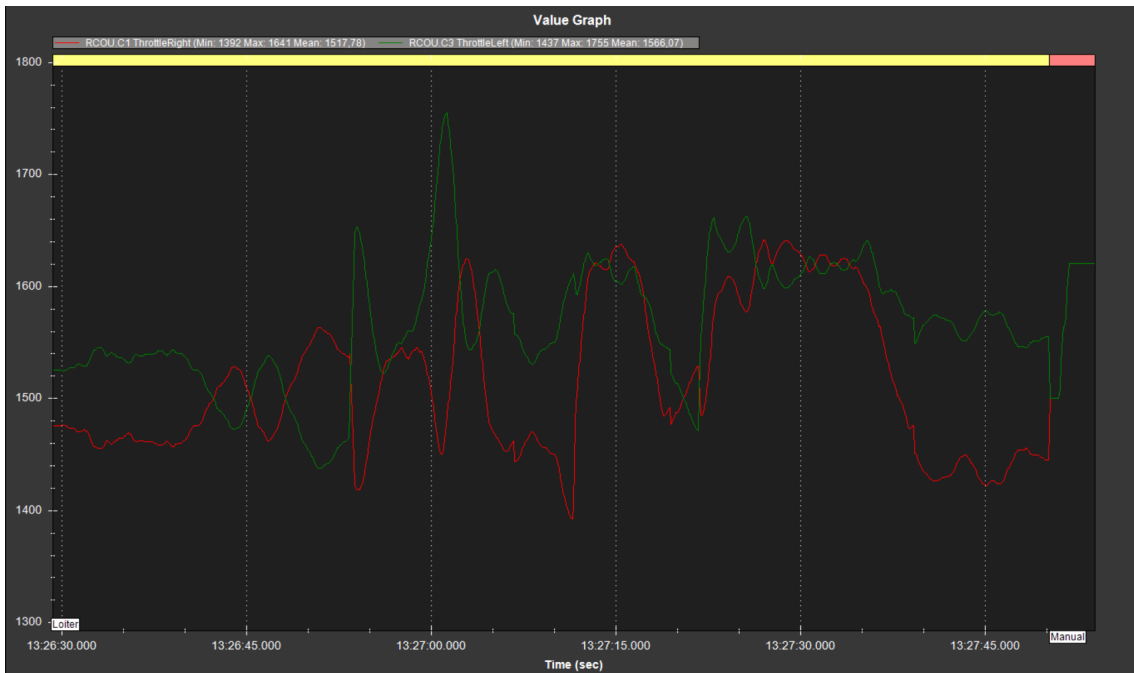


Figure 7.12: Throttle performance during Loiter, where throttle right is displayed in red, and throttle left is displayed in green

Guided mode was attempted by selecting various set points on the Herelink's interface. From the various tests that were performed, all points were successfully reached. One such example is presented later in Figure 7.13

Return to Launch makes the USV attempt to move back to the location from where it was first started. During testing, all attempts to navigate back were successful. However, the vessel has tendencies to not take the shortest way back, and instead turns more than necessary, meaning that it must adjust its path several times while navigating back.

Figure 7.13 presents one of the autopilot tests that was performed. In the Figure, the vessel enters from the right side in guided-mode, navigating to the set point, before being prompted to return with the RTL-mode. During this mission, the vessel returned to the origin successfully. However, it did not follow the most optimal path. The thrusters' throttle during the same mission is displayed in Figure 7.14, where the right throttle is displayed in red, while left is displayed in green.



Figure 7.13: Path of the USV during guided- and RTL-mode

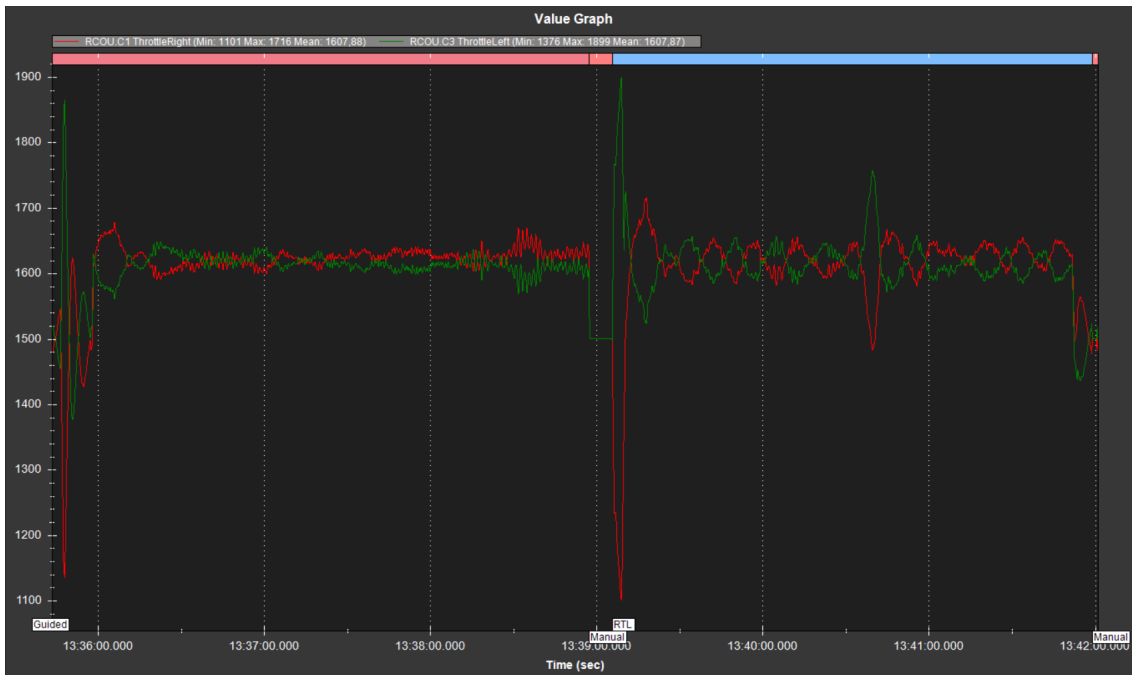


Figure 7.14: Throttle performance during Guided and RTL, where throttle right is displayed in red, and throttle left is displayed in green

Observed Values during Operation The following values have been observed during operation. The measured current during the entirety of the operation is shown in Figure 7.15. The graph shows a minimum current of 1.84A, a maximum current of 119.97A, and a mean current of 12.76A. A brief increase of current can be seen every time the USV changes direction, indicating a sudden spike in current to give an instant response for the thrusters. Figure 7.16 presents the measured current during the Guided- and RTL mission displayed in Figure 7.13. The graph shows that the USV operated at a mean measured current of 19.71A during relatively consistent movement at 30% thrust. The minimum current and maximum current for this mission is 2.02A and 119.7A respectively.

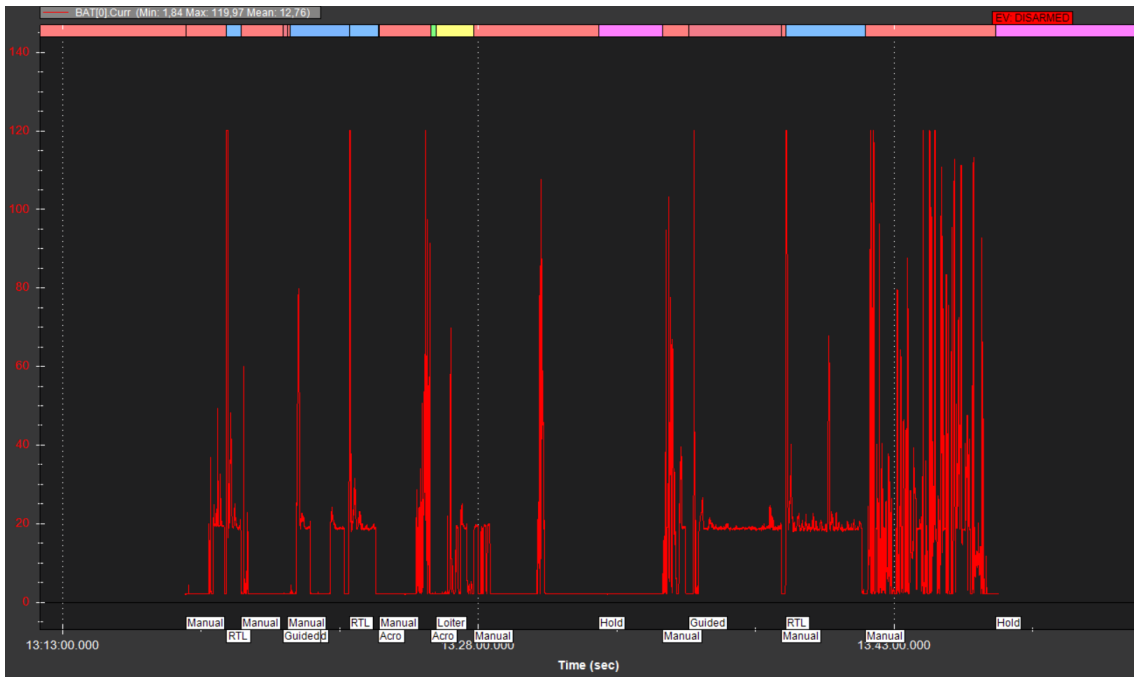


Figure 7.15: The measured current of the battery during the entire initial test

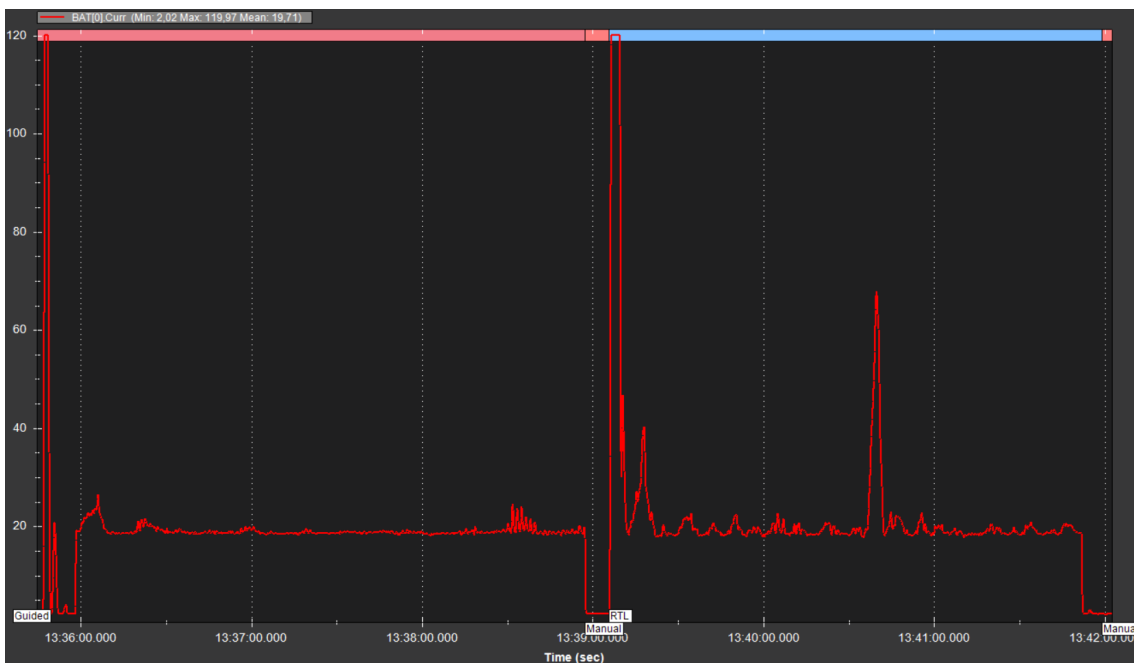


Figure 7.16: The measured current of the battery during the Guided- and RTL mission

The speed of the USV during the entire initial test is presented in the graph below. As mentioned, the throttle was set to 30% with the goal to maximize the battery efficiency while keeping sufficient speed. The maximum speed was therefore at 0.98m/s, with a mean speed at 0.18m/s. The speed of the USV during the Guided- and RTL mission is shown in Figure 7.18. The maximum speed was at 0.98m/s, with a mean speed at 0.43m/s.

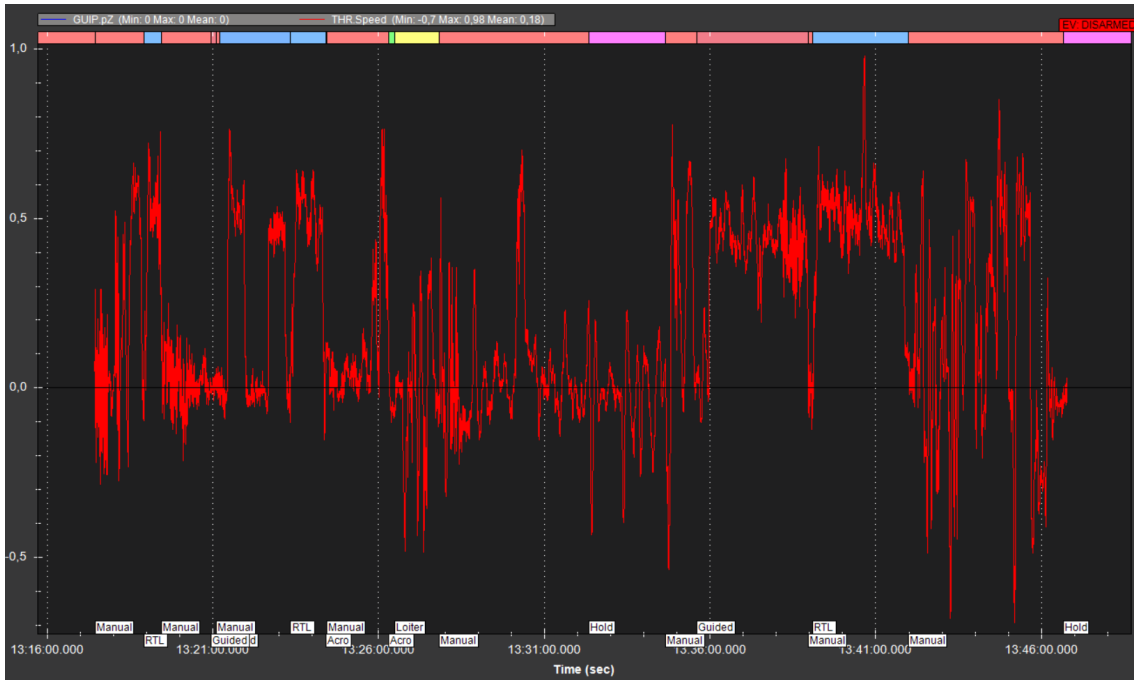


Figure 7.17: The measured speed of the USV during the entire test

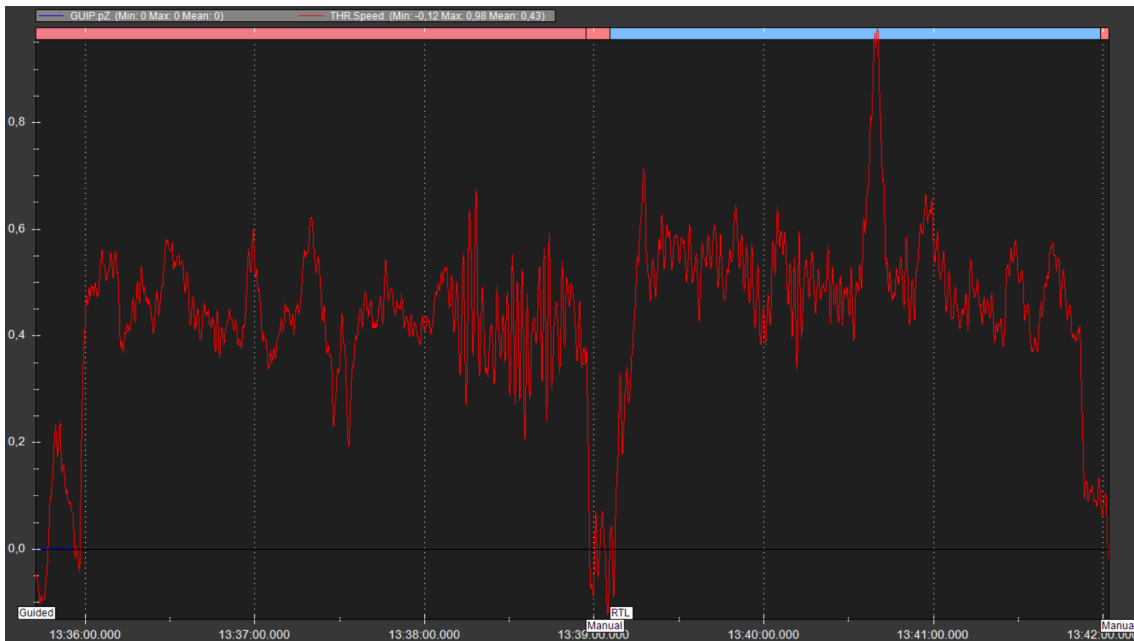


Figure 7.18: The measured speed of the USV during the Guided- and RTL mission

The cross-track error (XTE) for the RTL/Guided mission is presented below. XTE refers to the deviation of the vehicle from the intended course and is displayed in meters. The XTE, in Figure 7.19, shows a maximum error, minimum error, and mean error of -4.44m, 0.73m, and -0.19m respectively.

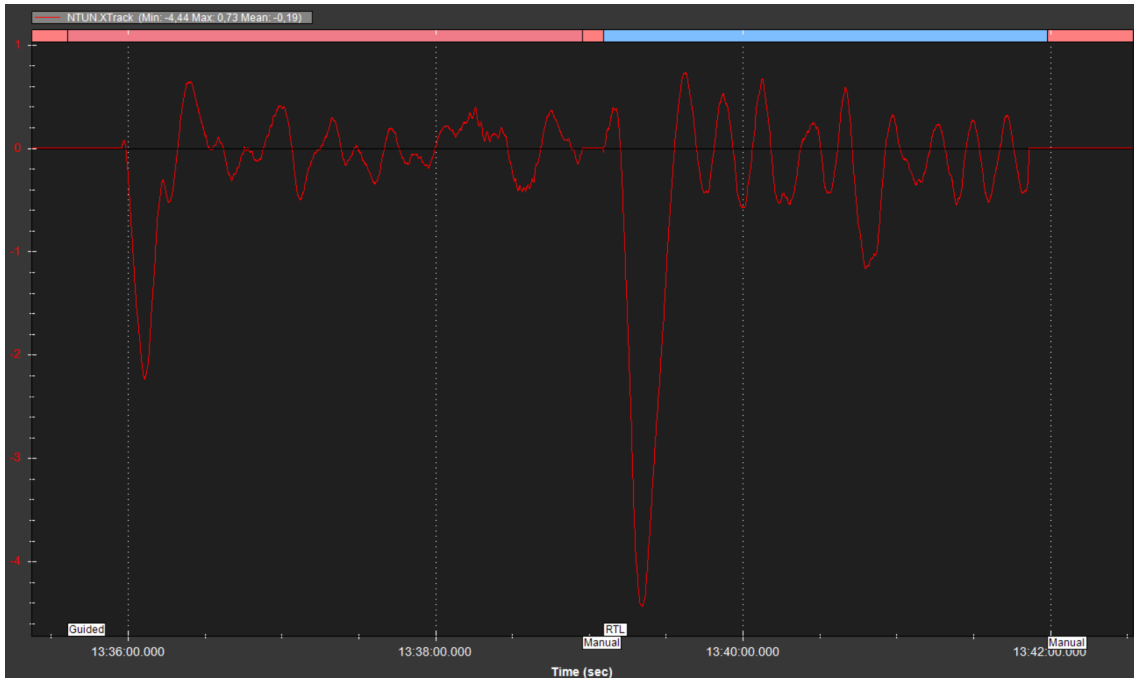


Figure 7.19: The cross-track error for the RTL/Guided mission

7.5 Second Test

Although the initial test was performed successfully, it was found that the USV was moving too slow. In addition, Auto mode was not attempted during this test. In order to overcome this limitation, a second test was conducted in Asker, Viken. On the second attempt, the throttle percentage set to 50%, opting for more time-efficient operating with a higher current draw as a trade-off. The test was conducted on May 5, 2023, at 13:05 in still water conditions without wind. The USV can be seen testing in Figure 7.20.



Figure 7.20: Completed USV during the second test

The following two Figures present the mission that was planned for the Auto mode, in addition to the actual navigation of the vessel. In total, eight waypoints were selected for the USV to navigate between, before returning to the origin with RTL.

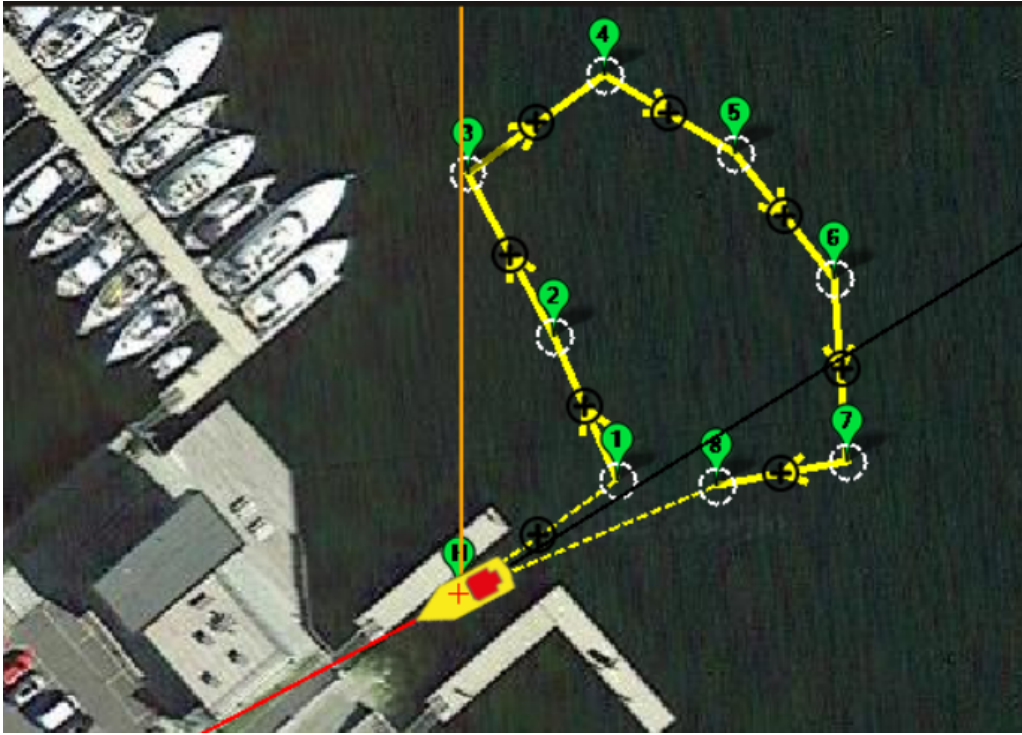


Figure 7.21: Predefined waypoints for the Auto mission



Figure 7.22: Map data from the Auto mission

Figure 7.23 shows the thruster performance during the Auto mission with the new 50% thrust of the vessel. During the mission, the USV had a mean throttle of 1637rpm.

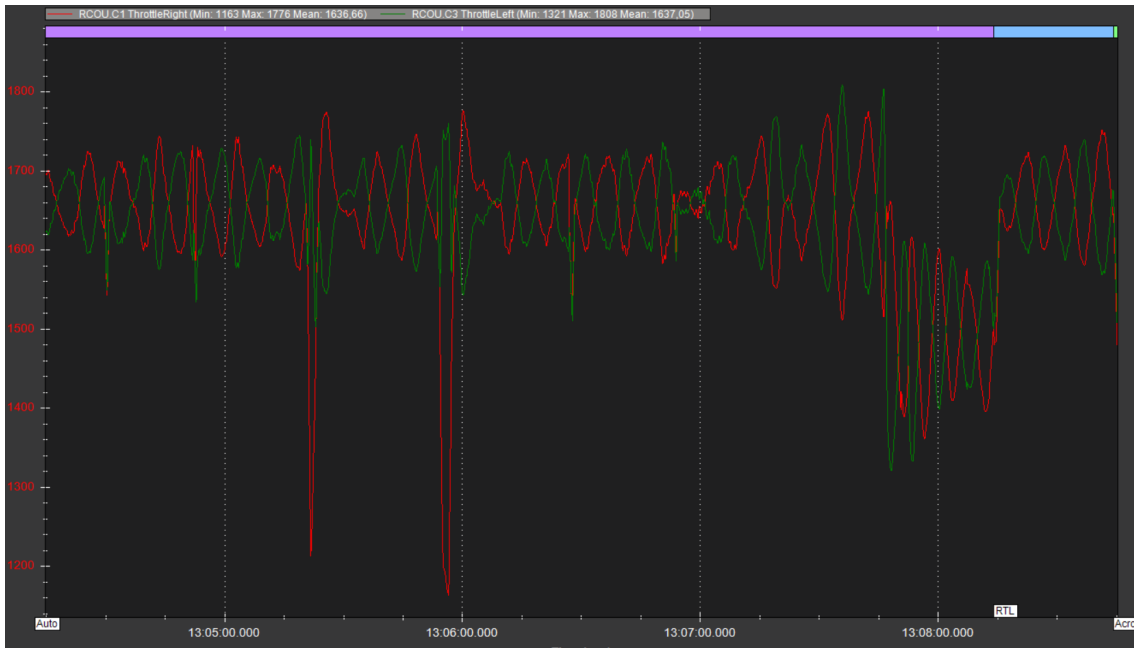


Figure 7.23: Thruster performance during Auto mission

Figure 7.24 shows the measured current during the Auto mission, showing a minimum current of 2.11A, a maximum current of 119.97A, and a mean current of 43.51A with the thrust set to 50%. Figure 7.25 shows the velocity of the USV during the same mission. The vessel performed with a mean velocity of 0.59m/s and a maximum of 1.02m/s.

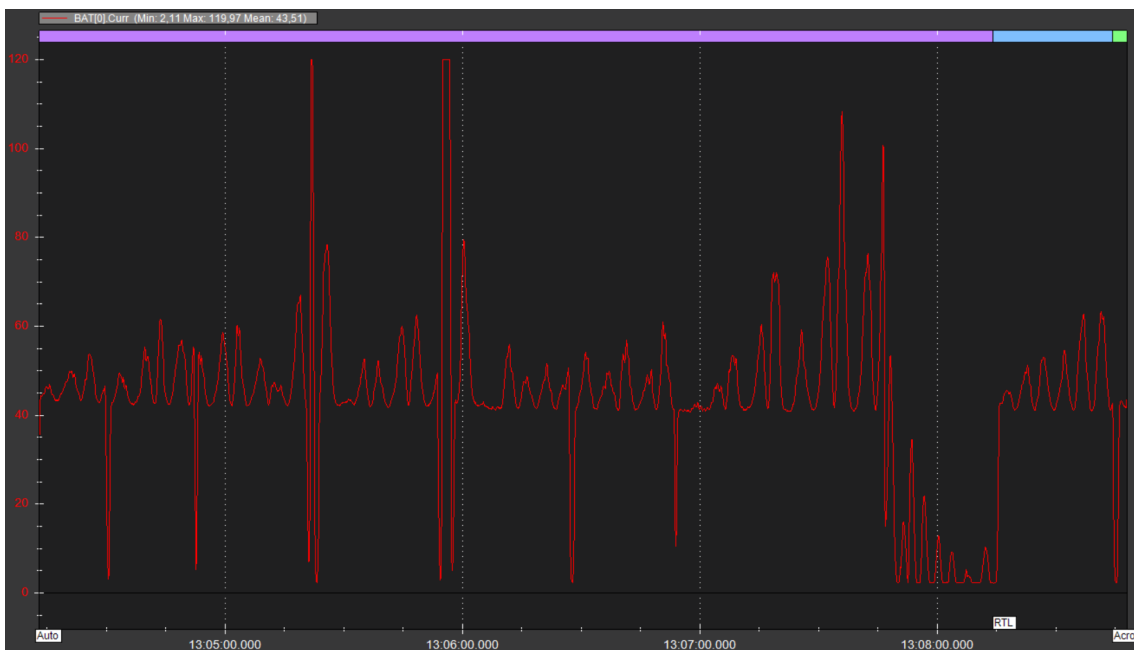


Figure 7.24: Measured current during Auto mission

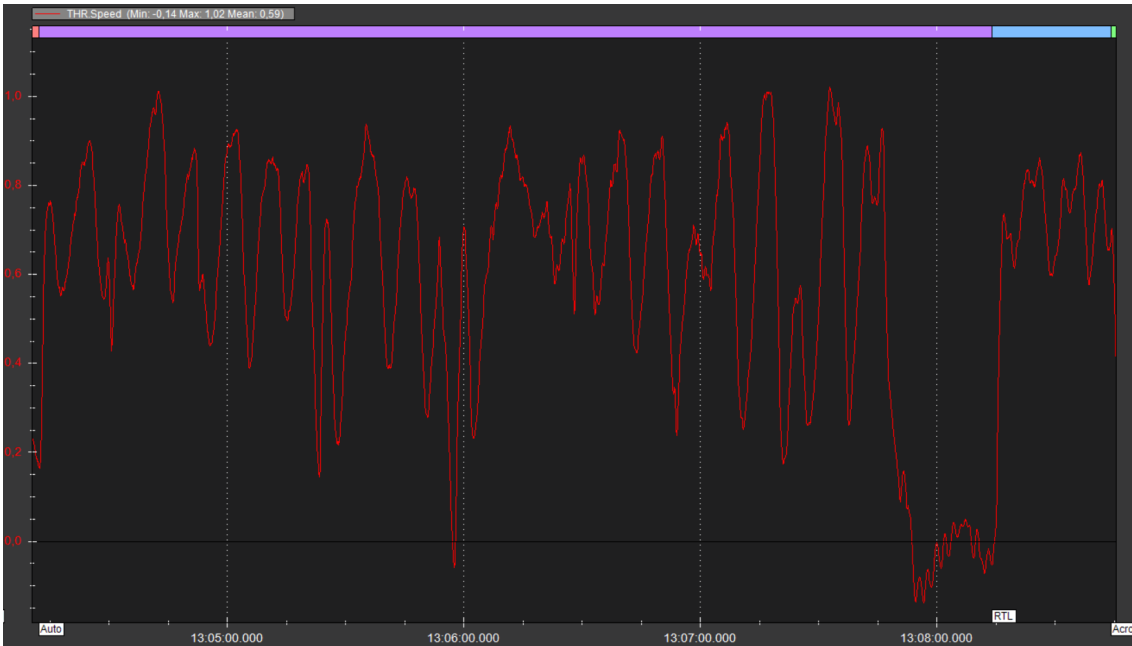


Figure 7.25: Measured speed during Auto mission

Figure 7.26 presents the XTE for this mission, measuring a minimum, maximum, and mean error of -3.45m, 1.48m, and -0.2m respectively.

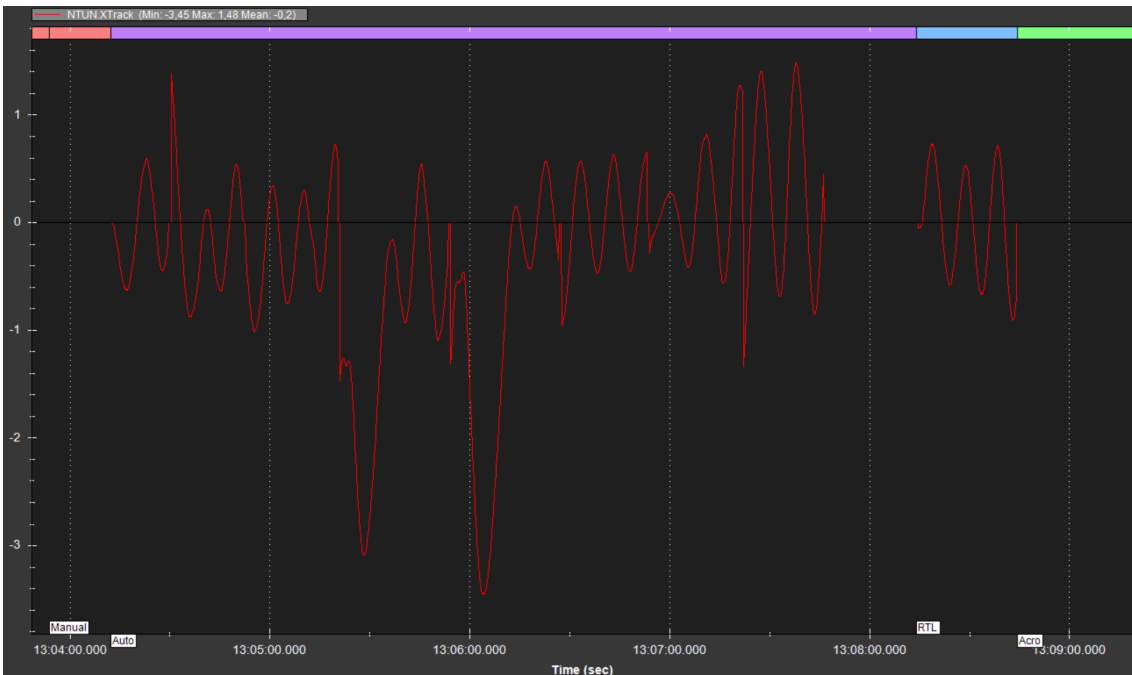


Figure 7.26: Cross-track error during the Auto mission

7.6 Operation Time

To calculate the estimated operation time of the USV, the power consumption described in Section 3.5 is used. The power (Wh) is calculated by multiplying the current over time by the voltage. The complete operation time for the USV can be formulated by subtracting the USV power usage from the battery capacity and adding the power provided by the solar panels.

$$h = C + \Delta Pt \quad (7.1)$$

$$h = (Ah_{Battery}V_{Battery}) + P_{solar}t - (V_{USV}A_{USV})t \quad (7.2)$$

where the following parameters are used. For the USV power usage, the mean values from the Guided/RTL mission from the initial test and the Auto mission from the second test was used.

- h = operation time in hours
- $Ah_{Battery} = 16Ah$
- $V_{Battery} = 16V$
- A_{USV} (30% throttle) = 19.71A
- V_{USV} (30% throttle) = 15.5V
- A_{USV} (50% throttle) = 43.51A
- V_{USV} (50% throttle) = 15.5V
- P_{solar} (assuming maximum power output) = 220W

Plotting the two equations for the different throttles give the following graphs, where t = time and $y = A$. At 30% throttle, the operation time is about 3 hours, while the operation time is about 30 minutes at 50%.

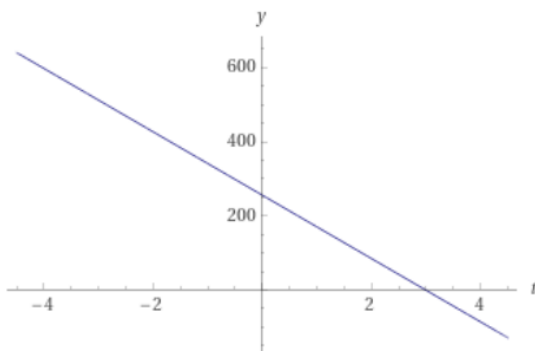


Figure 7.27: Estimated operation time at 30% throttle

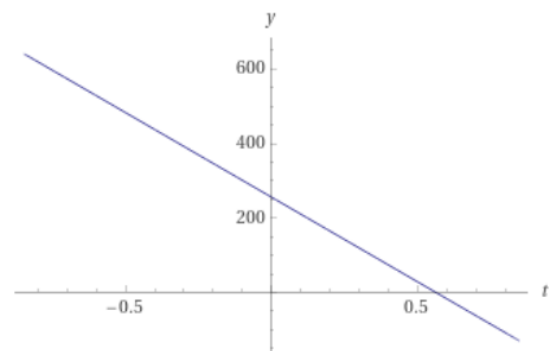


Figure 7.28: Estimated operation time at 50% throttle

Plotting the two equations without the power provided by the solar panels gives the following results. At 30% throttle, the operation time is about 0.8 hours (about 48 minutes), while the operation time is about 0.4 hours (about 24 minutes) at 50%.

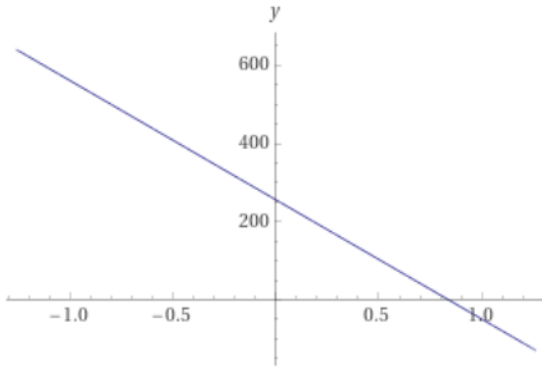


Figure 7.29: Estimated operation time at 30% throttle without solar panels

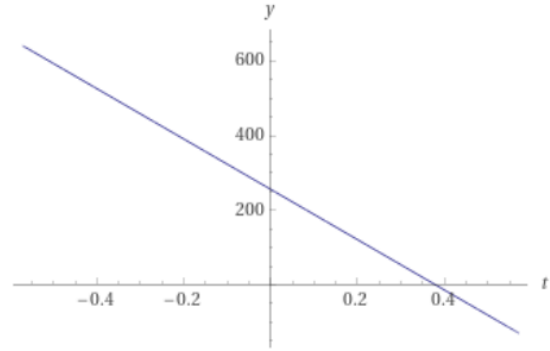


Figure 7.30: Estimated operation time at 50% throttle without solar panels

It is important to mention that the two missions are different and that the power consumption is dependant on several other factors, such as weather conditions and thruster values. Nevertheless, the estimated values provided above offer a rough idea of the expected operation time during missions.

7.7 Sensor Data

This Section shows test results of the probes during the second test in Asker. It should be noted that the solar charge controller did not provide enough power for the Raspberry Pi running the four probes. Therefore, no sensor data was collected during the initial test. For the seconds test a power bank was used to power the Raspberry Pi and the sensors instead.

The purpose of this experiment was to evaluate the water quality of a fjord using a solar-powered unmanned surface vehicle (USV) equipped with pH, dissolved oxygen (DO), temperature, and conductivity sensors. The testing took place on May 5, 2023, in the Oslo fjord in Leangen, Asker.

Table 7.3 displays the trends in pH, DO, temperature, and conductivity over the course of the mission presented in Figure 7.22. In all, 144 measurements were taken with the 4 sensors over a time span of 18 minutes.

Table 7.3: Efficiency comparison between 30% and 50% throttle

| Sensor | Mean | Standard Deviation | Range |
|--------------|-------|--------------------|----------------|
| DO (mg/L) | 5.26 | 0.19 | 5.19 - 5.94 |
| pH | 7.94 | 1.18 | 2.182 - 9.964 |
| Temp (°C) | 9.54 | 0.51 | 9.272 - 10.961 |
| Cond (μS/cm) | 20122 | 2634 | 5924 - 21330 |

In reference to Section 3.1.2, the results indicate that the water quality of the Oslo fjord in Leangen, Asker, during the testing period was within acceptable levels for pH, DO, and temperature. However, the conductivity measurements were higher than expected, indicating a possible pollution source or incorrect

calibration of the probe. The complete file is to be found in the Github repository, referenced to in Appendix 10.

7.8 Frame Stability during Operation

During, and after, the operation of the vessel, some flaws were discovered that were not accounted for while constructing the frame.

Since the side frames of the frame are connected with hinges, they have a tendency to move up and down depending on the thrusters. This was particularly noticeable during manual testing, where the side frames were observed to be lifted noticeably while turning at full throttle.

After the initial test, it was observed that some of the aluminum profiles in the frame had shifted from their original position. Most of the screws for the hinges and angle brackets had to be tightened after the first test.

Chapter 8

Discussion and Future Work

The following Sections feature reflections on the results, which are then compared to initial ideas. In addition, each section also addresses some of the concerns regarding the current design, and provides suggestions for future attempts at a low-cost, solar powered unmanned surface vessel.

8.1 Price

Section 7.1, Results, presented the overall estimated price of the vessel. The final price stands at roughly 43.000NOK, including only major parts and ignoring shipping prices. Overall, it is estimated that the final price should be assumed to be near 50.000NOK, which is in line with the initial objective of designing a low-cost solution. It is important to note that the actual cost of the USV may vary depending on several factors, including the location of the project and shipping prices. In addition, for future recreations, the total price also depends on the manufacturer's design choice regarding a recreation of this particular vessel.

The off-the-shelf components used in this project were chosen for their low price and availability. It is possible to reduce costs even further by using cheaper alternatives. However, it is essential to ensure that the quality and reliability of the components are not compromised.

The cost of the SUP board makes up a significant portion of the total cost, but it is a crucial component for achieving the project's objective of being fast to deploy, easy to transport, and providing high maneuverability. One of the reasons for choosing this particular hull is its size. Disregarding the solar panels for future attempts leaves the possibility to explore other smaller, and cheaper hulls, as explained later in Section 8.2.

The use of solar panels is another essential feature of this USV as it prolongs the battery life and reduces the reliance on external power sources. The cost of the solar panels is reasonable and should provide a reliable power source for the USV. However, ignoring these components reduces the price by roughly 3.300NOK, while also reducing the battery life as a trade off. One should consider the estimated operation time when deciding whether to include the solar panels and

the solar charge controller or not.

Other substantial components are the Herelink Ground Station and Air Unit, which together cost 11.622NOK as of the writing of this report. While purchasing alternative components would drastically lower the price, the project would no longer benefit from the quality and advantages from these components. For instance, the Herelink provides the operator with an interface which not only facilitates the operation, but also allows for real-time monitoring of the vehicle's performance. In addition, these components provide a range of up to 20km, which is significantly higher than many other ground stations available on the market. In all, these features were noticeably helpful during the testing of the USV, and are recommended for future constructions of this particular project.

Lastly, there are other parts such as connectors and the Whiteboxes which are not necessary for the USV, but rather complement the modularity of the vessel. For instance, the T1 Whiteboxes, used for the Raspberry Pi and sensors, are not necessary to take measurements. Soldering these components instead of purchasing the Whiteboxes saves additional 2180NOK but removes the ability to freely exchange probes and EZO boards.

In all, the estimated price of the USV is within a reasonable range, and the use of off-the-shelf components has helped to keep the cost low. While the current design leaves a lot of room for variations, it is crucial to ensure that the quality and reliability of the components are not compromised while considering cheaper alternatives.

8.2 Design

As previously mentioned, the frame and USV is designed to be modular, easy to construct, cheap, and fit for operation in marine environments. Overall, it fulfills this purpose, while leaving room for improvement.

The frame has been found to be easy to assemble and transport during testing, with a weight of 10.5kg. The handle design, which consists of two top- and bottom layers and an infill of 20%, has proven successful in securely locking the frame in place when folded and withstanding the weight of the frame while being carried. The first attempt at constructing the frame took about five hours, but it is expected that future attempts would require significantly less time, demonstrating that the current design is both simple and efficient to construct while requiring some experience with the tools and methods described in this report.

Improvements should be made to further strengthen the frame however. Some of the aluminum profiles in the frame had shifted from their position, suggesting that the screws used to secure them were either not tightened adequately or that additional reinforcement is required to strengthen the frame. This might indicate that larger angle brackets should be used, such as the ones used for the thruster arms. This way, the aluminium profiles are secured at multiple anchor-

age points and can withstand the force produced by the thrusters while operating. In addition, the side frames were found to be too flexible during operation. At times where the USV made quick turns, the side frames were often lifted, indicating that the side frames should be able to be locked in place when the frame is open. This could either be done by using hinges that cannot rotate as easily, or by mounting brackets to the main frame that could secure the side frames in place during operation.

Although the aluminium profiles can withstand marine environments, other components, such as the hinges and some of the angle brackets can not. It is suggested that future attempts at this design make use of components constructed of stainless steel instead of being galvanized, as to extend the quality and lifespan of the vessel.

While the quality and durability of the Peli cases are not in question, their size has been found to be impractical for containing the hardware. Although the current design with two Peli cases has proven sufficient, maintaining a good hardware structure inside the cases would be easier if they were larger. Therefore, for future work, it is suggested to replace the current cases with larger ones or use a single, larger case instead, in order to optimize hardware containment.

The finite element analysis presented in Section 6.2.2 predicted that the thruster arms would withstand the force exerted by the thrusters, and the physical test confirmed this by showing no signs of structural weakness. While the design of these arms have proven to be sufficient, some adjustments could be made to how the arms are lowered. The USV has to be placed at the edge of the pier, as seen in Figure 7.7 in Section 7.3, such that the arms can be lowered. While this method works, it is slightly impractical and could be improved upon. Future attempts should investigate other possible ways to lower the arms for operation.

The choice of hull has been demonstrated as a sufficient choice as it is both simple to transport, deploy, and highly maneuverable. The overall design of the USV also leaves the manufacturer of future attempts room to experiment with other hulls. For instance, the hull can be manufactured from scratch such as related work has demonstrated, or by choosing different types of pre-build platforms, such as other SUP boards, surf boards, kayaks, etc.

8.3 Hardware

The hardware setup for the USV has been designed with a focus on using connectors wherever possible to enable easy upgrading and replacement of components. When deploying the vessel, the connectors make it efficient to plug or unplug certain parts, and to power the system. Moreover, the use of these connectors significantly enhances the modularity of the USV, allowing users to swap out components as per their requirements.

The design of the 3D-printed mountings for the thrusters have proven to be

effective in securing the them to the thruster arms. After both tests, no signs of structural weakness was found on the thruster brackets when printing them with two top- and bottom layers and an infill of 20%.

The use of two-component epoxy adhesive and glue gun glue to secure the cable glands has also proven to be efficient. During testing no leakages were found, suggesting that this method needs no further improvement unless the USV is used in harsher environments.

For a prototype, the choice of battery has been sufficient for testing. However, connecting two 16.000mAh batteries in series, should be considered to further extend the operation time for serious testing. The vessel has the potential to carry even more, or larger, batteries than this and is currently only restrained by the limited storing space provided by the Peli Cases. This means that the vessel could be powered for multiple hours given enough battery capacity. This could improve on the 3 hours of operation that the vessel is currently capable of with solar panels and 30% throttle. It should also be noted that the current estimated battery life is derived from a calculation. Future work should thus measure the battery after testing to come to a more specific answer in this regard.

One potential limitation of the current hardware setup is the length of the thruster cables. As noted in Section 6.4, the cables were too short for the particular frame used in this project and had to be extended by soldering additional high temperature silicone wires. This limitation could be addressed in future work by using longer thruster cables or by designing a different frame that accommodates the current cable length.

To compare the efficiency of different throttle levels, measurements were taken at both 30% and 50% throttle. The table below summarizes the observed values for each test. The values recorded during the Guided/RTL mission for the initial tests are listed, while the Auto mission for the second test is included for comparison.

Table 8.1: Efficiency comparison between 30% and 50% throttle

| Values | 30% Throttle | 50% Throttle |
|---------------------|--------------|--------------|
| Mean current (A) | 19.71 | 43.51 |
| Minimum current (A) | 2.02 | 2.11 |
| Maximum current (A) | 119.97 | 119.97 |
| Mean speed (m/s) | 0.43 | 0.59 |
| Maximum speed (m/s) | 0.98 | 1.02 |

It is important to note that while the two missions are not identical, these results give a good indication of the overall efficiency of the two throttles. On average, the measured current is more than twice as high for the 50% throttle as for the 30% throttle. However, the average velocity is only 0.16m/s higher at 50% throttle.

These results suggest that increasing the throttle by 20% is not worth the significant increase in power consumption. As presented in Section 7.6, the opera-

tion time is about 2.5 hours longer while operating at 30% throttle, compared to 50%. However, it is important to note that more tests may be necessary to confirm these findings and to determine the optimal throttle level for specific applications. To create more accurate results in this regard, the USV should perform the same mission with both thruster values. In addition, it is worth noting that both missions were hindered by the lack of tuning of the PID controller, leading to suboptimal navigation, as discussed later in this report. As a result, oscillating movement occurred during both missions which decreased the average speed of the USV.

The previously calculated operation times demonstrate that the solar panels are an effective addition to the hardware of this design. At 30% throttle, the addition of solar panels roughly increase the operation time from 48 minutes to 3 hours. At 50% throttle the operation time increases from 24 minutes to 30 minutes. These findings further support the idea that the vessel is best operated near 30% thrust.

8.4 Software and Navigation

The results of the initial test indicate that the implementation of ArduPilot was successful in facilitating the operation of the vessel. The various flight modes that were attempted, including Manual, Loiter, Guided, RTL, and Auto each produced desirable results.

However, some limitations were identified, such as the relatively slow speed of the vessel during straight-line movement in Manual mode. As mentioned, the USV's thrust was initially set to 30% to operate at high efficiency. This results in the vessel moving at roughly 0.5m/s. In all, this makes the USV relatively slow, but very responsive in turning. While the overall maneuverability of the vessel was satisfactory, it was assumed that the USV could benefit from a lower thrust during turns, and slightly higher thrust during straight movement. Therefore, the thrust was increased to 50% on the second attempt increasing the speed average speed from 0.42m/s to 0.59m/s.

During Loiter, the USV successfully held its position. As mentioned in Section 7.3, this flight mode was tested by trying to wind the spool which the vessel was connected to, and thus pulling it towards the pier. The USV correctly responded by trying to maneuver back to its original position, as shown by the thruster response in figure 7.12, thus verifying that the mode works as intended. This implies that the vessel is able to hold its position during wind and waves.

In Guided, the USV moves to a user-defined destination by selecting it on the Herelink ground station. All results from the initial test demonstrated that the vessel successfully reached its destination. Return-to-Launch, or RTL, makes the vessel attempt to navigate back to its original position. All RTL tests showed success as well. However, there are minor concerns about the vessel's ability to take the shortest path during these modes. As seen in Section 7.3, in Figures 7.13 and

7.14, it is evident that the vessel must often readjust its path to its destination, which may affect the efficiency of future missions.

Auto mode was tested on the second test, which demonstrated that the USV successfully passed all the waypoints, as depicted in Figure 7.21. However, there are some concerns regarding the efficiency of the movement. As seen in the thruster performance graph and the map data, Figures 7.23 and 7.22, the vessel oscillates heavily while moving between the waypoints and is overall struggling to smoothly transition between the waypoints. While this issue was also noticeable during the initial test in both Guided and RTL, it is likely that the increased thruster performance has worsened the issue. The mean cross-track errors are -0.19m and -0.2m for the first and second test respectively. While these errors are very low, the minimum and maximum errors of these tests show that the vessel sometimes deviates a lot from its intended course. The highest errors the first and second test have are -4.44m and -3.45m respectively. During the initial test, the highest error occurred during the switch from Guided to RTL, which is visualized in Figure 7.13. The highest error during the second test occurred while transitioning from one waypoint to the next. This indicates that the navigation performs worst during flightmode changes and hard turns. Figures 7.19 and 7.26 further demonstrate the oscillation during autonomous flight modes. It is therefore recommended for future work to tune the PID controller in Mission Planner such that the vessel more effectively and efficiently navigates while moving autonomously.

To further enhance the sensing- and navigation capabilities of the USV, one possible improvement is to integrate additional sensors or cameras. Presently, the vessel lacks any means of object detection and avoidance, which makes it heavily dependent on an external operator. By adding object detection and avoidance capabilities, the USV can become more autonomous and safer when operating far from the operator or beyond line of sight. An off-the-shelf 3D camera like the Intel RealSense D435 could be utilized for object detection, while a lidar sensor could assist with obstacle detection and localization in low-light conditions, thereby reducing operator dependency.

8.5 Sensor Data

As the purpose of the USV is to monitor water quality measurements, four separate probes were connected to the USV, controlled by a Raspberry Pi. The probes used in this project were purchased from Atlas Scientific and measure dissolved oxygen, pH, temperature, and conductivity. The measurements were taken right below the water surface of the fjord by attaching the probes to one of the thruster arms of the USV. The testing took place on May 5, 2023, and a total of 144 measurements were taken with the four sensors over a time span of 18 minutes.

The results indicate that the water quality of the fjord was within acceptable levels according to the information given in Section 3.1.2. However, the conductivity measurements were higher than expected, indicating a possible pollution

source or incorrect calibration of the probe. Table 8.2 summarizes the average values of the findings and compares them to the ideal ranges of saltwater parameters shown earlier in Section 3.1.3.

Table 8.2: Comparison of findings against ideal parameters

| Water Quality Parameter (SI Unit) | Mean Value of Findings | Saltwater Ideal Range |
|--|------------------------|-----------------------|
| pH | 7.94 | 7.5 - 8.4 |
| DO (mg/L) | 5.26 | 5 - 11 |
| Water Temperature (°C) | 9.54 | 5 - 25 |
| Conductivity ($\mu\text{S}/\text{cm}$) | 20122 | 50,000 - 70,000 |

It is important to note that the probes were controlled separately from the USV, meaning that the exact location of the sensor data is inconvenient to pin point. To do so, one must match the timestamps of the measurements to the longitude and latitude of the USV at the given time, making it difficult and time consuming to compare. To obtain more accurate measurements, it is recommended to connect a GPS module to the Raspberry Pi to create separate map data.

Lastly, one should consider to adjust the `i2c_continuous.py` for better formatting of the measured data. The current solution writes each measurement as one single column without any clear separation, as seen in the figure below. Future work should thus make it easier to work with the data sets that are created during missions by separating the timestamp, status message, I2C address, and measurement with commas.

```
New Session at 26-04-2023 17:17:05:
26-04-2023 17:17:09 Success DO 97: 5.92
26-04-2023 17:17:11 Success pH 99: 8.220
26-04-2023 17:17:12 Success EC 100: 21310,11509,12.77,1.011
```

Figure 8.1: Current formatting of data

8.6 Ethical Concerns

Initially, the following ethical concerns were addressed in Section 1.2:

- Hazardous materials
- Navigation and collision
- Environmental sensitivity

With the USV constructed and tested, the following paragraphs investigate these concerns in regards to the current design and its results.

The vessel carries components that are potentially hazardous to the environment. As explained throughout this thesis, the USV is designed in a way that minimizes the risk of losing parts during operation. All parts are properly secured to the hull, or inside the Peli cases. During testing, the vessel was also deemed rigid such that this concern is no longer as valid. Still, it is important that the operator makes sure that all components of the USV are properly secured before deploying it.

As previously mentioned, the USV has no obstacle avoidance, meaning that the point of navigation and collision is still a valid concern. It is therefore important that the vessel is in line of sight with the operator at all times.

Initial tests showed that the USV was capable of causing disturbances to marine environments, habitats, or water quality. The level of disturbance caused by the USV is however assumed to be minimal, as it stays on the surface while also producing little noise. It is however still important to consider the potential impact on the environment, but further testing is required to come to a definitive answer in this regard. One possible solution is to use the methods presented by [58] such that the USV can perform with less disturbance.

Overall, it lies within the user to deploy and operate the USV with responsibility. As such, the vessel should never be deployed in populated or trafficked areas, and it should always be operated in line of sight with the user.

Chapter 9

Conclusion

The goal of this thesis was to create a low-cost solar powered unmanned surface vessel for the use of water quality inspection and monitoring in coastal areas and fjords. This project particularly focused on making up for the weaknesses of the heavier, more expensive, and less user-friendly alternatives. Thus, a large section of this project was to design the vessel in such a way that it only uses off-the-shelf components that have a low price and high market availability. In addition, the vessel should be easy to mass produce, transport, deploy and operate.

The unmanned surface vessel consists of a stand-up-paddle board as the hull with an aluminium frame strapped to it. The frame carries two cases that house all of the hardware. As this project makes use of the Ardupilot autopilot, the hardware consists of the Pixhawk 4, with accommodating components, and the Herelink ground station. The thrusters for this project are Blue Robotics' T200 thrusters. For measuring water quality, the hull carries a pH-, dissolved oxygen-, temperature-, and conductivity probe. For a prototyping phase, these sensors start measuring once they are powered, and write all data to a CSV file. The data can then provide an overall indication of the water quality of the tested water body. Lastly, the vessel carries two solar panels that are connected to a solar charge controller with the goal to minimize reliance on external power sources, and to extend the vessels operation time.

The frame was first designed in Solidworks with the goal to quickly prototype a design and identify potential problems. After multiple revisions, the frame is now able to be folded in to a portable case and able to be unfolded for operation. In regards to the complete design, the vessel costs roughly 50.000NOK and weighs 27kg. Depending on the team size and expertise, the vessel can be fully build in roughly one day, making it suitable for mass production.

Tests of the vessel demonstrated that the goal of simple operation, transportation, and deployment is achieved. The USV has several flight modes that all work as intended, including Manual, Loiter, Guided, RTL, and Auto. The USV was tested at both 30% and 50% throttle, with the 30% throttle opting to be more power efficient and 50% being more time efficient. It was found that the increase from 30% to 50% drastically increased the power consumption of the vessel while not gaining significant advantages in terms of speed. It is therefore rec-

ommended to keep the USV near 30% throttle for optimized operation. At this throttle, the USV can operate for roughly 3 hours, given optimal conditions.

The probe setup was proven to be viable approach for giving approximate data for water bodies. However, the current approach comes short when trying to accurately pin point exact locations of water quality measurements. A solution would be to connect a GPS module to the Raspberry Pi, such that map data can be formed with the various probes.

Future work should make attempts to improve on the solidity of the frame by swapping galvanized components with counterparts made of stainless steel instead. In addition, the side frames must be more rigid when operating as they are easily moved by the force of the thrusters. Furthermore, the Peli cases could be replaced with one or two larger cases to make it easier to maintain a good hardware structure. Future attempts should also tune the PID controller of the autopilot such that the USV navigates more optimally to its destination in Guided, RTL, and Auto mode. The autonomy of the vessel could be improved by the use of more sensors and the implementation of object detection and obstacle avoidance.

Bibliography

- [1] Federal Aviation Administration. Satellite navigation - gps - how it works. https://www.faa.gov/about/office_org/headquarters_offices/ato/service_units/techops/navservices/gnss/gps/howitworks.
- [2] Kofi Sarpong Adu-Manu, Cristiano Tapparelo, Wendi Heinzelman, Ferdinand Apietu Katsriku, and Jamal-Deen Abdulai. Water quality monitoring using wireless sensor networks: Current trends and future research directions. *ACM Transactions on Sensor Networks (TOSN)*, 13(1):1–41, 2017.
- [3] Harris Aerial. Herelink 2.4ghz long range hd video transmission system. <https://www.harrisaerial.com/product/herelink/>.
- [4] Barden. Sunpower spr-e-flex-110. <http://barden-uk.com/product/sunpower-spr-e-flex-110/>.
- [5] Ishrat Bashir, Farooq A Lone, Rouf Ahmad Bhat, Shafat A Mir, Zubair A Dar, and Shakeel Ahmad Dar. Concerns and threats of contamination on aquatic ecosystems. *Bioremediation and biotechnology: sustainable approaches to pollution degradation*, pages 1–26, 2020.
- [6] Bauhaus. Sup brett aqua marina hyper 350cm max 150kg. https://www.bauhaus.no/sup-brett-aqua-marina-hyper-350cm-max-150kg?gclid=CjwKCAjw3P0hBhBQEiwAqTCuBhmiw\1zzLRqLEnQpfHj3EHWxx53tHg2GV1VeyX7qi2Z5tbvWwoRoCgp0QAvD_BwE. (accessed: 17.04.2023).
- [7] BOATERexam. Boat hull types designs. <https://www.boaterexam.com/boating-resources/boat-hull-types-designs/>.
- [8] M.G. Budynas and J.K. Nisbett. *Shigley's Mechanical Engineering Design*. McGraw Hill, 10 edition, 2015.
- [9] William D Callister and David G Rethwisch. *Materials Science & Engineering*. John Wiley & Sons, 9th edition, 2013.
- [10] Joseph R Davis. *Corrosion of Aluminum and Aluminum Alloys*. ASM international, 2000.
- [11] T Dube, O Mutanga, K Seutloali, S Adelabu, and C Shoko. Water quality monitoring in sub-saharan african lakes: a review of remote sensing applications. *African Journal of Aquatic Science*, 40(1):1–7, 2015.

- [12] Moustafa Elkolali, Ahmed Al-Tawil, Lennard Much, Ryan Schrader, Olivier Masset, Marina Sayols, Andrew Jenkins, Sara Alonso, Alfredo Carella, and Alex Alcocer. A low-cost wave/solar powered unmanned surface vehicle. In *Global Oceans 2020: Singapore–US Gulf Coast*, pages 1–10. IEEE, 2020.
- [13] Bayu Erfianto, Adysti Adrienne, and Ramzy Rashaun Arif. On the experiment of path planning using multi-way points with a* algorithm for autonomous surface vehicle. *Kinetik: Game Technology, Information System, Computer Network, Computing, Electronics, and Control*, 2021.
- [14] Fondriest. Algae, phytoplankton and chlorophyll.
<https://www.fondriest.com/environmental-measurements/parameters/water-quality/algae-phytoplankton-chlorophyll/>.
- [15] Fondriest. Algae, phytoplankton and chlorophyll.
<https://www.fondriest.com/environmental-measurements/parameters/water-quality/algae-phytoplankton-chlorophyll/>.
- [16] Fondriest. Conductivity, salinity total dissolved solids.
<https://www.fondriest.com/environmental-measurements/parameters/water-quality/conductivity-salinity-tds/>.
- [17] Fondriest. Dissolved oxygen.
<https://www.fondriest.com/environmental-measurements/parameters/water-quality/dissolved-oxygen/>.
- [18] Fondriest. ph of water.
<https://www.fondriest.com/environmental-measurements/parameters/water-quality/ph/>.
- [19] Fondriest. Turbidity, total suspended solids water clarity.
<https://www.fondriest.com/environmental-measurements/parameters/water-quality/turbidity-total-suspended-solids-water-clarity/>.
- [20] Fondriest. Water temperature.
<https://www.fondriest.com/environmental-measurements/parameters/water-quality/water-temperature/>.
- [21] Thor I Fossen. *Handbook of marine craft hydrodynamics and motion control, Second Edition*. John Wiley Sons, 2021.
- [22] Subhodeep Ghosh. Types of hulls used for vessels.
<https://www.marineinsight.com/naval-architecture/types-of-hulls-used-for-vessels/>.
- [23] Roy Gilboa. *Design and System Identification of a Low-Cost USV for Coastal Observation*. PhD thesis, University of Rhode Island, 2022.
- [24] Allan R Hambley. *Electrical Engineering: Principles and Applications*. Pearson, 2018.

- [25] Dr. John Cairns Jr. *Restoration of Aquatic Ecosystems: Science, Technology, and Public Policy*. International series of monographs on physics. National Academies Press, 1992.
- [26] Binghao Li, Jiahuang Zhang, Peter Mumford, and Andrew G Dempster. How good is assisted gps. In *Proceedings of the International Global Navigation Satellite Systems Society (IGNSS Symposium 2011), Sydney, Australia*, pages 15–17. Citeseer, 2011.
- [27] Zhixiang Liu, Youmin Zhang, Xiang Yu, and Chi Yuan. Unmanned surface vehicles: An overview of developments and challenges. *Annual Reviews in Control*, 41:71–93, 2016.
- [28] Lihua Ma and Shangli Zhou. Positional accuracy of gps satellite almanac. *Artificial Satellites*, 49(4):225–231, 2014.
- [29] Dario Madeo, Alessandro Pozzebon, Chiara Mocenni, and Duccio Bertoni. A low-cost unmanned surface vehicle for pervasive water quality monitoring. *IEEE Transactions on Instrumentation and Measurement*, 69(4):1433–1444, 2020.
- [30] Thuy Mai. Global positioning system. nasa.gov/directorates/heo/scan/communications/policy/GPS.html.
- [31] Justin E Manley. Unmanned surface vehicles, 15 years of development. In *OCEANS 2008*, pages 1–4. Ieee, 2008.
- [32] Anglican Missions. United nation sustainable development goals (sdgs). <https://anglicanmissions.org.nz/united-nations-sustainable-development-goals-sdgs/>.
- [33] United Nations. Goal 13 climate action. https://www.undp.org/sustainable-development-goals/climate-action?utm_source=EN&utm_medium=GSR&utm_content=US_UNDP_PaidSearch_Brand_English&utm_campaign=CENTRAL&c_src=CENTRAL&c_src2=GSR&gclid=CjwKCAjw5pShBhB_EiwAvmnNVyGbbpc1UjhdWk_hRAvm1gUUtCRb2jQWZxK7Ma20ZF2fGbo2zYm8PxoCus4QAvD_BwE.
- [34] United Nations. Goal 14 life below water. https://www.undp.org/sustainable-development-goals/below-water?utm_source=EN&utm_medium=GSR&utm_content=US_UNDP_PaidSearch_Brand_English&utm_campaign=CENTRAL&c_src=CENTRAL&c_src2=GSR&gclid=CjwKCAjw5pShBhB_EiwAvmnNVyGbbpc1UjhdWk_hRAvm1gUUtCRb2jQWZxK7Ma20ZF2fGbo2zYm8PxoCus4QAvD_BwE.
- [35] United Nations. Goal 6 clean water and sanitation. https://www.undp.org/sustainable-development-goals/clean-water-and-sanitation?utm_source=EN&utm_medium=GSR&utm_content=US_UNDP_PaidSearch_Brand_English&utm_campaign=CENTRAL&c_src=CENTRAL&c_src2=GSR&gclid=CjwKCAjw5pShBhB_EiwAvmnNVyGbbpc1UjhdWk_hRAvm1gUUtCRb2jQWZxK7Ma20ZF2fGbo2zYm8PxoCus4QAvD_BwE.

- [36] United Nations. What are the sustainable development goals? https://www.undp.org/sustainable-development-goals?utm_source=EN&utm_medium=GSR&utm_content=US_UNDP_PaidSearch_Brand_English&utm_campaign=CENTRAL&c_src=CENTRAL&c_src2=GSR&gclid=CjwKCAjw5pShBhB_EiwAvmnNVyGbbpc1UjhdWk_hRAvm1gUUtCRb2jQWZxK7Ma20ZF2fGbo2zYm8PxoCus4QAvD_BwE.
[Online; accessed 30-March-2023].
- [37] Stan Pankratz, Adetoyese Olajire Oyedun, Xiaolei Zhang, and Amit Kumar. Algae production platforms for Canada's northern climate. *Renewable and Sustainable Energy Reviews*, 80:109–120, 2017.
- [38] Sanghyuk Park, John Deyst, and Jonathan How. A new nonlinear guidance logic for trajectory tracking. In *AIAA guidance, navigation, and control conference and exhibit*, page 4900, 2004.
- [39] Ruth G Patterson, Emily Lawson, Vinay Udyawer, Gary B Brassington, Rachel A Groom, and Hamish A Campbell. Uncrewed surface vessel technological diffusion depends on cross-sectoral investment in open-ocean archetypes: A systematic review of usv applications and drivers. *Frontiers in Marine Science*, 8:2015, 2022.
- [40] Junuthula Narasimha Reddy. *Introduction to the finite element method*. McGraw-Hill Education, 2019.
- [41] Blue Robotics. T200 thruster.
<https://bluerobotics.com/store/thrusters/t100-t200-thrusters/t200-thruster-r2-rp/>.
- [42] Improve Sailing. The illustrated guide to boat hull types (11 examples).
<https://improvesailing.com/guides/boat-hull-types>.
- [43] Atlas Scientific. Conductivity probe k 10.
<https://atlas-scientific.com/probes/conductivity-probe-k-10/>.
- [44] Atlas Scientific. Dissolved oxygen in water: Ppm for fish.
<https://atlas-scientific.com/blog/dissolved-oxygen-in-water-ppm-for-fish/>.
- [45] Atlas Scientific. How do dissolved oxygen probes work?
<https://atlas-scientific.com/blog/how-do-dissolved-oxygen-probes-work/>.
- [46] Atlas Scientific. How do temperature sensors work?
<https://atlas-scientific.com/blog/how-do-temperature-sensors-work/>.
- [47] Atlas Scientific. How does a ph probe work?
<https://atlas-scientific.com/blog/how-does-a-ph-probe-work/>.
- [48] Atlas Scientific. Lab grade dissolved oxygen probe.
<https://atlas-scientific.com/probes/dissolved-oxygen-probe/>.

- [49] Atlas Scientific. Lab grade gen 2 d.o. probe.
https://files.atlas-scientific.com/LG_D0_probe.pdf.
- [50] Atlas Scientific. Lab grade ph probe.
<https://atlas-scientific.com/probes/ph-probe/>.
- [51] Atlas Scientific. Pt-1000 temperature probe.
<https://atlas-scientific.com/probes/pt-1000-temperature-probe/>.
- [52] Atlas Scientific. Pt-1000 temperature probe.
<https://files.atlas-scientific.com/PT-1000-probe.pdf>.
- [53] Atlas Scientific. What applications industries use conductivity meters?
<https://atlas-scientific.com/blog/how-do-conductivity-meters-work/>.
- [54] Li Shen and Peter R Stopher. Review of gps travel survey and gps data-processing methods. *Transport reviews*, 34(3):316–334, 2014.
- [55] William Springer and Ing-Chang Jong. Teaching von mises stress: From principle axes to nonprincipal axes. 2022.
- [56] Sterlitech. Measuring total suspended solids in water.
<https://www.sterlitech.com/blog/post/measuring-total-suspended-solids-in-water>.
- [57] PX4 Dev Team. Pixhawk 4.
https://docs.px4.io/v1.9.0/en/flight_controller/pixhawk4.html.
- [58] Atle Totland and Espen Johnsen. Kayak drone—a silent acoustic unmanned surface vehicle for marine research. 2022.
- [59] João Carvalho Vasconcelos. Design of autonomous surface vessels, 2015.
- [60] Chandrabhan Verma, Eno E Ebenso, and MA Quraishi. Corrosion inhibitors for ferrous and non-ferrous metals and alloys in ionic sodium chloride solutions: A review. *Journal of Molecular Liquids*, 248:927–942, 2017.
- [61] Megan Wallace. What is gps?
https://www.nasa.gov/directorates/heo/scan/communications/policy/what_is_gps.
- [62] Joseph Peter Wichlinski. *Fabrication and Automation of a Power-Conserving USV in Moving Water*. PhD thesis, Purdue University Graduate School, 2021.
- [63] World Health Organization. *Guidelines for Drinking-water Quality*. WHO Press, fourth edition, 2011.

Chapter 10

Appendix

Appendix A: Github Repository

The following link references to the Github repository for this project. It contains all relevant 3D models, code, and data for this project.

<https://github.com/Jan-PhilipR/low-cost-solar-powered-USV.git>

Appendix B: 3D Models

This Appendix presents all 3D models that were designed in Solidworks. All parts mention here are included in the completed 3D model of the USV depicted in the Methodology, Figure 6.4. It should be noted that the SUP board is modelled after the Aqua Marina Hypers length, width, and height, but the actual shape of the model does not perfectly represent the physical board. All other parts were measured from their physical counterparts and modelled with those measurements. The aluminium profiles in the complete model all originate from the model depicted in Figure 10.10, but were individually modelled with different lengths, or with holes, when needed.

The models for the T200 and Peli case were retrieved from other sources on the 16th of February 2023:

Model: BlueRobotics T200 Thruster

Author: Rustom Jehangir

URL: <https://grabcad.com/library/bluerobotics-t200-thruster-1>

Model: pelican case¹

Author: Jared

URL: <https://grabcad.com/library/pelican-case-2>

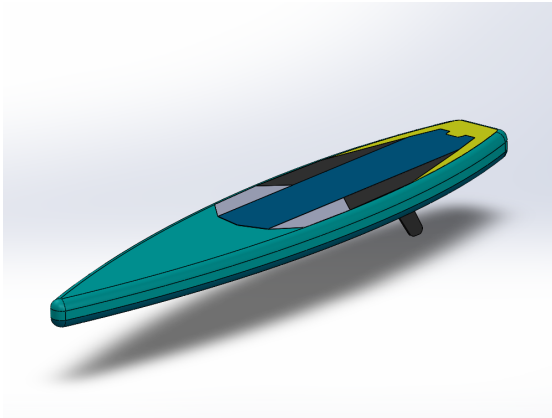


Figure 10.1: SUP board

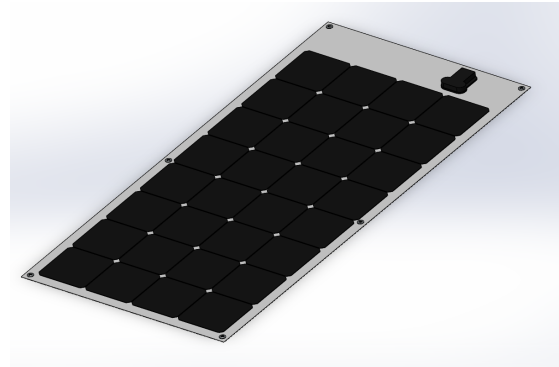


Figure 10.2: Solar panel

¹The model depicted in Figure 10.3 is coloured yellow, after the physical model, although the source model is coloured black.

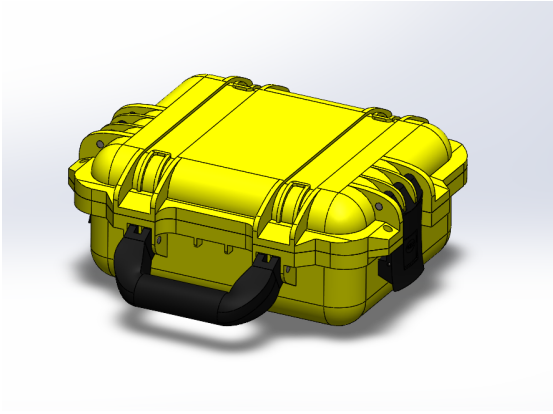


Figure 10.3: pelican case

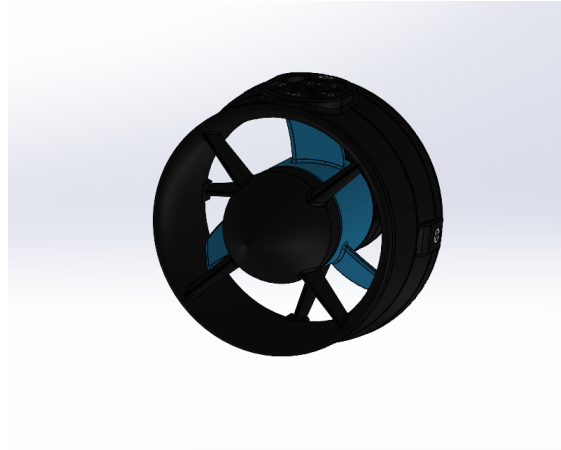


Figure 10.4: T200 thruster

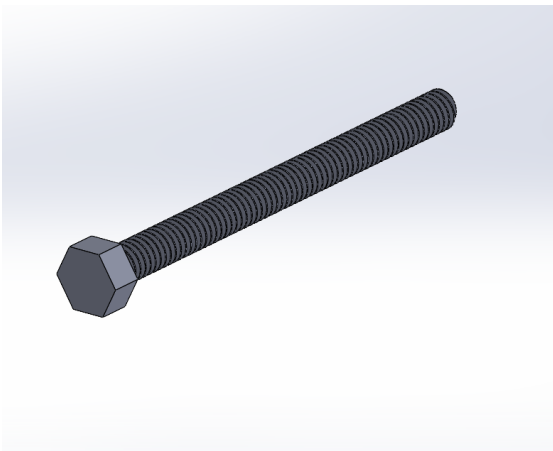


Figure 10.5: Bolt

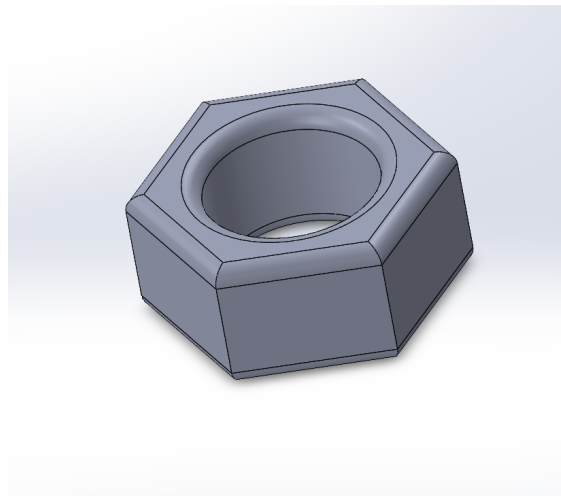


Figure 10.6: Nut

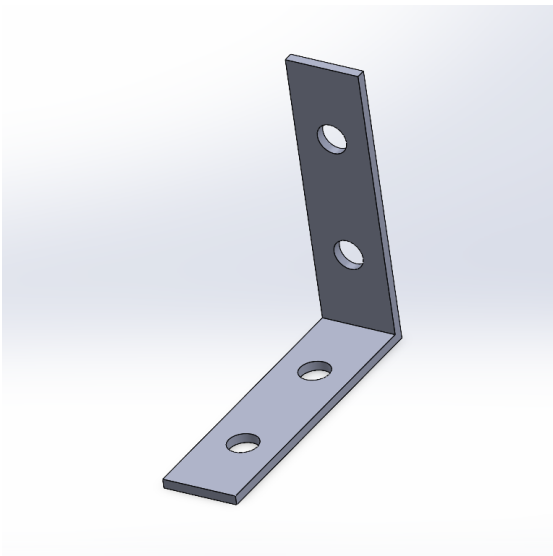


Figure 10.7: Angle bracket 75x75mm

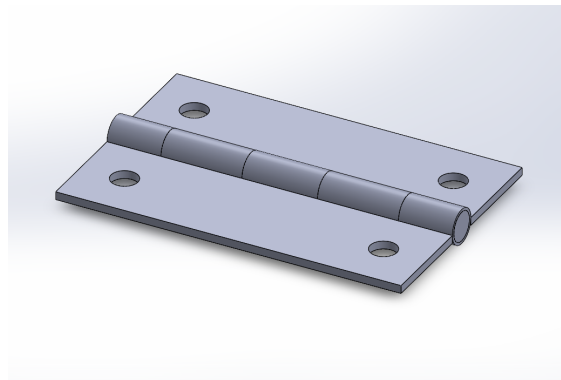


Figure 10.8: Hinge (consisting of three parts)

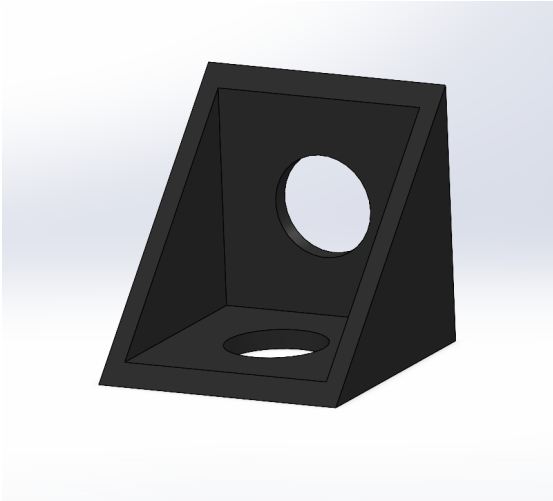


Figure 10.9: Ratrig angle bracket

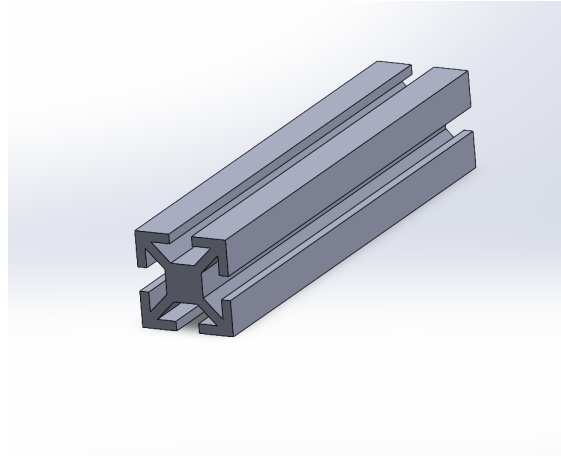


Figure 10.10: Ratrig aluminium profile

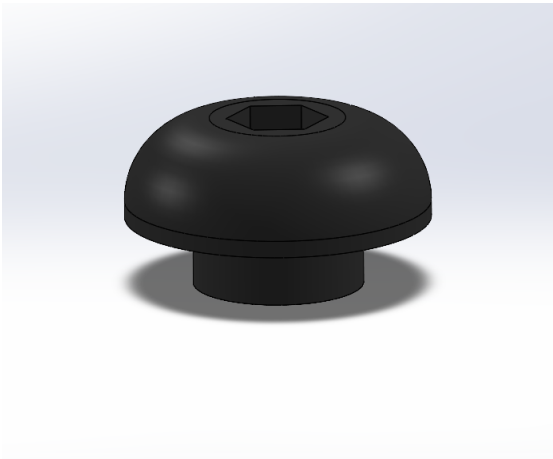


Figure 10.11: Ratrig screw

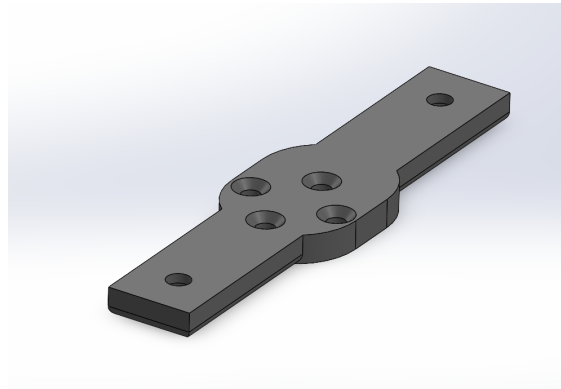


Figure 10.12: Thruster profile

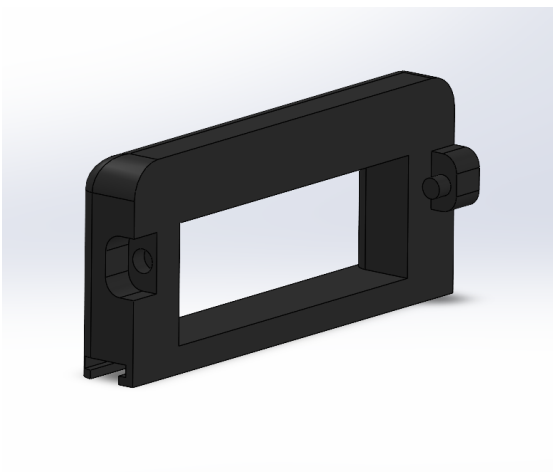


Figure 10.13: Handle

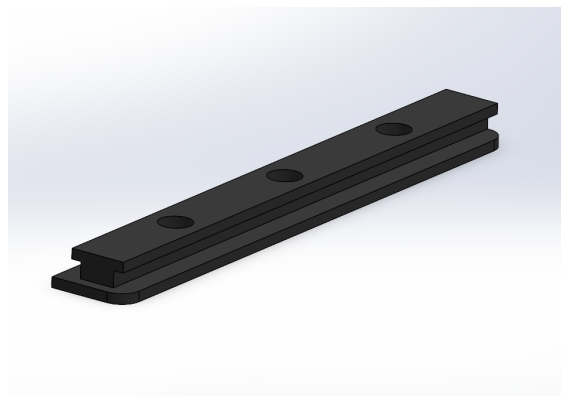


Figure 10.14: Handle bracket